



University of Strathclyde
Department of Mathematics and Statistics

STOCHASTIC DIFFERENTIAL EQUATIONS WITH
SWITCHING AND NUMERICAL SIMULATION FOR
GENE REGULATION NETWORKS

by

Somkid Intep

A thesis presented in fulfilment of the requirements
for the degree of Doctor of Philosophy

2010

Declaration

This thesis is the result of the authors original research. It has been composed by the author and has not been previously submitted for examination which has led to the award of a degree.

The copyright of this thesis belongs to the author under the terms of the United Kingdom Copyright Acts as qualified by University of Strathclyde Regulation 3.50. Due acknowledgement must always be made of the use of any material contained in, or derived from, this thesis.

Signed:

Date:

Acknowledgements

First of all, I would like to thank my supervisor, Professor Desmond J. Higham, very much. He always encouraged and supported me in everything since the first day I came to this department until this final thesis was submitted. It was very happy and enjoyable to work with him.

I would also like to thank my second supervisor, Professor Xuerong Mao, who gave insights on our analysis when we needed it.

This thesis would not have been possible if I had not been funded by Thailand's Commission on Higher Education, so I am very grateful to them.

Next, I would like to thank all of my fellows who are already titled 'Dr' and who are going to defend for it. I would also like to thank the ex-PhD student who is now titled with 'Dr', Dr Richard A. Rankin. He was very kind to help me with the small things, from latex to the language.

Finally, I would like to thank my family who supported me through everything. I would also like to thank my wife who came here with me since the beginning and shared happiness and sadness with me for more than three years.

Abstract

We analyse a hierarchy of three regimes for modelling gene regulation where the tools of stochastic calculus can be used to analyse first and second moments for all time. A technical issue to be addressed is that the state space for the discrete-valued switch is infinite. We show that the infinite ‘switch plus diffusion’ regime preserves the mean and variance, whereas the ‘switch plus ODE’ model uniformly underestimates the variance in the protein level.

We then compare three stochastic models in gene regulation; zero, one, and two-switch models. The steady state variance for the three models can either increase or decrease when switches are incorporated, depending on the rate constants and initial conditions. We find that one or two switches are always noisier than none. However, moving from one to two switches may either increase or decrease the noise strength. Although the underlying chemical kinetics appears to be second order in the two-switch model, we show that the hybrid diffusion model matches the moments of underlying Markov jump model for all time while the hybrid ODE model underestimates the variances. We also consider the case where the gene activity in the two-switch model is controlled by a pair of independent switches in AND and OR modes, and find that the OR mode may be more or less noisy than the AND mode depending on the model parameters.

After that, we analyse an autoregulation gene network in which a protein can

enhance its own transcription rate. We show that the moments of mRNA and protein increase monotonically with the feedback rate, and find that, at the stable steady state, increasing the feedback rate increases the variances and noise strengths of both mRNA and protein monotonically.

Contents

1	Introduction	1
1.1	Overview	2
2	Stochastic Differential Equations and Related Topics	4
2.1	Notation	5
2.2	Itô's Formula and Generalised Itô's Formula	5
2.3	Existence and Uniqueness of Solution for SDEs and Switch-SDEs	8
2.4	Numerical Solutions and Convergences	10
3	Biochemical Modelling	14
3.1	Modelling Genetic Networks	15
3.2	An Example	18
3.3	Noise Strength	20
4	Switching and Diffusion Models for Gene Regulation Networks	24
4.1	Theory and Simulation for Infinite State Space Switch	25
4.1.1	Examples of Finite and Infinite Markov Chains	25
4.1.2	Set-up	26

4.1.3	Existence and Uniqueness	28
4.1.4	Numerical Simulation	29
4.2	Hybrid Diffusion Moments	30
4.3	Hybrid ODE Moments	35
4.4	A Related Active/Inactive Gene Model	41
4.5	Tests With a Second Order Reaction	44
4.6	Summary	45
5	Zero, One and Two-switch Models of Gene Regulation	49
5.1	Gene Regulation Model	50
5.2	AND Mode: Moments for Two Switches	53
5.3	Comparing Noise Strengths	58
5.3.1	One-Switch versus Zero-Switch	58
5.3.2	Two-Switch versus Zero-Switch	62
5.3.3	One-Switch versus Two-Switch	63
5.4	Hybrid Moments	65
5.4.1	Hybrid Diffusion Moments	67
5.4.2	Hybrid ODE Moments	70
5.5	OR Mode	72
5.5.1	Moments for OR Mode	73
5.5.2	Mean, Variance, and Noise Strength: AND Mode versus OR Mode	75
5.6	Summary	76
6	Autoregulation Models for Gene Regulation Networks	81
6.1	Feedback Gene Regulation Model	82
6.2	Feedback Moments	83

6.3	Analytical Solutions	86
6.4	Feedback Effect	88
6.5	Steady State Variances and Noise Strengths with Feedback	97
6.6	Summary	99
7	Conclusions and Further Work	101
7.1	Conclusions	101
7.2	Further Work	102

Chapter 1

Introduction

Recently, switching stochastic differential equations (SDEs) are more and more popular to model many phenomena. In mathematical finance, for example, SDEs with switches are used to model the evolution of asset prices and interest rates in financial markets [21, 56]. This is because the values can change abruptly if, for example, the markets change from confident to nervous. In a gene regulation network, a gene, roughly speaking, can switch between an active state and inactive state [31, 43]. This causes mRNA to be transcribed if the gene is active, otherwise new mRNA is not produced. From this point of view, a switching SDE is reasonable to describe the evolution of the system.

It is popular to summarise the level of fluctuation observed in a system in term of the *noise strength* or *Fano factor*. For instance, the mRNA or protein noise strengths may be of interest in gene expression, see more details in section 3.3.

This thesis considers SDEs with switches along with their numerical simulation for gene regulation networks. We judge our models by their ability to reproduce the noise strength of the Chemical Master Equation (CME), under the assumption that the CME gives the most accurate solutions.

SDEs with a Markovian switch taking values in a finite state space have been already explored [37]. However, it is necessary to extend this theory to the case where the switch has an infinite state space. Consequently, hybrid models that use an infinite switch are considered in this thesis.

Increasing complexity of gene activity, and a protein feedback loop affecting its own transcription rate are the other issues we consider.

1.1 Overview

We designed this thesis as a self-contained study, so the first two chapters provide with some necessary ideas for the analysis in the main chapters.

Chapter 2 introduces some useful theorems and lemmas for SDEs and switch-SDEs, including existence and uniqueness of solutions, numerical simulation, and convergence.

In Chapter 3, we familiarise the reader with the general idea of how to model gene regulation. We give an example of how to form mathematical frameworks arising from chemical reactions. The noise strength is briefly discussed here.

Chapter 4 through 6 are the main body of research. In Chapter 4, we establish the existence and uniqueness, and consider numerical solution for SDEs with switches taking values in an infinite state space. Hybrid models are produced and judged via their noise strengths. This chapter is based on the paper [29].

Chapter 5 introduces a more complex type of gene activity in gene regulation, which could be regarded as a second order reaction network. We consider this complex gene activity into two senses: AND and OR operation modes. Most of the material in this chapter appeared in the paper [28].

In Chapter 6, the last of our research chapters, we look at the effect of increasing

the protein feedback rate when the protein affects its own transcription rate.

In the final chapter, we summarise our findings and leave some interesting open question for further research in this area.

Chapter 2

Stochastic Differential Equations and Related Topics

Nowadays stochastic differential equations (SDEs) are widely used to model many phenomena of science, economics, and engineering. This includes an interesting area, biochemical systems, which involves stochasticity. Recently, many authors have tried to understand and predict the behaviour of a biological systems such as gene expression [25, 31, 44, 47, 49, 51]. Some modelled the system by SDEs [51], and others modelled by SDEs with switches [25, 31]. In this thesis we will study SDEs with switches as our main aim. More precisely, we will develop and analyse approximate switching hybrid models and consider numerical simulation issues.

Here we assume that the reader is familiar with stochastic differential equations. For the reader who needs more details we refer to [32, 36, 42]. In the next sections, we define the notation used in this thesis, and state useful theorems and lemmas.

2.1 Notation

Let

- $\mathbb{E}[\cdot]$ denote expectation of \cdot .
- $\mathbb{P}(\cdot)$ denote probability of \cdot .
- $\mathcal{L}^p([a, b]; \mathbb{R}^n)$ denote a family of \mathbb{R}^n -valued \mathcal{F}_t -adapted processes $\{f(t)\}_{a \leq t \leq b}$ such that $\int_a^b |f(t)|^p dt < \infty$ all most surely (a.s.).
- $L^p_{\mathcal{F}_t}(\Omega; \mathbb{R}^n)$ denote a family of \mathbb{R}^n -valued \mathcal{F}_t -measurable random variables ξ such that $\mathbb{E}[|\xi|^p] < \infty$.
- $\mathcal{M}^p([a, b]; \mathbb{R}^n)$ denote a family of processes $\{f(t)\}_{a \leq t \leq b}$ in $\mathcal{L}^p([a, b]; \mathbb{R}^n)$ such that $\mathbb{E} \int_a^b |f(t)|^p dt < \infty$.
- $C^{2,1}(D \times \mathbb{R}_+; \mathbb{R})$ denote the family of all real-valued functions $V(x, t)$ defined on $D \times \mathbb{R}_+$ which are continuously twice differentiable in $x \in D$ and once differentiable in $t \in \mathbb{R}_+$.
- $[[a, b]]$ denote a stochastic closed interval, where a or b may be random variables.

2.2 Itô's Formula and Generalised Itô's Formula

In this section we will state the useful Itô's formula.

Definition 2.2.1. [37, p 39]

An n -dimensional Itô process is an \mathbb{R}^n -valued continuous adapted process $x(t) = (x_1(t), \dots, x_n(t))^T$ on $t \geq 0$ of the form

$$x(t) = x(0) + \int_0^t f(s) ds + \int_0^t g(s) dW(s),$$

where $f = (f_1, \dots, f_n)^T \in \mathcal{L}^1(\mathbb{R}_+; \mathbb{R}^n)$, $g = (g_{ij})_{n \times m} \in \mathcal{L}^2(\mathbb{R}_+; \mathbb{R}^{n \times m})$, and $W(t) = (W_1(t), \dots, W_m(t))^T, t \geq 0$ is an m -dimensional Brownian motion defined on a complete probability space $(\Omega, \mathcal{F}, \mathbb{P})$ adapted to the filtration $\{\mathcal{F}_t\}_{t \geq 0}$.

For $V \in C^{2,1}(\mathbb{R}^n \times \mathbb{R}_+; \mathbb{R})$, we set

$$V_t = \frac{\partial V}{\partial t}, \quad V_x = \left(\frac{\partial V}{\partial x_1}, \dots, \frac{\partial V}{\partial x_n} \right), \quad \text{and} \quad V_{xx} = \left(\frac{\partial^2 V}{\partial x_j \partial x_k} \right)_{n \times n}.$$

Theorem 2.2.1. (Itô's Formula) [37, p 39]

Let $x(t)$ be an n -dimensional Itô process on $t \geq 0$ with the stochastic differential

$$dx(t) = f(t)dt + g(t)dW(t),$$

where $f \in \mathcal{L}^1(\mathbb{R}_+; \mathbb{R}^n)$ and $g \in \mathcal{L}^2(\mathbb{R}_+; \mathbb{R}^{n \times m})$. Let $V \in C^{2,1}(\mathbb{R}^n \times \mathbb{R}_+; \mathbb{R})$. Then $V(x(t), t)$ is a real-valued Itô process with its stochastic differential given by

$$\begin{aligned} dV(x(t), t) &= [V_t + V_x f(t) + \frac{1}{2} \text{trace}(g^T(t) V_{xx} g(t))] dt \\ &\quad + V_x g(t) dW(t) \quad \text{a.s.} \end{aligned}$$

This theorem tells us that a function V maps the Itô process $x(t)$ to another Itô process $V(x(t), t)$, while the next theorem, known as the generalised Itô formula, will reveal that a function \widehat{V} maps a paired process $(x(t), r(t))$ to a new process $\widehat{V}(x(t), t, r(t))$ where $r(t)$ is a right-continuous Markov chain.

Let $r(t), t \geq 0$, be a right-continuous Markov chain on a complete probability space taking values in a finite state space $\mathbb{S} = \{1, 2, \dots, N\}$ with generator $\Gamma = (\gamma_{ij})_{N \times N}$ given by

$$\mathbb{P}\{r(t + \Delta) = j | r(t) = i\} = \begin{cases} \gamma_{ij} \Delta + o(\Delta) & \text{if } i \neq j, \\ 1 + \gamma_{ii} \Delta + o(\Delta) & \text{if } i = j, \end{cases}$$

where $\Delta > 0$, and $\gamma_{ij} \geq 0$ is the transition rate from state i to j if $i \neq j$ and

$$\gamma_{ii} = - \sum_{j \neq i} \gamma_{ij}.$$

Here we assume that the Markov chain $r(t)$ is independent of the Brownian motion $W(t)$.

Now for $\widehat{V} \in C^{2,1}(\mathbb{R}^n \times \mathbb{R}_+ \times \mathbb{S}; \mathbb{R})$, we set

$$\widehat{V}_t(x, t, i) = \frac{\partial \widehat{V}(x, t, i)}{\partial t}, \quad \widehat{V}_x(x, t, i) = \left(\frac{\partial \widehat{V}(x, t, i)}{\partial x_1}, \dots, \frac{\partial \widehat{V}(x, t, i)}{\partial x_n} \right),$$

$$\text{and } \widehat{V}_{xx}(x, t, i) = \left(\frac{\partial^2 \widehat{V}(x, t, i)}{\partial x_j \partial x_k} \right)_{n \times n},$$

and define an operator L from $\mathbb{R}^n \times \mathbb{R}_+ \times \mathbb{S}$ to \mathbb{R} such that

$$\begin{aligned} L\widehat{V}(x, t, i) &= \widehat{V}_t(x, t, i) + \widehat{V}_x(x, t, i)f(t) \\ &\quad + \frac{1}{2} \text{trace}[g^T(t)\widehat{V}_{xx}(x, t, i)g(t)] + \sum_{j=1}^N \gamma_{ij}\widehat{V}(x, t, j). \end{aligned}$$

Note that in the case that the Markov chain $r(t)$ takes values in an infinite state space, the upper summation index N in the last term of the equation above becomes infinity.

We are now in a position to state the generalised Itô formula.

Theorem 2.2.2. (Generalised Itô Formula) [37, 46]

If $\widehat{V} \in C^{2,1}(\mathbb{R}^n \times \mathbb{R}_+ \times \mathbb{S}; \mathbb{R})$, then for any $t \geq 0$

$$\begin{aligned} \widehat{V}(x(t), t, r(t)) &= \widehat{V}(x(0), 0, r(0)) + \int_0^t L\widehat{V}(x(s), s, r(s))ds \\ &\quad + \int_0^t \widehat{V}_x(x(s), s, r(s))g(x(s), s, r(s))dW(s) \\ &\quad + \int_0^t \int_{\mathbb{R}} \left(\widehat{V}(x(s), s, i_0 + h(r(s), l)) - \widehat{V}(x(s), s, r(s)) \right) \mu(ds, dl), \end{aligned}$$

where the details of the function h and the measure μ can be found in [37].

Note that we do not state the explicit forms of the function h and the martingale measure $\mu(ds, dl)$ because they are not relevant to our work. This is because they vanish when we take expectation.

2.3 Existence and Uniqueness of Solution for SDEs and Switch-SDEs

We first consider an SDE of the form

$$dx(t) = f(x(t), t)dt + g(x(t), t)dW(t), \quad t_0 \leq t \leq T \quad (2.1)$$

with an initial condition $x(t_0) = x_0 \in L^2_{\mathcal{F}_{t_0}}(\Omega; \mathbb{R}^n)$, and

$$f : \mathbb{R}^n \times \mathbb{R}_+ \rightarrow \mathbb{R}^n \quad \text{and} \quad g : \mathbb{R}^n \times \mathbb{R}_+ \rightarrow \mathbb{R}^{n \times m}.$$

An existence of a unique solution of the SDE (2.1) is accounted by the following condition.

Theorem 2.3.1. [36, p 51]

Assume that f and g satisfy a Lipschitz condition; that is, there exists a positive constant \bar{K} such that

$$|f(x, t) - f(y, t)|^2 \vee |g(x, t) - g(y, t)|^2 \leq \bar{K}|x - y|^2$$

for all $x, y \in \mathbb{R}^n$ and $t \in [t_0, T]$. Then there exists a unique solution $x(t)$ to SDE (2.1) and the solution belongs to $\mathcal{M}^2([t_0, T]; \mathbb{R}^n)$.

Now let us consider a Markovian switching SDE of the form

$$dx(t) = f(x(t), t, r(t))dt + g(x(t), t, r(t))dW(t), \quad t_0 \leq t \leq T \quad (2.2)$$

with initial conditions $x(t_0) = x_0 \in L^2_{\mathcal{F}_{t_0}}(\Omega; \mathbb{R}^n)$ and $r(t_0) = r_0$. Here r_0 is an \mathbb{S} -valued \mathcal{F}_{t_0} -measurable random variable,

$$f : \mathbb{R}^n \times \mathbb{R}_+ \times \mathbb{S} \rightarrow \mathbb{R}^n \quad \text{and} \quad g : \mathbb{R}^n \times \mathbb{R}_+ \times \mathbb{S} \rightarrow \mathbb{R}^{n \times m},$$

and $r(t)$ is a right-continuous Markov chain, as defined in section 2.2.

Definition 2.3.1. (*Solution of switch-SDEs*)[37, p 88]

An \mathbb{R}^n -valued stochastic process $\{x(t)\}_{t_0 \leq t \leq T}$ is called a solution of SDE (2.2) if it has the following properties:

1. $\{x(t)\}_{t_0 \leq t \leq T}$ is continuous and \mathcal{F}_t -adapted;
2. $\{f(x(t), t, r(t))\}_{t_0 \leq t \leq T} \in \mathcal{L}^1([t_0, T]; \mathbb{R}^n)$ and $\{g(x(t), t, r(t))\}_{t_0 \leq t \leq T} \in \mathcal{L}^2([t_0, T]; \mathbb{R}^{n \times m})$;
3. For any $t \in [t_0, T]$,

$$x(t) = x(t_0) + \int_{t_0}^t f(x(s), s, r(s))ds + \int_{t_0}^t g(x(s), s, r(s))dW(s)$$

holds with probability 1.

We say that a solution $\{x(t)\}_{t_0 \leq t \leq T}$ is unique if we cannot distinguish any other solution $\{\bar{x}(t)\}_{t_0 \leq t \leq T}$ from $\{x(t)\}_{t_0 \leq t \leq T}$.

The following condition is sufficient for there to exist a unique solution to the SDE (2.2).

Theorem 2.3.2. [37, p 89]

Assume that there exist a positive constant \bar{K} such that

(Lipschitz condition for switch-SDE) for all $x, y \in \mathbb{R}^n$, $t \in [t_0, T]$ and $i \in \mathbb{S}$

$$|f(x, t, i) - f(y, t, i)|^2 \vee |g(x, t, i) - g(y, t, i)|^2 \leq \bar{K}|x - y|^2. \quad (2.3)$$

Then there exists a unique solution $x(t)$ to switch-SDE (2.2) and, moreover,

$$\mathbb{E} \left(\sup_{t_0 \leq t \leq T} |x(t)|^2 \right) \leq (1 + 3\mathbb{E}|x_0|^2)e^{3\bar{K}(T-t_0)(T-t_0+4)} \quad (2.4)$$

so the solution belongs to $\mathcal{M}^2([t_0, T]; \mathbb{R}^n)$.

Note that the Lipschitz condition (2.3) implies automatically a *linear growth condition*; that is, there exist a positive constant K such that for all $(x, t, i) \in \mathbb{R}^n \times [t_0, T] \times \mathbb{S}$,

$$|f(x, t, i)|^2 \vee |g(x, t, i)|^2 \leq K(1 + |x|^2).$$

2.4 Numerical Solutions and Convergences

Generally we cannot obtain analytical solutions of SDEs with Markovian switching. So, it is necessary to obtain a good approximate solution. In this section we will introduce the Euler–Maruyama (EM) method. Now, consider an autonomous SDE with Markovian switching of the form

$$dx(t) = f(x(t), r(t))dt + g(x(t), r(t))dW(t), \quad 0 \leq t \leq T, \quad (2.5)$$

with initial conditions $x(0) = x_0 \in \mathbb{R}^n$ and $r(0) = r_0 \in \mathbb{S}$, where

$$f : \mathbb{R}^n \times \mathbb{S} \rightarrow \mathbb{R}^n \quad \text{and} \quad g : \mathbb{R}^n \times \mathbb{S} \rightarrow \mathbb{R}^{n \times m}.$$

Here we assume that f and g satisfy the condition (2.3) so that the SDE (2.5) has a unique solution. Note that x_0 and r_0 are now non-random.

To establish the EM approximate solution of (2.5), we will show first how to simulate the Markov chain $r(t)$. Given a fixed stepsize $\Delta > 0$, let $r_k^\Delta = r(k\Delta)$ for $k \geq 0$. We then have a discrete-time Markov chain $\{r_k^\Delta, k = 0, 1, 2, \dots\}$ with the one-step transition probability matrix [2, 37]

$$P(\Delta) = (P_{ij}(\Delta))_{N \times N} = e^{\Delta\Gamma},$$

where the generator Γ is defined in section 2.2. We note that $\sum_{j=1}^N P_{ij}(\Delta) = 1$ for all $i \in \mathbb{S}$. We now can construct the discrete-time Markov chain $\{r_k^\Delta\}$ as follows, see, for example, [37]:

1. Compute the one-step transition probability matrix

$$P(\Delta) = (P_{ij}(\Delta))_{N \times N} = e^{\Delta \Gamma},$$

and set $r_0^\Delta = r_0 \in \mathbb{S}$.

2. Generate an independent uniform (0,1) random number ξ_1 and find the smallest integer $r_1^\Delta := r_1 \in \mathbb{S}$ such that

$$\xi_1 < \sum_{j=1}^{r_1} P_{r_0, j}(\Delta).$$

3. Generate an independent uniform (0,1) random number ξ_2 and find the smallest integer $r_2^\Delta := r_2 \in \mathbb{S}$ such that

$$\xi_2 < \sum_{j=1}^{r_2} P_{r_1, j}(\Delta).$$

4. Repeating this procedure we can obtain a path from the discrete-time Markov chain $\{r_k^\Delta, k = 0, 1, 2, \dots\}$.

We are now in a position to define the EM approximate solution of (2.5).

A natural EM method for simulating the switching SDE (2.5) takes the form

$$X_{k+1} = X_k + f(X_k, r_k^\Delta)\Delta + g(X_k, r_k^\Delta)\Delta W_k. \quad (2.6)$$

Here, $\Delta > 0$ is a fixed stepsize, X_k is the approximation to $X(t_k)$, with $t_k = k\Delta$, $r_k^\Delta = r(k\Delta)$, $\Delta W_k = W(t_{k+1}) - W(t_k)$ and the initial conditions for the iteration are $X_0 = X(0) = x_0$ and $r_0^\Delta = r_0$.

For the purpose of analysis, it is convenient to work with a continuous time approximation, $X(t)$, that is defined as

$$X(t) = X_0 + \int_0^t f(\bar{X}(s), \bar{r}(s))ds + \int_0^t g(\bar{X}(s), \bar{r}(s))dW(s), \quad (2.7)$$

where the ‘step processes’ $\bar{X}(t)$ and $\bar{r}(t)$ take the form

$$\bar{X}(t) = X_k, \quad \bar{r}(t) = r_k^\Delta \quad \text{for } t \in [t_k, t_{k+1}).$$

Note that $X(t_k) = \bar{X}(t_k) = X_k$, so that $X(t)$ and $\bar{X}(t)$ coincide with the discrete numerical solution at the gridpoints t_k .

The following general moment bounds hold for both the exact and numerical solutions.

Lemma 2.4.1. [37, p 113]

Assume that f and g satisfy a linear growth condition; that is, there exists a constant $K > 0$ such that

$$|f(x, i)| \vee |g(x, i)| \leq K(1 + |x|) \quad \forall (x, i) \in \mathbb{R}^n \times \mathbb{S}. \quad (2.8)$$

Then for any $p \geq 2$ there is a constant H , which is dependent on only p, T, K, x_0 but independent of Δ , such that the exact solution $x(t)$ in (2.5) and the EM approximate solution $X(t)$ in (2.7) have the property that

$$\mathbb{E} \left[\sup_{0 \leq t \leq T} |x(t)|^p \right] \vee \mathbb{E} \left[\sup_{0 \leq t \leq T} |X(t)|^p \right] \leq H.$$

Now there is a question arising is of how close is an approximate solution to a true solution and how to measure their difference. Here we introduce two error measures: strong and weak convergence.

Definition 2.4.1. Strong Convergence [22]

A numerical method is said to have **strong order of convergence** equal to γ if there exists a constant C , independent of Δ , such that

$$\mathbb{E}|x(t_k) - X_k| \leq C\Delta^\gamma \quad (2.9)$$

for any fixed $t_k = k\Delta \in [0, T]$ and Δ sufficiently small.

If a numerical method has a strong order of convergence γ in (2.9), this means that if we decrease the time-step size Δ by a factor of 2, say, then the strong error between the true and approximate solutions will decrease by at least a factor of 2^γ .

In the case that the true solution is not known, we then use a numerical solution with a very small time-step size Δ instead.

Definition 2.4.2. Weak Convergence [22]

A numerical method is said to have **weak order of convergence** equal to γ if there exists a constant C , independent of Δ , such that for all functions p in some class

$$|\mathbb{E}[p(x(t_k))] - \mathbb{E}[p(X_k)]| \leq C\Delta^\gamma \quad (2.10)$$

for any fixed $t_k = k\Delta \in [0, T]$ and Δ sufficiently small.

Typically, the functions p in (2.10) are required to satisfy smoothness and polynomial growth conditions. The simplest choice for p is the identity function.

In the next theorem, we will bound the strong error of the EM approximate solution $X(t)$, in (2.7), under the global Lipschitz condition.

Theorem 2.4.1. Strong Convergence: Global Lipschitz Condition [37, p 115]

Assume that f and g satisfy the global Lipschitz condition; that is, there exists a constant $\bar{K} > 0$ such that

$$|f(x, i) - f(y, i)| \vee |g(x, i) - g(y, i)| \leq \bar{K}|x - y| \quad (2.11)$$

for all $x, y \in \mathbb{R}^n$ and $i \in \mathbb{S}$. Then, as $\Delta \rightarrow 0$,

$$\mathbb{E} \left[\sup_{0 \leq t \leq T} |X(t) - x(t)|^2 \right] \leq C\Delta + o(\Delta), \quad (2.12)$$

where C is a positive constant independent of Δ .

Chapter 3

Biochemical Modelling

In this chapter we familiarise the reader with the general idea of how to model gene regulation. In general, living biological systems are very complex. For example, protein synthesis involves lots of complex processes which combine together to perform transcription and translation. However, we can ignore the details of such processes if we are only interested in the control and downstream effects [55]. Therefore, we may model the process as follows: a gene (DNA) transcribes an mRNA, then the mRNA is translated to a protein, and the mRNA and protein can decay. This could be written in chemical reaction notation as [49]



where \widehat{D} denotes the amount of gene, and M and P denote the amount of mRNA and protein, respectively. The symbol \emptyset denotes the degradation of species. We will now explain the meaning of the chemical reaction notation used above, which we use quite often in this thesis. Reaction (3.1) says that a gene can create a

molecule of mRNA with transcription rate u_M , without destroying itself. Reaction (3.2) says that a molecule of mRNA can create a protein with synthesis rate u_P , without destroying itself. In (3.3) and (3.4) a molecule of mRNA, or protein, can degrade with reaction rate constant d_M or d_P , respectively. The equations (3.1) and (3.2) represent “*catalytic production from a source*” of mRNA and protein or “*birth*” of new mRNA and protein, and the equations (3.3) and (3.4) are known as “*degradation*” or “*death*”.

In the next section we discuss a general framework in which chemical reaction systems can be converted into mathematical models.

3.1 Modelling Genetic Networks

Gene regulation is typically modelled using the language of chemical kinetics. At one extreme, discrete-valued stochastic models can be adopted, giving rise to a *Chemical Master Equation* (CME), from which sample paths can be simulated via the Stochastic Simulation Algorithm (SSA) which is also known as Gillespie’s algorithm [14, 15, 55]. At the other extreme, continuous-valued deterministic modelling leads to a set of ordinary differential equations (ODEs) that are sometimes said to arise through the *law of mass action* [9].

The ODE framework is typically (a) more amenable to analysis [1, 27], (b) cheaper to simulate with [51, 52] and (c) better suited to the important inverse problem of estimating rate constants and comparing models based on sparsely observed data [53]. However, in the case where small numbers of molecules are present, the modelling assumptions that give rise to the mass action ODE are not valid [14, 15, 33] and the discrete/stochastic effects captured by the CME should not be ignored. For example, the stochastic version of a bi-stable ODE model can

account for switching between “almost stable” states [50, 54].

Although progress is being made on solving the CME [35] and on optimising Gillespie’s direct simulation method [12, 20], the fully discrete CME setting remains computationally infeasible for most realistic systems. Tau-leaping [8, 19] was introduced in an attempt to speed up stochastic simulation without resorting to a fully deterministic model. This tau-leaping approach can also be used as a means to derive an intermediate stochastic differential equation (SDE) model, known as the *Chemical Langevin Equation* (CLE) [18]. In the more general context of population dynamics this type of *diffusion limit* has also been defined as an approximation to a Markov jump process [33, 45].

We next give the reader more details of the mathematical approaches. Suppose we have a well-stirred system which is in thermal equilibrium, and that the volume of the system is fixed. In the system, N *chemical species* $\{S_1, \dots, S_N\}$ of a process can interact through M *chemical reactions* or *chemical channels* $\{R_1, \dots, R_M\}$. Let $\mathbf{X}(0) = \mathbf{x}_0$ be the initial state, and $P(\mathbf{x}, t)$ denote the probability that $\mathbf{X}(t) = \mathbf{x}$ at time t , where $\mathbf{X}(t) = (X_1(t), \dots, X_N(t))^T$ is a state vector such that $X_i(t)$ records the number of molecules of species S_i at time t . Then the CME takes the form

$$\frac{d}{dt}P(\mathbf{x}, t) = \sum_{j=1}^M [a_j(\mathbf{x} - \boldsymbol{\nu}_j)P(\mathbf{x} - \boldsymbol{\nu}_j, t) - a_j(\mathbf{x})P(\mathbf{x}, t)],$$

where $\boldsymbol{\nu}_j$ is the *stoichiometric* or *state-change* vector when reaction j th takes place such that state vector $\mathbf{X}(t)$ is changed to $\mathbf{X}(t) + \boldsymbol{\nu}_j$, and $a_j(\mathbf{X}(t))$ is the propensity function such that, in the next infinitesimal time interval $[t, t + dt)$, the probability that the j th reaction will occur is $a_j(\mathbf{X}(t))dt$. For further details the reader may refer to [16, 39]. We can construct the propensity function as follows. If R_j is the monomolecular reaction $S_m \xrightarrow{c_j}$ products, we have $a_j(\mathbf{X}(t)) = c_j X_m(t)$. If R_j is the bimolecular reaction $S_m + S_n \xrightarrow{c_j}$ products, we have $a_j(\mathbf{X}(t)) = c_j X_m(t) X_n(t)$ if

$m \neq n$, or $a_j(\mathbf{X}(t)) = c_j \frac{1}{2} X_m(t) (X_m(t) - 1)$ if $m = n$. These propensity functions were derived by Gillespie [14, 15] using first principle modelling arguments.

To avoid computing $P(\mathbf{x}, t)$ directly, the SSA, which was introduced by Gillespie [14], computes numerical realisations of the state vector $\mathbf{X}(t)$. The trajectories or realisations of $\mathbf{X}(t)$ can be simply simulated as in the following algorithm [14, 15, 23]. Suppose that an initial state $\mathbf{X}(0)$ is given.

1. Compute $\{a_k(\mathbf{X}(t))\}_{k=1}^M$ and $a_0(\mathbf{X}(t)) := \sum_{k=1}^M a_k(\mathbf{X}(t))$.
2. Generate two independent uniform $(0, 1)$ random numbers, ξ_1 and ξ_2 .
3. Find the smallest integer j satisfying $\xi_1 a_0(\mathbf{X}(t)) < \sum_{k=1}^j a_k(\mathbf{X}(t))$.
4. Set $\tau = \ln(1/\xi_2)/a_0(\mathbf{X}(t))$.
5. Update the state and time: $\mathbf{X}(t + \tau) = \mathbf{X}(t) + \boldsymbol{\nu}_j$ and $t = t + \tau$.
6. Record $(\mathbf{X}(t), t)$ as desired. Return to step 1, or else end the simulation.

SSA still has similar problems to the CME if there are too many molecule species present in the system, it is slow and expensive. To speed up the SSA, tau-leaping [8, 19] was introduced. After further modelling assumptions are imposed, this leads to the CLE [18] which has the following form

$$d\mathbf{Y}(t) = \sum_{j=1}^M \boldsymbol{\nu}_j a_j(\mathbf{Y}(t)) dt + \sum_{j=1}^M \boldsymbol{\nu}_j \sqrt{a_j(\mathbf{Y}(t))} dW_j(t), \quad (3.5)$$

where $W_j(t)$ are independent scalar Brownian motions, and $\mathbf{Y}(t)$ is the state vector that records the amount of each species present. We note that $\mathbf{Y}(t)$ is now a real-valued random variable. It is known that, in general, Langevin equations of this type introduce technical difficulties due to solution components becoming negative [24, 48]. Throughout this thesis, we assume that solutions with bounded first and

second moments exists—more precisely, we implicitly derive results that are valid up to an appropriate stopping time.

If we remove the diffusion term of the CLE (3.5), we have the set of ODEs called the Reaction Rate Equation (RRE)

$$\frac{d\mathbf{y}(t)}{dt} = \sum_{j=1}^M \boldsymbol{\nu}_j a_j(\mathbf{y}(t)). \quad (3.6)$$

Here we use the lower case symbol $\mathbf{y}(t)$ in order to distinguish the RRE from the CLE. We also note that $\mathbf{y}(t)$ is now a real-valued deterministic variable.

We are now in a position to illustrate how to model a chemical system through a concrete example.

3.2 An Example

The Michaelis–Menten enzyme system [40, 55] is represented by the chemical reactions:



Overall, an enzyme E converts a substrate S to a product P . Here the c_i are reaction rate constants. For this example, $\mathbf{X}(t)$ is a state vector that records the number of molecules of enzyme, substrate, complex, and product. In (3.7), an enzyme E combines with a substrate S to form a enzyme-substrate complex ES with reaction rate constant c_1 . When this reaction takes place, we lose one molecule of enzyme and one molecule of substrate, and get one molecule of complex, but it does not change the number of molecules of product P . So, we have

the stoichiometric vector

$$\boldsymbol{\nu}_1 = \begin{bmatrix} -1 \\ -1 \\ 1 \\ 0 \end{bmatrix},$$

and propensity function $a_1(\mathbf{X}) = c_1 X_1 X_2$ for this reaction. Similarly, in (3.8), a complex may dissociate back to an enzyme and a substrate. When this reaction takes place, we lose a molecule of complex but gain a molecule of enzyme and a molecule of substrate (again it does not change the number of molecules of product). In (3.9), a complex may release a free enzyme and create a new product. Therefore, the stoichiometric and propensity functions associated with these two reactions are

$$\boldsymbol{\nu}_2 = \begin{bmatrix} 1 \\ 1 \\ -1 \\ 0 \end{bmatrix}, \text{ and } \boldsymbol{\nu}_3 = \begin{bmatrix} 1 \\ 0 \\ -1 \\ 1 \end{bmatrix},$$

and $a_2(\mathbf{X}) = c_2 X_3$ and $a_3(\mathbf{X}) = c_3 X_3$. If we plug these stoichiometrics and propensity functions into (3.5) and (3.6), we have the CLE

$$\begin{aligned} dX_1 &= (-c_1 X_1 X_2 + (c_2 + c_3) X_3) dt - \sqrt{c_1 X_1 X_2} dW_1 + \sqrt{c_2 X_3} dW_2 \\ &\quad + \sqrt{c_3 X_3} dW_3, \\ dX_2 &= (-c_1 X_1 X_2 + c_2 X_3) dt - \sqrt{c_1 X_1 X_2} dW_1 + \sqrt{c_2 X_3} dW_2, \\ dX_3 &= (c_1 X_1 X_2 - (c_2 + c_3) X_3) dt + \sqrt{c_1 X_1 X_2} dW_1 - \sqrt{c_2 X_3} dW_2 \\ &\quad - \sqrt{c_3 X_3} dW_3, \\ dX_4 &= c_3 X_3 dt + \sqrt{c_3 X_3} dW_3, \end{aligned}$$

and the RRE

$$\begin{aligned}\frac{dX_1}{dt} &= -c_1X_1X_2 + (c_2 + c_3)X_3, \\ \frac{dX_2}{dt} &= -c_1X_1X_2 + c_2X_3, \\ \frac{dX_3}{dt} &= c_1X_1X_2 - (c_2 + c_3)X_3, \\ \frac{dX_4}{dt} &= c_3X_3,\end{aligned}$$

to model the Michaelis–Menten enzyme system.

3.3 Noise Strength

Gene expression is a fundamental biological process that attracts a great deal of attention from both experimental and theoretical scientists. Because some important components are present at very low copy numbers, mathematical models typically involve discrete-valued state variables and have a stochastic nature [30, 43, 44, 47, 49].

The *noise strength* or *Fano factor* is often used to summarise the level of fluctuations observed in a system; for a random variable X , this is simply the ratio of variance to mean [44, 49]:

$$\text{ns}[X] := \frac{\text{var}[X]}{\mathbb{E}[X]}. \quad (3.10)$$

Typically, the steady state noise strength in the mRNA or protein level may be of interest. Experimental or computer simulation-based measurements can then be recorded for different parameter regimes in order to understand which sources contribute to enhancing and suppressing intrinsic noise [44, 47, 49].

Raser and O’Shea [44] considered a gene regulation involving inactive and active DNA in eukaryotics. There, the DNA can only produce an mRNA when it is active.

They examined noise strength for three different regimes by varying the kinetic reaction rate constants at steady state and comparing with a real experimental data, and found that two promoters can give the same mean with different noise strength. A promoter undergoing high activation rates but low transcription will result in small noise strength, while a promoter undergoing low activation rates but high transcription can produce large noise strength.

In 2001 Thattai and Oudenaarden [49] considered a simpler gene expression model in prokaryotes that covers the essential processes of transcription, translation, and degradation represented by the reactions (3.1)–(3.4).

In 2005 Gadgil et al. [11] used the master equation for a system of first-order chemical reactions to obtain a closed system of ODEs that describe the evolution of the first and second moments and correlations. This result allows us to analyse the fluctuation noise strength for all time. For the CLE formulation, we may analyse the noise strength for all time of the first-order reaction network using the Itô lemma.

We now re-visit the reactions (3.1)–(3.4). In this model, the amount of gene stays fixed, so \widehat{D} remains constant. We may therefore take the state vector for the amount of mRNA and protein to be

$$\begin{bmatrix} X_1 \\ X_2 \end{bmatrix}.$$

The stoichiometric vectors [23, 55] for the four reactions are

$$\boldsymbol{\nu}_1 = \begin{bmatrix} 1 \\ 0 \end{bmatrix}, \quad \boldsymbol{\nu}_2 = \begin{bmatrix} 0 \\ 1 \end{bmatrix}, \quad \boldsymbol{\nu}_3 = \begin{bmatrix} -1 \\ 0 \end{bmatrix}, \quad \boldsymbol{\nu}_4 = \begin{bmatrix} 0 \\ -1 \end{bmatrix},$$

with corresponding propensity functions

$$a_1(X) = u_M \widehat{D}, \quad a_2(X) = u_P X_1, \quad a_3(X) = d_M X_1, \quad a_4(X) = d_P X_2.$$

Because \widehat{D} is fixed, we will re-name $u_M \widehat{D}$ as u_M . This gives the CLE

$$d \begin{bmatrix} M \\ P \end{bmatrix} = \begin{bmatrix} u_M - d_M M \\ u_P M - d_P P \end{bmatrix} dt + \begin{bmatrix} \sqrt{u_M} & 0 & -\sqrt{d_M M} & 0 \\ 0 & \sqrt{u_P M} & 0 & -\sqrt{d_P P} \end{bmatrix} \begin{bmatrix} dW_1 \\ dW_2 \\ dW_3 \\ dW_4 \end{bmatrix}. \quad (3.11)$$

We are now in a position to study the means and variances of mRNA and protein. We interpret the system (3.1)–(3.4) as a Markov process defined by the CME, letting $M(t)$ and $P(t)$ denote the stochastic processes that specify the levels of mRNA and protein, respectively. The system fits into the framework of a *first-order reaction network*. Therefore we may use the general result of [11] to obtain a closed system of ODEs

$$\frac{d}{dt} \mathbb{E}[M] = -d_M \mathbb{E}[M] + u_M, \quad (3.12)$$

$$\frac{d}{dt} \mathbb{E}[P] = u_P \mathbb{E}[M] - d_P \mathbb{E}[P], \quad (3.13)$$

$$\frac{d}{dt} \mathbb{E}[P^2] = u_P \mathbb{E}[M] + d_P \mathbb{E}[P] + 2u_P \mathbb{E}[MP] - 2d_P \mathbb{E}[P^2], \quad (3.14)$$

$$\frac{d}{dt} \mathbb{E}[M^2] = u_M + (2u_M + d_M) \mathbb{E}[M] - 2d_M \mathbb{E}[M^2], \quad (3.15)$$

$$\frac{d}{dt} \mathbb{E}[MP] = u_P \mathbb{E}[M^2] + u_M \mathbb{E}[P] - (d_M + d_P) \mathbb{E}[MP]. \quad (3.16)$$

By solving this linear ODE, we have the mean and variance of the mRNA and protein for all time, from which we can compute their noise strength.

In the CLE formulation, applying the Itô formula Theorem 2.2.1 to the equation

(3.11), we find that

$$\begin{aligned}
d \begin{bmatrix} M^2 \\ P^2 \\ MP \end{bmatrix} &= \begin{bmatrix} u_M + (2u_M + d_M)M - 2d_M M^2 \\ u_P M + d_P P - 2d_P P^2 + 2u_P MP \\ u_M P + u_P M^2 - (d_M + d_P)MP \end{bmatrix} dt \\
&+ \begin{bmatrix} 2\sqrt{u_M}M & 0 & -2M\sqrt{d_M M} & 0 \\ 0 & 2P\sqrt{u_P M} & 0 & -2P\sqrt{d_P P} \\ \sqrt{u_M}P & M\sqrt{u_P M} & -P\sqrt{d_M M} & -M\sqrt{d_P P} \end{bmatrix} \begin{bmatrix} dW_1 \\ dW_2 \\ dW_3 \\ dW_4 \end{bmatrix}.
\end{aligned} \tag{3.17}$$

Taking the expectation in (3.11) and (3.17), we arrive at the same ODEs (3.12)–(3.16). This shows that the CME and CLE versions produce the same first and second moments and correlations. Gillespie [17] showed that this property holds for all scalar first order networks, and this was generalised to any first order network in [25]. We note that third and higher order moments do not match, in general [17].

In later chapters, we produce approximate models, namely hybrid models, for the sake of computational efficiency, and we will judge them by their ability to reproduce the noise strength of the CME.

Chapter 4

Switching and Diffusion Models for Gene Regulation Networks

In this chapter we are going to produce approximate models for the chemical reactions (3.1)–(3.4). For the CME, these reactions have the ODE, (3.12)–(3.16), that describes the evolution of the first and second moments and correlations, as discussed in section 3.3.

It is intuitively appealing, and potentially extremely beneficial, to mix together the CME, RRE, and CLE regimes so that different species, different reactions, or different time periods are treated by simulation methods that are as cheap as possible while preserving the overall accuracy [7, 10]. An interesting example that applies specifically to a simple gene regulation setting was proposed by Paszek [43]. Here, a hybrid model was put forward that uses the CME regime for low copy number species and the ODE framework for relatively abundant species. In this chapter, which follows from a simpler context in [25], we exploit the fact that the hybrid model may be regarded as a system of ODEs driven by an independent Markovian switch. The switch has an infinite state space, but we show that ex-

istence and uniqueness, and numerical simulation theories, carry through. This viewpoint makes it possible to analyse the first and second moments of the model using the tools of stochastic calculus, and to consider an alternative where the ODE is replaced by a diffusion approximation.

4.1 Theory and Simulation for Infinite State Space Switch

4.1.1 Examples of Finite and Infinite Markov Chains

In this subsection we will give examples to distinguish between Markov chains with finite state space and infinite state space.

Example 4.1. (*Telephone Exchange*) [41]

Consider a telephone exchange system that can connect phone calls. In this system, the maximum number of calls that can be connected at once is m , and new additional calls are lost when the exchange is full. In this setting, if we let $x(t)$ denote the number of connected calls at time t , then $x(t)$ represents a Markov chain because the number of connected calls for the next infinitesimal time $x(t+dt)$ depends only on the current $x(t)$. We also see that the Markov chain takes values in a finite state space $\mathbb{S} = \{0, 1, 2, \dots, m\}$. It is clear that $x(t) = 0$ represents that there are no calls at time t , and $x(t) = m$ represents the exchange is full with m calls at time t .

Example 4.2. (*Immigration-Death Process*) [55]

In an immigration-death process, individuals arrive into the population with constant rate λ , and each individual can die independently with constant rate

μ . Therefore, when an immigration event occurs, the population of individuals increases by one. On the other hand, the population decreases by one when a death event occurs. Let $X(t)$ denote the population of individuals at time t , then the transition equations are

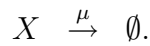
$$\mathbb{P}(X(t + dt) = s + 1 \mid X(t) = s) = \lambda dt,$$

$$\mathbb{P}(X(t + dt) = s - 1 \mid X(t) = s) = \mu s dt,$$

$$\mathbb{P}(X(t + dt) = s \mid X(t) = s) = 1 - (\lambda - \mu s) dt,$$

$$\text{and } \mathbb{P}(X(t + dt) = y \mid X(t) = s) = 0, \quad \forall y \notin \{s - 1, s, s + 1\}.$$

These equations clearly define a Markov process with infinite state space $\widehat{\mathbb{S}} = \{0, 1, 2, \dots\}$. In the context of chemical kinetics, this model arises from the system



We can see from the example 4.1 that the Markov chain $x(t)$ has a value in the finite state space $\mathbb{S} = \{0, 1, 2, \dots, m\}$ no matter how much time is allowed. On the other hand, the Markov chain $X(t)$ in the example 4.2 can take an arbitrarily large value if we give time to the process long enough.

4.1.2 Set-up

Stochastic differential equations driven by switches are becoming more common as models in science and engineering. A switch typically takes a finite number of possible values, but in this work we need to consider a countably infinite state space, enumerated by the non-negative integers. This is because if we model the number of molecules of mRNA through the reactions (3.1) and (3.3) as a Markov process $\widehat{r}(t)$, we see that the number of $\widehat{r}(t)$ can potentially increase up to infinity

since the number of genes \widehat{D} is fixed, and always available to produce mRNA in the system. This requires us to extend the theory for existence, uniqueness, and numerical simulation that can be found, for example, in [37], from finite to countably infinite state spaces. We begin by setting up our notation and problem formulation.

Let $\widehat{r}(t)$ be again a Markov chain on a complete probability space but taking values in an infinite state space $\widehat{\mathbb{S}} = \{0, 1, 2, \dots\}$ with generator $\widehat{\Gamma} = (\gamma_{ij})_{i,j \in \widehat{\mathbb{S}}}$ given by

$$\begin{aligned} \lim_{\Delta \rightarrow 0} \frac{\mathbb{P}\{\widehat{r}(t+\Delta) = j \mid \widehat{r}(t) = i\} - 1}{\Delta} &= \gamma_{ii}, \quad \text{if } i = j, \quad \text{and} \\ \lim_{\Delta \rightarrow 0} \frac{\mathbb{P}\{\widehat{r}(t+\Delta) = j \mid \widehat{r}(t) = i\}}{\Delta} &= \gamma_{ij}, \quad \text{if } i \neq j, \end{aligned}$$

where $\gamma_{ij} \geq 0$ is the transition rate from state i to j if $i \neq j$ and

$$\gamma_{ii} = - \sum_{j \neq i} \gamma_{ij}.$$

We assume that the transition rate γ_{ij} satisfies the following condition:

$$\max_{i \in \widehat{\mathbb{S}}} |\gamma_{ii}| < \infty.$$

Now, consider an autonomous SDE with Markovian switch of the form

$$dx(t) = f(x(t), \widehat{r}(t))dt + g(x(t), \widehat{r}(t))dW(t), \quad 0 \leq t \leq T, \quad (4.1)$$

with initial conditions $x(0) = x_0 \in L^p_{\mathcal{F}_t}(\Omega; \mathbb{R}^n)$ and $\widehat{r}(0) = \widehat{r}_0$, where \widehat{r}_0 is an $\widehat{\mathbb{S}}$ -valued, \mathcal{F}_0 -measurable random variable and

$$f : \mathbb{R}^n \times \widehat{\mathbb{S}} \rightarrow \mathbb{R}^n \quad \text{and} \quad g : \mathbb{R}^n \times \widehat{\mathbb{S}} \rightarrow \mathbb{R}^{n \times m}.$$

Here $W(t)$ is an m -dimensional Brownian motion that is independent of the Markov chain.

4.1.3 Existence and Uniqueness

We begin with an existence, uniqueness, and moment bound result based on the finite state treatment in [37] that was summarised in Chapter 3. We make the traditional global Lipschitz assumptions on the coefficients. For the case where the diffusion coefficients arise through the chemical Langevin regime, these results apply only up to a stopping time—so that excursions taking population sizes close to zero can be avoided. Deriving more general results that apply directly to nonglobally Lipschitz problems is currently an active area of research [26, 38].

To keep the analysis compact, without loss of any generality, we set the initial conditions x_0 and \widehat{r}_0 be non-random; that is $x_0 \in \mathbb{R}^n$ and $\widehat{r}_0 \in \widehat{\mathbb{S}}$.

Theorem 4.1.1. *Assume that f and g satisfy a global Lipschitz condition; that is, there exists a positive constant K such that*

$$|f(x, i) - f(y, i)| \vee |g(x, i) - g(y, i)| \leq K|x - y| \quad (4.2)$$

for all $x, y \in \mathbb{R}^n$ and $i \in \widehat{\mathbb{S}}$.

Then there exists a unique solution $x(t)$ to (4.1), and, moreover,

$$\mathbb{E} \left(\sup_{0 \leq t \leq T} |x(t)|^2 \right) \leq (1 + 3\mathbb{E}|x_0|^2)e^{3KT(T+4)}, \quad (4.3)$$

so the solution belongs to $\mathcal{M}^2([0, T]; \mathbb{R}^n)$.

Proof. Since almost every sample path of $\widehat{r}(\cdot)$ is a step function, there is a sequence $\{\tau_k\}_{k \geq 0}$ of stopping times such that $t_0 = \tau_0 < \tau_1 < \tau_2 < \cdots < \tau_k < \cdots$ and $\widehat{r}(t) = \widehat{r}(\tau_k)$ for $t \in [\tau_k, \tau_{k+1})$.

First, we consider (4.1) on the interval $t \in [[\tau_0, \tau_1]]$; that is,

$$dx(t) = f(x(t), \widehat{r}_0)dt + g(x(t), \widehat{r}_0)dW(t), \quad (4.4)$$

with initial conditions $x(t_0) = x_0$ and $\widehat{r}(t_0) = \widehat{r}_0$. Now, (4.4) is an SDE without Markovian switch. So, by Theorem 2.3.1, (4.1) has a unique solution which belongs

to $\mathcal{M}^2([\tau_0, \tau_1]; \mathbb{R}^n)$. In particular, $x(\tau_1) \in L^2_{\mathcal{F}_{\tau_1}}(\Omega; \mathbb{R}^n)$. After that, we consider (4.1) on the interval $t \in [[\tau_1, \tau_2]]$ which becomes

$$dx(t) = f(x(t), \widehat{r}(\tau_1))dt + g(x(t), \widehat{r}(\tau_1))dW(t), \quad (4.5)$$

with initial conditions $x(\tau_1)$ and $\widehat{r}(\tau_1)$. Again by Theorem 2.3.1, (4.1) has a unique solution which belongs to $\mathcal{M}^2([\tau_1, \tau_2]; \mathbb{R}^n)$. By repeating this procedure we can see that (4.1) has a unique solution $x(t)$ on $[0, T]$. Finally, the bound (4.3) follows by arguing in the same way as [37, Lemma 3.1]. \square

4.1.4 Numerical Simulation

Like in section 2.4, the natural Euler–Maruyama method for simulating the switching SDE (4.1) takes the form

$$X_{k+1} = X_k + f(X_k, \widehat{r}_k^\Delta)\Delta + g(X_k, \widehat{r}_k^\Delta)\Delta W_k.$$

Here again, $\Delta > 0$ is a fixed stepsize, X_k is the approximation to $X(t_k)$, with $t_k = k\Delta$, $\widehat{r}_k^\Delta = \widehat{r}(k\Delta)$, $\Delta W_k = W(t_{k+1}) - W(t_k)$, and the initial conditions for the iteration are $X_0 = x_0$ and $\widehat{r}_0^\Delta = \widehat{r}_0$. Keep in mind that in this chapter we focus on the Markovian switch that arises from the simple chemical reactions (3.1) and (3.3). So, the switch has an infinite state space; see section 4.2 for details of how to define and simulate the switch. Therefore, we do not need to worry about how to simulate $\widehat{r}(t)$ in general case.

Let $X(t)$ be a continuous time approximation that is defined as

$$X(t) = X_0 + \int_0^t f(\bar{X}(s), \bar{r}(s))ds + \int_0^t g(\bar{X}(s), \bar{r}(s))dW(s), \quad (4.6)$$

where the “step processes” $\bar{X}(t)$ and $\bar{r}(t)$ take the form

$$\bar{X}(t) = X_k, \quad \bar{r}(t) = \widehat{r}_k^\Delta \quad \text{for } t \in [t_k, t_{k+1}).$$

The following general moment bounds hold for both the exact and numerical solutions.

Lemma 4.1.1. *Assume that f and g satisfy a linear growth condition; that is, there exists a constant $\bar{K} > 0$ such that*

$$|f(x, i)| \vee |g(x, i)| \leq \bar{K}(1 + |x|) \quad \forall (x, i) \in \mathbb{R}^n \times \widehat{\mathbb{S}}. \quad (4.7)$$

Then for any $p \geq 2$ there is a constant H , which is dependent on only p, T, \bar{K}, x_0 but independent of Δ , such that the exact solution $x(t)$ in (4.1) and the Euler–Maruyama approximate solution $X(t)$ in (4.6) have the property that

$$\mathbb{E} \left[\sup_{0 \leq t \leq T} |x(t)|^p \right] \vee \mathbb{E} \left[\sup_{0 \leq t \leq T} |X(t)|^p \right] \leq H.$$

Proof. To prove this lemma, we can follow the proof in [37, Lemma 4.1]. \square

This result then allows us to establish a strong convergence result for the numerical method.

Theorem 4.1.2. *Assume that f and g satisfy the global Lipschitz condition (4.2).*

Then,

$$\mathbb{E} \left[\sup_{0 \leq t \leq T} |X(t) - x(t)|^2 \right] \leq C\Delta, \quad (4.8)$$

where C is a positive constant independent of Δ .

Proof. It is easy to see that the global Lipschitz condition (4.2) implies the linear growth condition (4.7), so that Lemma 4.1.1 applies. Following the proof in [37, Theorem 4.1] and using Lemma 4.1.1, the required assertion follows. \square

4.2 Hybrid Diffusion Moments

Now we look at a hybrid model based on (3.1)–(3.4), where the number of mRNA molecules is modelled as a Markov process, as in section 3.3, but the evolution

of the protein level in (3.2) and (3.4) is modelled with the CLE regime. We are motivated by the assumption that the protein is typically more abundant than the mRNA—Paszek [43] adopted this approach but used an ODE in the protein regime, as discussed in section 4.3. This gives rise to an Itô SDE, driven by an independent switch, of the form

$$dP^*(t) = (u_P \widehat{r}(t) - d_P P^*(t))dt + \sqrt{u_P \widehat{r}(t)}dW_1(t) - \sqrt{d_P P^*(t)}dW_2(t). \quad (4.9)$$

Here, $\widehat{r}(t)$ denotes the number of mRNA molecules present at time t , when reactions (3.1) and (3.3) are interpreted through the CME, and $P^*(t)$ denotes the number of protein molecules present at time t , when reactions (3.2) and (3.4) are interpreted through the CLE. We use $P^*(t)$ to distinguish this process from the protein level $P(t)$ arising from the full CME regime, as discussed in section 3.3; this emphasises that $P(t)$ and $P^*(t)$ are different stochastic processes; in particular $P(t)$ is discrete valued and $P^*(t)$ is continuous valued. In (4.9), $W_1(t)$ and $W_2(t)$ are mutually independent Brownian motions that are also independent of $\widehat{r}(t)$.

The switch $\widehat{r}(t)$, as mentioned in subsection 4.1.2, can take values in the set of non-negative integers $\{0, 1, 2, \dots\}$, with no upper limit. We let γ_{ij} denote the transition rate for the switch from state i to j so that, for $i \neq j$,

$$\lim_{\Delta \rightarrow 0} \frac{\mathbb{P}\{\widehat{r}(t + \Delta) = j \mid \widehat{r}(t) = i\}}{\Delta} = \gamma_{ij}, \quad (4.10)$$

and $\gamma_{ii} := -\sum_{j \neq i} \gamma_{ij}$ is such that

$$\lim_{\Delta \rightarrow 0} \frac{\mathbb{P}\{\widehat{r}(t + \Delta) = i \mid \widehat{r}(t) = i\} - 1}{\Delta} = \gamma_{ii}. \quad (4.11)$$

For this switch, the only possible change of state is an increase or a decrease by one. The chance of decay is proportional to the current number of molecules, and new molecules are being produced at a rate that is independent of the state. We therefore find that

$$\gamma_{i,i-1} = id_M, \quad \gamma_{i,i+1} = u_M, \quad \gamma_{i,i} = -id_M - u_M, \quad (4.12)$$

and all other transition rates are zero.

Suppose that an initial state $\widehat{r}(0)$ and a fixed time-step size Δ are given, a path from the Markovian switch $\widehat{r}(t)$ can be simulated as follows:

1. Compute: $\text{Up} := u_M \Delta$ and $\text{Down} := \widehat{r}(t) d_M \Delta$.
2. Generate an independent uniform $(0, 1)$ random number ξ .
3. Update state:
 - (a) If $\xi \leq \text{Up}$, then $\widehat{r}(t + \Delta) = \widehat{r}(t) + 1$.
 - (b) If $\text{Up} < \xi \leq \text{Up} + \text{Down}$, then $\widehat{r}(t + \Delta) = \widehat{r}(t) - 1$.
 - (c) If $\xi > \text{Up} + \text{Down}$, then $\widehat{r}(t + \Delta) = \widehat{r}(t)$.
4. Update time: $t = t + \Delta$.
5. Record $(\widehat{r}(t), t)$ as desired. Return to step 1, or else end the simulation.

Now, let \mathcal{L} denote the infinitesimal generator of a Markov process [13, 57].

Then

$$\begin{aligned}
 \mathcal{L}\widehat{r}(t) &= \lim_{\Delta \rightarrow 0} \frac{1}{\Delta} \mathbb{E} [\widehat{r}(t + \Delta) - \widehat{r}(t) \mid \widehat{r}(t) = r] \\
 &= \lim_{\Delta \rightarrow 0} \frac{1}{\Delta} \left[\sum_j j \mathbb{P}(\widehat{r}(t + \Delta) = j \mid \widehat{r}(t) = r) - r \right] \\
 &= \lim_{\Delta \rightarrow 0} \frac{1}{\Delta} \left[\sum_{j \neq r} j (\gamma_{rj} \Delta + o(\Delta)) + r(1 + \gamma_{rr} \Delta + o(\Delta)) - r \right] \\
 &= \lim_{\Delta \rightarrow 0} \frac{1}{\Delta} \left[\sum_{j=0}^{\infty} j \gamma_{rj} \Delta + o(\Delta) \right] \\
 &= \sum_{j=0}^{\infty} j \gamma_{rj}.
 \end{aligned} \tag{4.13}$$

Therefore, by Dynkin's formula [57, Theorem 2.7], using (4.12) and (4.13), we have

$$\begin{aligned}
d\widehat{r}(t) &= (\mathcal{L}\widehat{r}(t))dt + d(\text{mart.}) \\
&= \left(\sum_{j=0}^{\infty} j\gamma_{rj} \right) dt + d(\text{mart.}) \\
&= ((r-1)\gamma_{r,r-1} + r\gamma_{rr} + (r+1)\gamma_{r,r+1})dt + d(\text{mart.}) \\
&= ((r-1)(d_M r) + r(-d_M r - u_M) + (r+1)(u_M))dt + d(\text{mart.}) \\
&= (u_M - d_M r)dt + d(\text{mart.}), \tag{4.14}
\end{aligned}$$

where “mart.” denotes a martingale whose precise form is not relevant to our analysis and it vanishes when we take expectation up to an appropriate stopping time.

To obtain the second moment $\mathbb{E}[P^{*\widehat{r}^2}]$ and correlation $\mathbb{E}[P^{*\widehat{r}}]$, we need to apply the generalised Itô formula Theorem 2.2.2 to the Itô SDE (4.9), which has the drift coefficient $f(t) = u_P \widehat{r}(t) - d_P P^*(t)$ and diffusion coefficient $g(t) = \left[\sqrt{u_P \widehat{r}(t)} \quad -\sqrt{d_P P^*(t)} \right]$. First, let $\widehat{V}(P^*, t, \widehat{r}) = P^* \widehat{r}$. We then have

$$\widehat{V}_t(P^*, t, \widehat{r}) = 0, \quad \widehat{V}_{P^*}(P^*, t, \widehat{r}) = \widehat{r}, \quad \text{and} \quad \widehat{V}_{P^* P^*}(P^*, t, \widehat{r}) = 0.$$

So, by using the operator L in section 2.2,

$$\begin{aligned}
L\widehat{V}(P^*, t, \widehat{r}) &= \widehat{V}_t(P^*, t, \widehat{r}) + \widehat{V}_{P^*}(P^*, t, \widehat{r})f(t) \\
&\quad + \frac{1}{2}\text{trace}[g^T(t)\widehat{V}_{P^* P^*}(P^*, t, \widehat{r})g(t)] + \sum_{j=0}^{\infty} \gamma_{ij}\widehat{V}(P^*, t, j) \\
&= \widehat{r}(u_P \widehat{r} - d_P P^*) \\
&\quad + \gamma_{\widehat{r}, \widehat{r}-1}(P^*(\widehat{r}-1)) + \gamma_{\widehat{r}, \widehat{r}}(P^* \widehat{r}) + \gamma_{\widehat{r}, \widehat{r}+1}(P^*(\widehat{r}+1)) \\
&= (u_P \widehat{r}^2 - d_P P^* \widehat{r}) \\
&\quad + d_M \widehat{r} P^*(\widehat{r}-1) + (-d_M \widehat{r} - u_M)(P^* \widehat{r}) + u_M P^*(\widehat{r}+1) \\
&= u_P \widehat{r}^2 + u_M P^* - (d_M + d_P)P^* \widehat{r}.
\end{aligned}$$

Now applying the generalised Itô formula Theorem 2.2.2, we have

$$d\widehat{V}(P^*, t, \widehat{r}) = L\widehat{V}(P^*, t, \widehat{r})dt + d(\text{mart.}).$$

Therefore,

$$d(P^*\widehat{r}) = (u_P\widehat{r}^2 + u_M P^* - (d_M + d_P)P^*\widehat{r})dt + d(\text{mart.}) \quad (4.15)$$

Now let $\widehat{V}(P^*, t, \widehat{r}) = P^{*2}$. We then have

$$\widehat{V}_t(P^*, t, \widehat{r}) = 0, \quad \widehat{V}_{P^*}(P^*, t, \widehat{r}) = 2P^*, \quad \text{and} \quad \widehat{V}_{P^*P^*}(P^*, t, \widehat{r}) = 2.$$

So,

$$\begin{aligned} L\widehat{V}(P^*, t, \widehat{r}) &= 2P^*(u_P\widehat{r} - d_P P^*) \\ &\quad + \frac{1}{2} \text{trace} \left[\begin{bmatrix} \sqrt{u_P\widehat{r}} \\ -\sqrt{d_P P^*} \end{bmatrix} (2) \begin{bmatrix} \sqrt{u_P\widehat{r}} & -\sqrt{d_P P^*} \end{bmatrix} \right] \\ &\quad + \sum_{j=0}^{\infty} \gamma_{\widehat{r},j} \widehat{V}(P^*, t, j) \\ &= 2P^*(u_P\widehat{r} - d_P P^*) + (u_P\widehat{r} + d_P P^*) + \sum_{j=0}^{\infty} \gamma_{\widehat{r},j} P^{*2}. \end{aligned}$$

Since $\sum_{j=0}^{\infty} \gamma_{\widehat{r},j} P^{*2} = P^{*2} \sum_{j=0}^{\infty} \gamma_{\widehat{r},j} = P^{*2}(0) = 0$, so

$$L\widehat{V}(P^*, t, \widehat{r}) = 2u_P P^*\widehat{r} - 2d_P P^{*2} + u_P\widehat{r} + d_P P^*.$$

Applying the generalised Itô formula, we have

$$d(P^{*2}) = (2u_P P^*\widehat{r} - 2d_P P^{*2} + u_P\widehat{r} + d_P P^*)dt + d(\text{mart.}). \quad (4.16)$$

Thus,

$$\begin{aligned} \frac{d}{dt} \mathbb{E}[P^*(t)] &= u_P \mathbb{E}[\widehat{r}(t)] - d_P \mathbb{E}[P^*(t)], \\ \frac{d}{dt} \mathbb{E}[P^{*2}(t)] &= 2u_P \mathbb{E}[P^*(t)\widehat{r}(t)] - 2d_P \mathbb{E}[P^{*2}(t)] + u_P \mathbb{E}[\widehat{r}(t)] + d_P \mathbb{E}[P^*(t)], \\ \frac{d}{dt} \mathbb{E}[P^*(t)\widehat{r}(t)] &= u_P \mathbb{E}[\widehat{r}^2(t)] + u_M \mathbb{E}[P^*(t)] - (d_M + d_P) \mathbb{E}[P^*(t)\widehat{r}(t)]. \end{aligned}$$

Since the switch $\widehat{r}(t)$ is identical to $M(t)$ from the full CME, we see from (3.13), (3.14), and (3.16) that this hybrid regime exactly reproduces the first two moments.

4.3 Hybrid ODE Moments

Here we consider the case where, as in section 4.2, the number of mRNA molecules is modelled as a Markov process, but now the evolution of the protein level is modelled with the law of mass action. This regime was introduced and studied by Paszek [43]. We have an ODE, driven by an independent switch, of the form

$$d\widehat{P}(t) = (u_P\widehat{r}(t) - d_P\widehat{P}(t))dt, \quad (4.17)$$

where, as in section 4.2, $\widehat{r}(t)$ denotes the number of mRNA molecules when (3.1) and (3.3) are modelled through the CME. We use $\widehat{P}(t)$ to denote the continuous-valued stochastic process that represents the protein level.

Instead of (4.15) and (4.16), we now have

$$d(\widehat{P}\widehat{r}) = (u_P\widehat{r}^2 + u_M\widehat{P} - (d_M + d_P)\widehat{P}\widehat{r})dt + d(\text{mart.})$$

and

$$d(\widehat{P}^2) = (2u_P\widehat{P}\widehat{r} - 2d_P\widehat{P}^2)dt + d(\text{mart.}).$$

In integral form, we have

$$\begin{aligned} \widehat{P}(t) &= \widehat{P}(0) + \int_0^t (u_P\widehat{r}(s) - d_P\widehat{P}(s)) ds, \\ \widehat{P}(t)\widehat{r}(t) &= \widehat{P}(0)\widehat{r}(0) + \int_0^t (u_P\widehat{r}(s)^2 + u_M\widehat{P}(s) - (d_M + d_P)\widehat{P}(s)\widehat{r}(s)) ds \\ &\quad + \int_0^t (\text{mart.}) ds, \\ \text{and } \widehat{P}(t)^2 &= \widehat{P}(0)^2 + \int_0^t (2u_P\widehat{P}(s)\widehat{r}(s) - 2d_P\widehat{P}(s)^2) ds + \int_0^t (\text{mart.}) ds. \end{aligned}$$

Since we consider implicitly up to an appropriate stopping time, then all components are finite, and the expectation exists. Taking the expectation, and then

differentiating, we have

$$\frac{d}{dt}\mathbb{E}[\widehat{P}(t)] = u_P\mathbb{E}[\widehat{r}(t)] - d_P\mathbb{E}[\widehat{P}(t)], \quad (4.18)$$

$$\frac{d}{dt}\mathbb{E}[\widehat{P}^2(t)] = 2u_P\mathbb{E}[\widehat{P}(t)\widehat{r}(t)] - 2d_P\mathbb{E}[\widehat{P}^2(t)], \quad (4.19)$$

$$\frac{d}{dt}\mathbb{E}[\widehat{P}(t)\widehat{r}(t)] = u_P\mathbb{E}[\widehat{r}(t)^2] + u_M\mathbb{E}[\widehat{P}(t)] - (d_M + d_P)\mathbb{E}[\widehat{P}(t)\widehat{r}(t)]. \quad (4.20)$$

Comparing these ODEs to (3.13), (3.14), and (3.16), and recalling that $\widehat{r}(t)$ is identical to $M(t)$, we see that this hybrid model matches the means and correlation of the full CME but does not reproduce the correct second moment.

We next analyse the discrepancy between the second moments in the CME and hybrid switch plus ODE models. First, we show that the error is always one-sided.

Theorem 4.3.1. *For the system (3.1)–(3.4), the variances for the protein arising from the CME and the hybrid model (4.17), $\text{var}[P(t)]$ and $\text{var}[\widehat{P}(t)]$, satisfy $\text{var}[\widehat{P}(t)] \leq \text{var}[P(t)]$ for all time, independently of the rate constants and initial conditions.*

Proof. Letting $y(t) := \text{var}[P(t)] - \text{var}[\widehat{P}(t)]$, because the means match we have $y(t) = \mathbb{E}[P^2(t)] - \mathbb{E}[\widehat{P}^2(t)]$. We then see from (3.14) and (4.19) that

$$\frac{dy(t)}{dt} = u_P\mathbb{E}[M(t)] + d_P\mathbb{E}[P(t)] - 2d_P y(t). \quad (4.21)$$

Now, by construction, the CME does not allow molecules to become negative, so $h(t) := u_P\mathbb{E}[M(t)] + d_P\mathbb{E}[P(t)] \geq 0$. Using an integrating factor in (4.21) we find that

$$y(t) = e^{-2d_P t} \int_0^t e^{2d_P s} h(s) ds,$$

and the result follows. \square

To obtain a precise expression for the error in the variance, we may first solve for $\mathbb{E}[M(t)]$ in (3.12) and then for $\mathbb{E}[P(t)]$ in (3.13). Substituting in (4.21) then

gives

$$\begin{aligned} \text{var}[P(t)] - \text{var}[\widehat{P}(t)] &= \frac{u_M u_P}{d_M d_P} (1 - e^{-d_P t}) \\ &\quad + \left(\mathbb{E}[M(0)] - \frac{u_M}{d_M} \right) \frac{u_P}{d_P - d_M} (e^{-d_M t} - e^{-d_P t}) \\ &\quad + \mathbb{E}[P(0)] (e^{-d_P t} - e^{-2d_P t}), \end{aligned} \quad (4.22)$$

when $d_M \neq d_P$, and

$$\begin{aligned} \text{var}[P(t)] - \text{var}[\widehat{P}(t)] &= \frac{u_M u_P}{d_M d_P} (1 - e^{-d_P t}) \\ &\quad + \left(\mathbb{E}[M(0)] - \frac{u_M}{d_M} \right) u_P t e^{-d_P t} \\ &\quad + \mathbb{E}[P(0)] (e^{-d_P t} - e^{-2d_P t}), \end{aligned} \quad (4.23)$$

when $d_M = d_P$.

We note from (4.22) and (4.23) that $\lim_{t \rightarrow \infty} \text{var}[P(t)] - \text{var}[\widehat{P}(t)] = u_M u_P / (d_M d_P)$, in agreement with the steady state analysis in [43].

To interpret the expressions (4.22) and (4.23) further, we focus on the case where the initial conditions satisfy

$$\mathbb{E}[M(0)] = u_M / d_M \quad \text{and} \quad \mathbb{E}[P(0)] > u_M u_P / (d_M d_P).$$

The error in the variance then simplifies to

$$\text{var}[P(t)] - \text{var}[\widehat{P}(t)] = \frac{u_M u_P}{d_M d_P} (1 - e^{-d_P t}) + \mathbb{E}[P(0)] (e^{-d_P t} - e^{-2d_P t}).$$

This expression has a unique maximum at time

$$t^* := \frac{1}{d_P} \log \left(\frac{2d_M d_P \mathbb{E}[P(0)]}{d_M d_P \mathbb{E}[P(0)] - u_M u_P} \right),$$

and the ratio of the maximum transient error to the steady state error is given by

$$\frac{\text{var}[P(t^*)] - \text{var}[\widehat{P}(t^*)]}{\lim_{t \rightarrow \infty} \text{var}[P(t)] - \text{var}[\widehat{P}(t)]} = \frac{1}{2} + \frac{d_M d_P \mathbb{E}[P(0)]}{4u_M u_P} + \frac{u_M u_P}{4d_M d_P \mathbb{E}[P(0)]}. \quad (4.24)$$

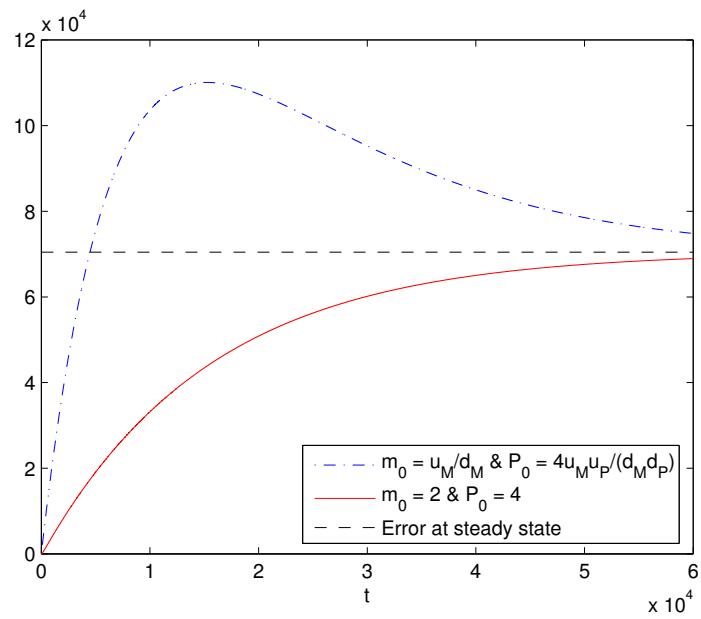


Figure 4.1: Modelling error in the protein variance for the switch plus ODE hybrid (4.17), using rate constants from [47].

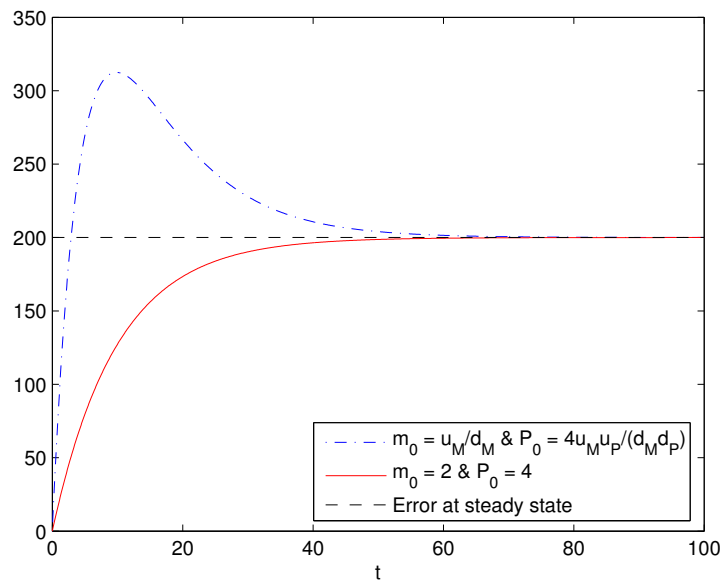


Figure 4.2: Modelling error in the protein variance for the switch plus ODE hybrid (4.17), using rate constants from [44].

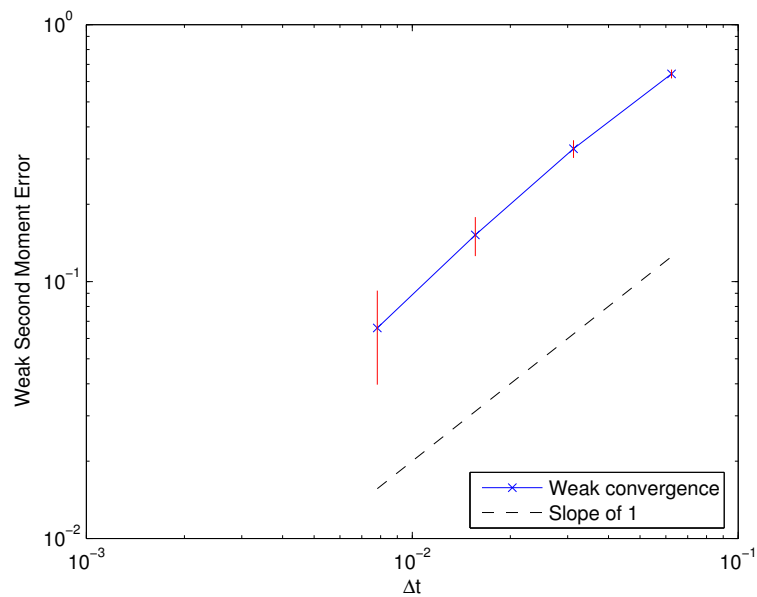


Figure 4.3: Weak convergence in the switch plus CLE framework using rate constants from [47]. Vertical axis measures the error $|\mathbb{E}[P^*(T)^2] - \mathbb{E}[\widehat{P}^*(T)^2]|$, for $T = 5$, where $P^*(t)$ in (4.9) denotes the protein level and $\widehat{P}^*(t)$ is the numerical approximation with the method described in the section 4.1. The quantity $\mathbb{E}[\widehat{P}^*(T)^2]$ is evaluated via Monte Carlo, and 95% confidence intervals are shown as vertical lines.

We see from (4.24) that the transient error in the variance can exceed the steady state error when $\mathbb{E}[P(0)]$ is large. In Figure 4.1, using biologically valid rate constants from [47], which are $u_M = 0.3$, $u_P = 0.1734$, $d_M = 0.0115$, and $d_P = 6.42 \times 10^{-5}$, we show how the error in the variance evolves when $\mathbb{E}[M(0)] = u_M/d_M$ and $\mathbb{E}[P(0)] = 4u_M u_P/(d_M d_P)$. Here the right-hand side of (4.24) is $25/16 \approx 3/2$, and we see that the maximum temporal error is about 50% above the steady state value. We also show the case where $\mathbb{E}[M(0)] = 2$ and $\mathbb{E}[P(0)] = 4$, for which it can be shown that the steady state value is an upper bound for the error. Figure 4.2 shows similar behaviour for rate constants appearing in [44], which are $u_M = 10$, $u_P = 10$, $d_M = 5$, and $d_P = 0.1$.

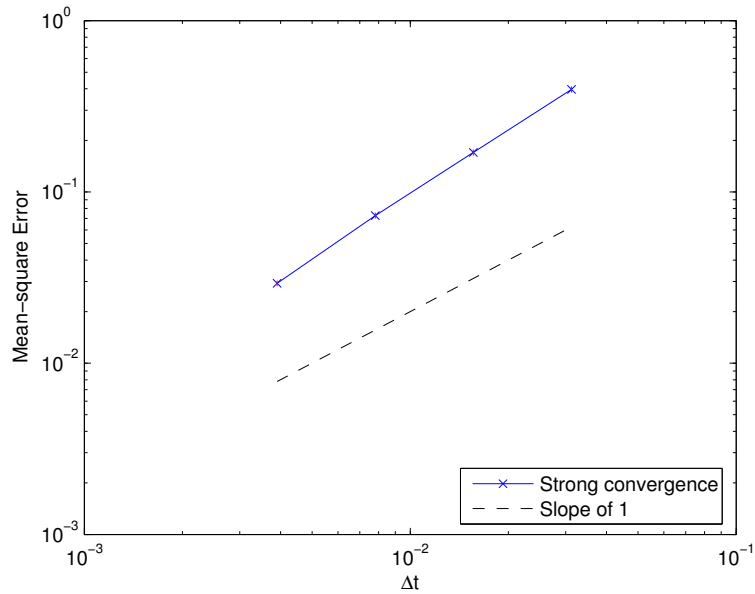


Figure 4.4: As for Figure 4.3 except that the strong error $\mathbb{E}[(P^*(T)^2 - \widehat{P}^*(T)^2)^2]$ is measured. Sample means are shown for 10^4 paths, and 95% confidence intervals are negligible.

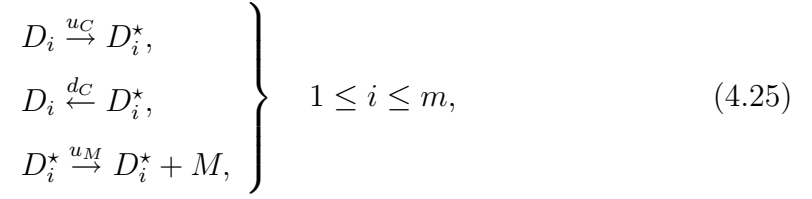
We conclude this section with the results of some numerical experiments to

demonstrate numerically that an Euler–Maruyama based method can successfully integrate the “switch plus CLE” model. For the same parameters as Figure 4.1, we show in Figure 4.3 the absolute error in the sample mean for $P^*(T)^2$, at $T = 5$, arising from the numerical method outlined in the subsection 4.1.4, for $\Delta t = 2^{-4}$, 2^{-5} , 2^{-6} , and 2^{-7} . The time interval $[0, 5]$ is different from that in Figure 4.1 because we are now interested in finite-time convergence of a numerical method and wish to observe asymptotic, small-stepsize behaviour. We used 10^7 sample paths, and all 95% confidence intervals, shown as vertical lines, were less than 0.055. The errors are plotted on a log-log scale, and we see that the results are consistent with a weak order of 1. A least squares fit gave an error behaviour of $\propto \Delta t^{1.1}$ with residual of 0.08. Similarly, we show in Figure 4.4 the second moment of the error in $P^*(T)^2$ for $\Delta t = 32 \times 2^{-10}$, 16×2^{-10} , 8×2^{-10} , and 4×2^{-10} . Here, we used 10^4 sample paths, and all 95% confidence intervals, shown as vertical lines, were less than 0.04. The errors are plotted on a log-log scale, and we see that the results are consistent with a strong order of $\frac{1}{2}$, that is, mean-square of order 1. A least squares fit gave a mean-square error behaviour of $\propto \Delta t^{1.3}$ with residual of 0.03.

4.4 A Related Active/Inactive Gene Model

Raser and O’Shea [44] extended the system (3.1)–(3.4) to the case where genes may alternate between an inactive state, where no mRNA is produced, and an active state. If there are m genes in total, and we let D_i^* denote the active state

of the i th gene, this system may be written as



and



Here, the initial condition for the i th gene must be either $D_i(0) = 0$ and $D_i^*(0) = 1$ (active) or $D_i(0) = 1$ and $D_i^*(0) = 0$ (inactive), and $D_i(t) + D_i^*(t) \equiv 1$ for all time.

Paszek [43] considered a hybrid model with the number of active genes forming a discrete-valued stochastic process in the CME regime, and with the levels of mRNA and protein taking real values. He chose mass action ODEs for the reactions involving mRNA and protein, and, as for the simpler system (3.1)–(3.4), found that this switch plus ODE hybrid gave a steady state variance that does not match the underlying CME. Khanin and Higham [31] showed that a hybrid switch plus diffusion model, where reactions involving mRNA and protein are treated with the CLE approach, reproduces the exact first and second moments for all time. Although the active/inactive model is in a sense more complex than the model in Chapter 3, we emphasise that the number of active genes forms a switch with a finite state space, and hence it is possible to appeal to standard work such as [37] for existence, uniqueness, and simulation theory, and stochastic calculus tools. Our main aim here is to point out that the uniform underestimation of the variance that we established in Theorem 4.3.1 also applies in this case.

Following [31], if we let $\widetilde{M}(t)$ and $\widetilde{P}(t)$ denote the mRNA and protein levels arising from the switch plus ODE model, then $\mathbb{E}[M(t)] = \mathbb{E}[\widetilde{M}(t)]$, $\mathbb{E}[P(t)] = \mathbb{E}[\widetilde{P}(t)]$,

and $\mathbb{E}[P(t)M(t)] = \mathbb{E}[\tilde{P}(t)\tilde{M}(t)]$, and the discrepancy in the second moments

$$y(t) := \begin{bmatrix} \mathbb{E}[M^2(t)] - \mathbb{E}[\tilde{M}^2(t)] \\ \mathbb{E}[P^2(t)] - \mathbb{E}[\tilde{P}^2(t)] \end{bmatrix}$$

satisfies

$$\frac{d}{dt}y(t) = -Ay(t) + g(t),$$

where

$$A = \begin{bmatrix} d_M & 0 \\ 0 & d_P \end{bmatrix} \quad \text{and} \quad g(t) = \begin{bmatrix} u_M \mathbb{E}[r(t)] + d_M \mathbb{E}[M(t)] \\ u_P \mathbb{E}[M(t)] + d_P \mathbb{E}[P(t)] \end{bmatrix}.$$

Here $r(t)$ is a Markovian switch taking values in a finite state space $\{0, 1, 2, \dots, m\}$.

It follows that

$$y(t) = e^{-At} \int_0^t e^{As} g(s) ds.$$

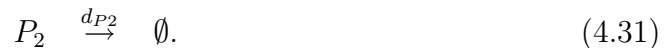
Since $g(t) \geq 0$ for all $t \geq 0$, we conclude that this hybrid model underestimates the true mRNA and protein variances for all time.

We also note that when the reversible reactions $D_i \rightarrow D_i^*$ and $D_i^* \rightarrow D_i$ in (4.25) are fast compared with the other reactions in the system, that is, both $u_C \gg 1$ and $d_C \gg 1$, with all other rate constants of $O(1)$, then we may introduce a slow-fast decoupling along the lines of [7]. Here, we replace $D_i^*(t)$ by its steady state in the D_i - D_i^* subsystem, which effectively reduces (4.25)–(4.28) to the fixed-gene system (3.1)–(3.4) with the amount of gene equal to $\hat{D} = D^*(0)u_C/(u_C + d_C)$. Paszek [43] refers to this as a thermodynamic limit for the full model. Analysis along the lines of that developed above can be used to show that this type of modelling approximation does not have a one-sided effect on the variance; the reduced model may produce a larger or smaller variance depending on the parameter regimes, and the error may change sign over time.

4.5 Tests With a Second Order Reaction

The results in the previous three sections rely on the first order nature of the reactions. In this section we give some brief numerical evidence that the ideas are relevant more generally when the first two moments do not form a closed system of ODEs. To do this, we add a protein dimerization stage to the simple gene regulation models.

For the Thattai–van Oudenaarden model (3.1)–(3.4), we add the three reactions



Here, in (4.29) two protein molecules combine to form a dimer, P_2 , and in (4.30) the process is reversed. In (4.31) the dimer decays. We note that it has been argued that a difference between the monomer and dimer decay rates can explain the phenomenon of “cooperative stability,” which makes a larger spread of protein levels available in vivo [5]. We chose rate constants $u_M = 0.3$, $u_P = 0.17$, $d_M = 0.012$ from [47], $d_P = 0.0007$, $u_{P_2} = 0.025$, $u_{-P_2} = 0.5$ from [6], and $d_{P_2} = 0.00023$ from [5]. Initial conditions were set to $D(0) = 4$, $M(0) = 2$, $P(0) = 4$, and $P_2(0) = 4$, and we record the levels at time $T = 20$.

For the systems given by (3.1)–(3.4) and (4.29)–(4.31), we compared the CME (via Gillespie’s algorithm) with the full CLE, switch plus diffusion, and switch plus ODE regimes using an Euler method with a stepsize of 0.004. (Comparable results were obtained with a larger stepsize.) Table 4.1 summarises the results.

Expected values are estimated with Monte Carlo simulation over 10^5 paths, and approximate 95% confidence intervals are given for each sample mean. In addition to moments and variances for the protein and dimer, we also show their

noise strength, $\text{ns}[P]$ and $\text{ns}[P_2]$, respectively, defined as the ratio of variance to mean.

We see from Table 4.1 that the CME, CLE, and switch plus diffusion regimes give comparable results for moments and noise strengths, whereas the switch plus ODE regime significantly underestimates the variance and noise strength for the protein and dimer.

Table 4.2 shows the results of an analogous experiment where the Raser and O’Shea system (4.25)–(4.28) was augmented with the dimerization reactions (4.29)–(4.31). We used $u_C = 0.1$ and $d_C = 0.1$ from [44], $u_M = 0.3$, $u_P = 0.17$, $d_M = 0.012$ from [47], $d_P = 0.0007$, $u_{P_2} = 0.025$, $u_{-P_2} = 0.5$ from [6], and $d_{P_2} = 0.00023$ from [5]. We see that the conclusions from Table 4.1 continue to hold.

4.6 Summary

The diffusion approximation to a Markov jump process is useful both analytically and computationally. In this chapter we have shown that the existence and uniqueness, and numerical simulation theories for solutions of the hybrid models driven by the independent Markovian switch, in which has the infinite state space, can be established. We also found that

- The switch plus ODE model uniformly underestimates the true protein variance, for all time.
- The steady state error in the protein variance for the switch plus ODE model may significantly underestimate the error in the transient.
- Replacing the switch plus ODE model with a switch plus diffusion model recovers the correct means and variances, for all time.

Table 4.1: Ninety-five percent confidence intervals for Monte Carlo sample mean approximations to the first and second moments, variance and noise strength in the CME, CLE, switch plus diffusion, and switch plus ODE formulations for (3.1)–(3.4) and (4.29)–(4.31). Average number of switches per path was 27.

	CME	CLE	CLE switch	ODE switch
$\mathbb{E}[P]$	[26.23, 26.30]	[26.22, 26.28]	[26.22, 26.29]	[26.54, 26.57]
$\mathbb{E}[P^2]$	[717.87, 721.55]	[717.28, 720.97]	[717.31, 721.00]	[712.22, 714.11]
$\mathbb{E}[P_2]$	[14.58, 14.63]	[14.56, 14.62]	[14.55, 14.61]	[14.42, 14.46]
$\mathbb{E}[P_2^2]$	[231.85, 233.59]	[231.20, 232.89]	[231.19, 232.91]	[217.79, 218.98]
$\text{var}[P]$	[29.60, 30.13]	[29.84, 30.39]	[29.68, 30.22]	[7.97, 8.11]
$\text{ns}[P]$	[1.125, 1.149]	[1.136, 1.159]	[1.129, 1.152]	[0.300, 0.305]
$\text{var}[P_2]$	[19.28, 19.63]	[19.06, 19.40]	[19.30, 19.66]	[9.80, 9.98]
$\text{ns}[P_2]$	[1.317, 1.347]	[1.304, 1.332]	[1.321, 1.351]	[0.678, 0.692]

Table 4.2: Ninety-five percent confidence intervals for Monte Carlo sample mean approximations to the first and second moments, variance and noise strength in the CME, CLE, switch plus diffusion, and switch plus ODE formulations for (4.25)–(4.28) and (4.29)–(4.31). Average number of switches per path was 8.

	CME	CLE	CLE switch	ODE switch
$\mathbb{E}[P]$	[19.65, 19.71]	[19.67, 19.74]	[19.64, 19.70]	[20.04, 20.06]
$\mathbb{E}[P^2]$	[411.30, 413.91]	[412.53, 415.14]	[411.15, 413.75]	[405.42, 406.41]
$\mathbb{E}[P_2]$	[8.47, 8.51]	[8.47, 8.52]	[8.46, 8.50]	[8.31, 8.33]
$\mathbb{E}[P_2^2]$	[83.95, 84.81]	[84.14, 84.99]	[83.62, 84.47]	[71.54, 71.88]
$\text{var}[P]$	[25.10, 25.56]	[25.36, 25.82]	[25.20, 25.66]	[3.98, 4.05]
$\text{ns}[P]$	[1.273, 1.301]	[1.285, 1.312]	[1.279, 1.306]	[0.198, 0.202]
$\text{var}[P_2]$	[12.16, 12.40]	[12.25, 12.49]	[12.04, 12.28]	[2.52, 2.56]
$\text{ns}[P_2]$	[1.428, 1.464]	[1.438, 1.474]	[1.417, 1.452]	[0.302, 0.308]

In addition, we have briefly shown that the hybrid switch plus ODE model, but the switch has the finite state space, arising through the active/inactive model (4.25)–(4.28) underestimates the variances in both mRNA and protein for all time.

We further did numerically experiments when the model (3.1)–(3.4) was combined with the protein dimerization stage (4.29)–(4.31), and found that, at the final time $T = 20$, the switch plus ODE model significantly underestimates the protein and dimer variances and noise strengths.

Chapter 5

Zero, One and Two-switch Models of Gene Regulation

In this chapter we are concerned with the way that intrinsic noise depends on the choice of mathematical model. We look at this issue in two senses.

First, we consider a hierarchy of three continuous-time discrete-space gene regulation models of increasing complexity, where either zero, one or two switches affect the activity of the transcription process. In this case we are able to derive explicit expressions for the first and second moments of the mRNA and protein at steady state and make clear statements about whether switches increase or decrease the noise strength. Second, we look at a simple case of a hybrid version of the two-switch model based on the type of multi-scale approximation that is commonly used to make simulations more tractable. This leads to a stochastic differential equation driven by a Markov chain, and we show that a generalised version of Itô's lemma can be used to analyse first and second moments.

5.1 Gene Regulation Model

Figure 5.1 illustrates a simple schematic of the process by which mRNA is created through transcription and protein is then created through translation. In this setting, as used, for example, in [49], an underlying gene is assumed to be creating mRNA at a constant rate, as mainly discussed in Chapter 4. In the language of chemical kinetics, this gives a first order reaction network [11] that can be interpreted as a Markov jump process, where $\emptyset \rightarrow \text{mRNA}$ represents production from a source, $\text{mRNA} \rightarrow \text{Protein}$ represents catalytic production, and $\text{mRNA} \rightarrow \emptyset$ and $\text{Protein} \rightarrow \emptyset$ represent degradation. This diagram can be written as the reaction network (3.1)–(3.4), which also discussed in Chapter 4.

In Figure 5.2, we follow [44] by supposing that the gene is not always available to create mRNA, but rather switches between an active state and an inactive state. The switch operates independently of the mRNA and protein levels, and we may regard $\text{Active} \leftrightarrow \text{Inactive}$ as reversible isometric reactions. This diagram represents the system discussed in section 4.4 with $m = 1$.

The biological mechanisms through which a gene is activated and deactivated are, of course, extremely complicated, and Figure 5.2 presents a very simplified view. Quoting from the Wikipedia website (June 2010)

http://en.wikipedia.org/wiki/Transcription_factor:

“In the field of molecular biology, a transcription factor (sometimes called a sequence-specific DNA binding factor) is a protein that binds to specific DNA sequences and thereby controls the transfer (or transcription) of genetic information from DNA to RNA. Transcription factors perform this function alone or with other proteins in a complex, by promoting (as an activator), or blocking (as a repressor) the

recruitment of RNA polymerase (the enzyme which performs the transcription of genetic information from DNA to RNA) to specific genes.”

and

“Transcription factors may be activated (or deactivated) through their signal-sensing domain by a number of mechanisms. . .”

This motivates the diagram in Figure 5.3, where gene activity is controlled by a pair of independent switches in AND mode. We may imagine that the gene is active only when a transcription factor (TF) is bound *and* this TF has become active. Either unbinding or deactivation of the TF will cause the rate at which the gene produces mRNA to drop to zero. Although we will use the bound/unbound active/inactive terminology throughout this work, we mention that the model could be motivated from other mechanisms, for example [4, Figure 2] describe a circumstance where two separate “activators” must operate in tandem for transcription to occur.

The AND operation in Figure 5.3 could be regarded as a second order (or bimolecular reaction)—the rate at which mRNA is produced depends on the product of two $\{0, 1\}$ valued species. Generally, second order reaction networks are not amenable to analysis; for example closed form ordinary differential equations cannot be derived for their moments. However, we will show in this chapter that the special structure of this network allows analysis to be performed, both in the discrete-space Markov jump setting, and in the case where a hybrid stochastic differential equation is used.

To simplify the language, we will say that Figures 5.1, 5.2 and 5.3 represent the zero, one and two-switch models, respectively.

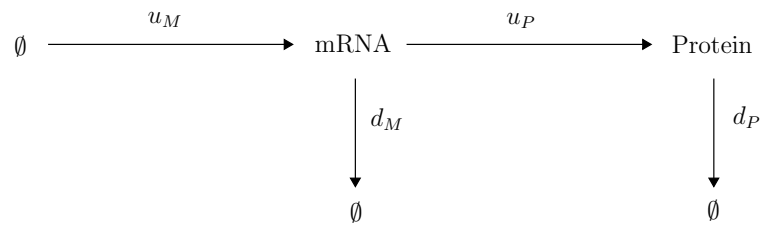


Figure 5.1: Zero-switch gene regulation diagram.

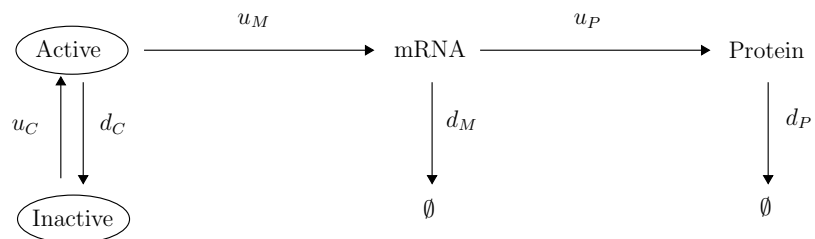


Figure 5.2: One-switch gene regulation diagram.

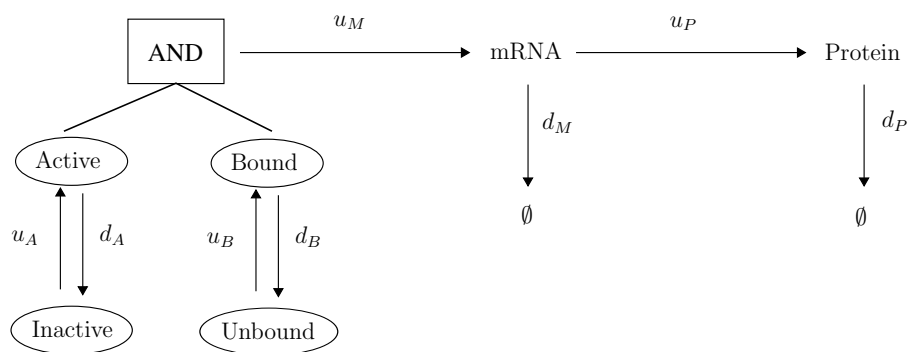


Figure 5.3: Two-switch gene regulation diagram.

5.2 AND Mode: Moments for Two Switches

Moment analysis for the zero-switch model has already been studied in section 3.3 and Chapter 4, and for the one-switch models has also appeared in the literature [31]. In this section, we focus on the new two-switch model. Interpreting Figure 5.3 as a discrete-space, continuous-time Markov jump process, we may introduce scalar processes $A(t)$ and $B(t)$ to record the activation and binding of the TF: at time t ,

- $A(t) = 1$ if the TF is active and $A(t) = 0$ if the TF is inactive,
- $B(t) = 1$ if the TF is bound and $B(t) = 0$ if the TF is unbound.

Given the rate constants u_A, d_A, u_B, d_B , we may characterise these processes by

$$\begin{aligned}\mathbb{P}(A(t + \Delta) = 1 \mid A(t) = 0) &= u_A \Delta + o(\Delta), \\ \mathbb{P}(A(t + \Delta) = 0 \mid A(t) = 1) &= d_A \Delta + o(\Delta), \\ \mathbb{P}(B(t + \Delta) = 1 \mid B(t) = 0) &= u_B \Delta + o(\Delta), \\ \mathbb{P}(B(t + \Delta) = 0 \mid B(t) = 1) &= d_B \Delta + o(\Delta).\end{aligned}$$

Now let $M^\oplus(t)$ denote the level of mRNA for the two-switch model at time t . Since mRNA is produced with rate constant u_M only when the TF is bound and active, we have

$$\mathbb{P}(M^\oplus(t + \Delta) = M^\oplus(t) + 1 \mid A(t), B(t)) = u_M A(t) B(t) \Delta + o(\Delta).$$

This takes the form of a second order reaction—the rate of production of the species $M^\oplus(t)$ depends on the product of the levels of “species” $A(t)$ and $B(t)$. In general, second order systems are not amenable to analysis [17, Section 2.7.B], but we will show in this section that the special form of this system can be exploited. To do this, we introduce artificial species $Y_i(t)$ for $i = 1, 2, 3, 4$, each of which takes values in $\{0, 1\}$. These are defined according to

- $Y_1(t) = 1 \iff A(t) = 0$ and $B(t) = 0$,
- $Y_2(t) = 1 \iff A(t) = 0$ and $B(t) = 1$,
- $Y_3(t) = 1 \iff A(t) = 1$ and $B(t) = 0$, and
- $Y_4(t) = 1 \iff A(t) = 1$ and $B(t) = 1$.

We note that $\sum_{i=1}^4 Y_i(t) = 1$ for all time t . Letting P^\oplus denote the protein level at time t , we may write the overall system in the form



This system now has the form of first-order reaction network. In the terminology of [11], reactions (5.1)–(5.8) are of *conversion* type, (5.9) and (5.10) are of *catalytic production* type, and (5.11) and (5.12) are of *degradation* type. So, we may use the general results in [11] to obtain a closed system of ODEs that express the evolution

of the first and second moments and correlations. In the notation of [11], we have

$$K^S = \mathbf{0} \in \mathbb{R}^{6 \times 6},$$

$$K^d = \begin{bmatrix} 0 & 0 & 0 & 0 & 0 & 0 \\ 0 & 0 & 0 & 0 & 0 & 0 \\ 0 & 0 & 0 & 0 & 0 & 0 \\ 0 & 0 & 0 & 0 & 0 & 0 \\ 0 & 0 & 0 & 0 & d_M & 0 \\ 0 & 0 & 0 & 0 & 0 & d_P \end{bmatrix}, \quad K^{\text{cat}} = \begin{bmatrix} 0 & 0 & 0 & 0 & 0 & 0 \\ 0 & 0 & 0 & 0 & 0 & 0 \\ 0 & 0 & 0 & 0 & 0 & 0 \\ 0 & 0 & 0 & 0 & 0 & 0 \\ 0 & 0 & 0 & u_M & 0 & 0 \\ 0 & 0 & 0 & 0 & u_P & 0 \end{bmatrix},$$

$$K^{\text{con}} = \begin{bmatrix} -(u_A + u_B) & d_B & d_A & 0 & 0 & 0 \\ u_B & -(u_A + d_B) & 0 & d_A & 0 & 0 \\ u_A & 0 & -(u_B + d_A) & d_B & 0 & 0 \\ 0 & u_A & u_B & -(d_A + d_B) & 0 & 0 \\ 0 & 0 & 0 & 0 & 0 & 0 \\ 0 & 0 & 0 & 0 & 0 & 0 \end{bmatrix},$$

$$\mathcal{K} = \begin{bmatrix} -(u_A + u_B) & d_B & d_A & 0 & 0 & 0 \\ u_B & -(u_A + d_B) & 0 & d_A & 0 & 0 \\ u_A & 0 & -(u_B + d_A) & d_B & 0 & 0 \\ 0 & u_A & u_B & -(d_A + d_B) & 0 & 0 \\ 0 & 0 & 0 & u_M & -d_M & 0 \\ 0 & 0 & 0 & 0 & u_P & -d_P \end{bmatrix},$$

and

$$\Gamma(t) = \begin{bmatrix} 0 & 0 & 0 & 0 & 0 & 0 \\ 0 & 0 & 0 & 0 & 0 & 0 \\ 0 & 0 & 0 & 0 & 0 & 0 \\ 0 & 0 & 0 & 0 & 0 & 0 \\ 0 & 0 & 0 & u_M \mathbb{E}[Y_4(t)] & 0 & 0 \\ 0 & 0 & 0 & 0 & u_P \mathbb{E}[M^\oplus(t)] & 0 \end{bmatrix}.$$

For convenience we will drop the time dependent t . Because $\sum_{i=1}^4 Y_i(t) = 1$, $Y_i(t)^2 = Y_i(t)$ and $Y_i(t)Y_j(t) = 0$ for $i \neq j$, we can eliminate some redundancy in order to obtain ODEs for the means

$$\frac{d}{dt} \mathbb{E}[Y_2] = u_B - (u_A + u_B + d_B) \mathbb{E}[Y_2] - u_B \mathbb{E}[Y_3] - (u_B - d_A) \mathbb{E}[Y_4], \quad (5.13)$$

$$\frac{d}{dt} \mathbb{E}[Y_3] = u_A - u_A \mathbb{E}[Y_2] - (u_A + u_B + d_A) \mathbb{E}[Y_3] - (u_A - d_B) \mathbb{E}[Y_4], \quad (5.14)$$

$$\frac{d}{dt} \mathbb{E}[Y_4] = u_A \mathbb{E}[Y_2] + u_B \mathbb{E}[Y_3] - (d_A + d_B) \mathbb{E}[Y_4], \quad (5.15)$$

$$\frac{d}{dt} \mathbb{E}[M^\oplus] = u_M \mathbb{E}[Y_4] - d_M \mathbb{E}[M^\oplus], \quad (5.16)$$

$$\frac{d}{dt} \mathbb{E}[P^\oplus] = u_P \mathbb{E}[M^\oplus] - d_P \mathbb{E}[P^\oplus], \quad (5.17)$$

correlations

$$\begin{aligned} \frac{d}{dt}\mathbb{E}[Y_2M^\oplus] &= u_B\mathbb{E}[M^\oplus] - (u_A + u_B + d_B + d_M)\mathbb{E}[Y_2M^\oplus] \\ &\quad - u_B\mathbb{E}[Y_3M^\oplus] - (u_B - d_A)\mathbb{E}[Y_4M^\oplus], \end{aligned} \quad (5.18)$$

$$\begin{aligned} \frac{d}{dt}\mathbb{E}[Y_2P^\oplus] &= u_B\mathbb{E}[P^\oplus] + u_P\mathbb{E}[Y_2M^\oplus] - (u_A + u_B + d_B + d_P)\mathbb{E}[Y_2P^\oplus] \\ &\quad - u_B\mathbb{E}[Y_3P^\oplus] - (u_B - d_A)\mathbb{E}[Y_4P^\oplus], \end{aligned} \quad (5.19)$$

$$\begin{aligned} \frac{d}{dt}\mathbb{E}[Y_3M^\oplus] &= u_A\mathbb{E}[M^\oplus] - u_A\mathbb{E}[Y_2M^\oplus] - (u_A + u_B + d_A + d_M)\mathbb{E}[Y_3M^\oplus] \\ &\quad - (u_A - d_B)\mathbb{E}[Y_4M^\oplus], \end{aligned} \quad (5.20)$$

$$\begin{aligned} \frac{d}{dt}\mathbb{E}[Y_3P^\oplus] &= u_A\mathbb{E}[P^\oplus] - u_A\mathbb{E}[Y_2P^\oplus] + u_P\mathbb{E}[Y_3M^\oplus] \\ &\quad - (u_A + u_B + d_A + d_P)\mathbb{E}[Y_3P^\oplus] - (u_A - d_B)\mathbb{E}[Y_4P^\oplus], \end{aligned} \quad (5.21)$$

$$\begin{aligned} \frac{d}{dt}\mathbb{E}[Y_4M^\oplus] &= u_A\mathbb{E}[Y_2M^\oplus] + u_B\mathbb{E}[Y_3M^\oplus] + u_M\mathbb{E}[Y_4] \\ &\quad - (d_A + d_B + d_M)\mathbb{E}[Y_4M^\oplus], \end{aligned} \quad (5.22)$$

$$\begin{aligned} \frac{d}{dt}\mathbb{E}[Y_4P^\oplus] &= u_A\mathbb{E}[Y_2P^\oplus] + u_B\mathbb{E}[Y_3P^\oplus] + u_P\mathbb{E}[Y_4M^\oplus] \\ &\quad - (d_A + d_B + d_P)\mathbb{E}[Y_4P^\oplus], \end{aligned} \quad (5.23)$$

$$\frac{d}{dt}\mathbb{E}[M^\oplus P^\oplus] = u_M\mathbb{E}[Y_4P^\oplus] + u_P\mathbb{E}[M^{\oplus 2}] - (d_M + d_P)\mathbb{E}[M^\oplus P^\oplus], \quad (5.24)$$

and second moments

$$\frac{d}{dt}\mathbb{E}[M^{\oplus 2}] = u_M\mathbb{E}[Y_4] + d_M\mathbb{E}[M^\oplus] + 2u_M\mathbb{E}[Y_4M^\oplus] - 2d_M\mathbb{E}[M^{\oplus 2}], \quad (5.25)$$

$$\frac{d}{dt}\mathbb{E}[P^{\oplus 2}] = u_P\mathbb{E}[M^\oplus] + d_P\mathbb{E}[P^\oplus] + 2u_P\mathbb{E}[M^\oplus P^\oplus] - 2d_P\mathbb{E}[P^{\oplus 2}]. \quad (5.26)$$

We are now in a position to compare the noise strengths of the three models.

5.3 Comparing Noise Strengths

5.3.1 One-Switch versus Zero-Switch

The one-switch model in Figure 5.2 may be interpreted as the first order reaction system (4.25)–(4.28), with $m = 1$. A closed, stable linear system of ODEs describing the evolution of the first and second moments and correlations can be found in [31]. As used in section 4.4, using $\widetilde{M}(t)$ and $\widetilde{P}(t)$ to denote the mRNA and protein levels for the one-switch model, in order avoid confusion with $M^\oplus(t)$ and $P^\oplus(t)$ from the two-switch model, we find that the steady state moments have the form

$$\lim_{t \rightarrow \infty} \mathbb{E}[\widetilde{M}(t)] = \frac{u_C u_M}{d_M(u_C + d_C)}, \quad (5.27)$$

$$\lim_{t \rightarrow \infty} \mathbb{E}[\widetilde{P}(t)] = \frac{u_P u_C u_M}{d_P d_M(u_C + d_C)}, \quad (5.28)$$

$$\begin{aligned} \lim_{t \rightarrow \infty} \mathbb{E}[\widetilde{M}(t)^2] &= \frac{u_M u_C}{d_M(u_C + d_C)} + \frac{u_M^2 u_C}{d_M(u_C + d_C)(u_C + d_C + d_M)} \\ &\quad + \frac{u_M^2 u_C^2}{d_M^2(u_C + d_C)(u_C + d_C + d_M)}, \end{aligned} \quad (5.29)$$

$$\begin{aligned} \lim_{t \rightarrow \infty} \mathbb{E}[\widetilde{P}(t)^2] &= \frac{u_P^2 u_M^2 u_C (d_M + u_C)(d_M + u_C + d_C + d_P)}{(u_C + d_C)(u_C + d_C + d_M)(u_C + d_C + d_P)(d_M + d_P)d_M^2 d_P} \\ &\quad + \frac{u_P^2 u_M^2 u_C^2}{(u_C + d_C)(u_C + d_C + d_P)(d_M + d_P)d_M d_P^2} \\ &\quad + \frac{u_P u_M u_C (d_M + d_P + u_P)}{(u_C + d_C)(d_M + d_P)d_M d_P}, \end{aligned} \quad (5.30)$$

$$\begin{aligned} \lim_{t \rightarrow \infty} \mathbb{E}[\widetilde{M}(t)\widetilde{P}(t)] &= \frac{u_M^2 u_C^2 u_P}{(u_C + d_C)(u_C + d_C + d_P)(d_M + d_P)d_M d_P} \\ &\quad + \frac{u_M^2 u_P u_C (u_C + d_M)(u_C + d_C + d_P + d_M)}{(u_C + d_C)(u_C + d_C + d_M)(u_C + d_C + d_P)(d_M + d_P)d_M^2} \\ &\quad + \frac{u_P u_M u_C}{(u_C + d_C)(d_M + d_P)d_M}. \end{aligned} \quad (5.31)$$

Recall that the zero-switch case in Figure 5.1 can be written as the reaction network (3.1)–(3.4), with $\widehat{D}(t) \equiv 1$ for all time. A linear ODE system for the first and second moments of this model was given in section 3.3. We then find the

steady state values

$$\lim_{t \rightarrow \infty} \mathbb{E}[M(t)] = \frac{u_M}{d_M}, \quad (5.32)$$

$$\lim_{t \rightarrow \infty} \mathbb{E}[P(t)] = \frac{u_P u_M}{d_P d_M}, \quad (5.33)$$

$$\lim_{t \rightarrow \infty} \mathbb{E}[M(t)^2] = \frac{u_M}{d_M} + \frac{u_M^2}{d_M^2}, \quad (5.34)$$

$$\lim_{t \rightarrow \infty} \mathbb{E}[P(t)^2] = \frac{u_P^2 u_M^2}{d_P^2 d_M^2} + \frac{u_P u_M (u_P + d_M + d_P)}{(d_M + d_P) d_M d_P}, \quad (5.35)$$

$$\lim_{t \rightarrow \infty} \mathbb{E}[M(t)P(t)] = \frac{u_P u_M}{d_M (d_M + d_P)} + \frac{u_P u_M^2}{d_P d_M^2}. \quad (5.36)$$

Comparing the steady state mRNA and protein variances from the two models, we find that

$$\begin{aligned} \text{var}[\widetilde{M}] - \text{var}[M] &= \frac{u_M u_C (d_M^2 + u_M u_C + d_M u_C + d_M d_C + d_M u_M)}{d_M^2 (u_C + d_C) (u_C + d_C + d_M)} \\ &\quad - \frac{u_M^2 u_C^2}{d_M^2 (u_C + d_C)^2} - \frac{u_M}{d_M} \end{aligned}$$

and

$$\begin{aligned} \text{var}[\widetilde{P}] - \text{var}[P] &= \frac{u_P u_M u_C (d_M + d_P + u_P)}{d_M d_P (u_C + d_C) (d_M + d_P)} \\ &\quad + \frac{u_P^2 u_M^2 u_C^2}{d_M d_P^2 (u_C + d_C) (u_C + d_C + d_P) (d_M + d_P)} \\ &\quad + \frac{u_P^2 u_M^2 u_C (u_C + d_M) (d_M + u_C + d_C + d_P)}{d_M^2 d_P (u_C + d_C) (u_C + d_C + d_M) (u_C + d_C + d_P) (d_M + d_P)} \\ &\quad - \frac{u_P^2 u_M^2 u_C^2}{d_P^2 d_M^2 (u_C + d_C)^2} \\ &\quad - \frac{u_P u_M (d_M + d_P + u_P)}{d_M d_P (d_M + d_P)}. \end{aligned}$$

Now recalling the definition of noise strength in (3.10), some further manipulation of (5.27)–(5.35) shows that

$$\text{ns}[\widetilde{M}] - \text{ns}[M] = \frac{u_M d_C}{(u_C + d_C) (u_C + d_C + d_M)}, \quad (5.37)$$

$$\text{ns}[\widetilde{P}] - \text{ns}[P] = \frac{u_P u_M d_C (u_C + d_C + d_M + d_P)}{(u_C + d_C) (d_P + d_M) (u_C + d_C + d_P) (u_C + d_C + d_M)} \quad (5.38)$$

It is clear that the right hand sides in (5.37) and (5.38) are always positive. Hence, at steady state, *adding a switch always increases the noise strength of both mRNA and protein*, for any choice of rate constants. This happens *despite the fact that the variances may increase or decrease*. For example, using rate constants $u_C = 0.1, d_C = 0.01, u_M = 0.3, d_M = 0.01, u_P = 0.3$ and $d_P = 0.001$, we find

$$\begin{aligned}\text{var}[\widetilde{M}] - \text{var}[M] &= 3.47, \\ \text{var}[\widetilde{P}] - \text{var}[P] &= 3.22 \times 10^4, \\ \text{ns}[\widetilde{M}] - \text{ns}[M] &= 0.2273, \\ \text{ns}[\widetilde{P}] - \text{ns}[P] &= 6.7568,\end{aligned}$$

whereas changing to $d_C = 0.2$ gives

$$\begin{aligned}\text{var}[\widetilde{M}] - \text{var}[M] &= -13.55, \\ \text{var}[\widetilde{P}] - \text{var}[P] &= -1.15 \times 10^5, \\ \text{ns}[\widetilde{M}] - \text{ns}[M] &= 0.6452, \\ \text{ns}[\widetilde{P}] - \text{ns}[P] &= 18.1799.\end{aligned}$$

Figure 5.4 illustrates that the conclusion above concerning the relative noise strengths *does not generalise to all t* . Here, we chose rate constants $u_M = 0.3, d_M = 0.012, u_P = 0.17$ from [47], $d_P = 0.0007$ from [6], $u_C = 0.1$ and $d_C = 0.9$. Deterministic initial conditions were used, with $D^*(0) = 1, M(0) = 20$ and $P(0) = 40$. We see that the time-dependent differences $\text{ns}[\widetilde{M}(t)] - \text{ns}[M(t)]$ and $\text{ns}[\widetilde{P}(t)] - \text{ns}[P(t)]$ can change sign before settling down to a positive value. Figure 5.5 repeats this experiment using rate constants $u_C = 0.1, d_C = 0.1, u_M = 10, d_M = 5, u_P = 10$, and $d_P = 0.1$ from [44] with the same initial conditions as in Figure 5.4. For these rate constants and initial conditions, the difference between noise strengths for mRNA and protein remains positive for all time.

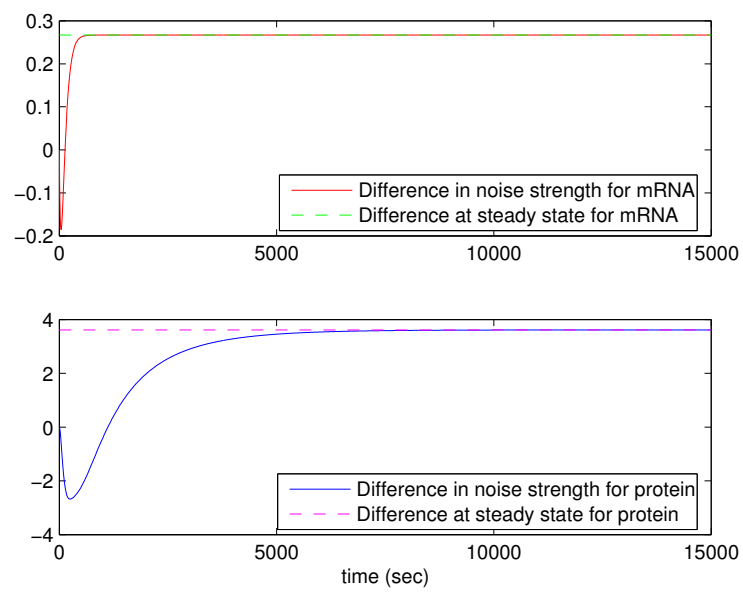


Figure 5.4: Difference in noise strengths between the one and zero-switch models. Upper: mRNA, $ns[\widetilde{M}(t)] - ns[M(t)]$. Lower: protein, $ns[\widetilde{P}(t)] - ns[P(t)]$. The moments were computed by solving the relevant ODEs. Horizontal lines show steady state values from (5.37) and (5.38). Rate constants are taken from [47] and [6].

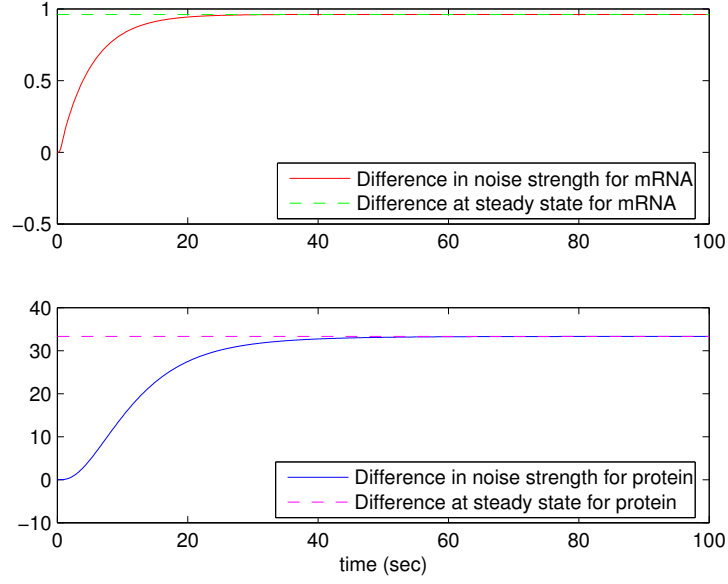


Figure 5.5: As for Figure 5.4 with rate constants taken from [44].

5.3.2 Two-Switch versus Zero-Switch

Equations (5.13)–(5.26) give a stable, linear ODE system for the moments of the two-switch model (5.1)–(5.12). Solving for the steady state and comparing with the result for the zero-switch model (3.1)–(3.4), we find that the difference between mRNA noise strengths is

$$\begin{aligned}
\text{ns}[M^\oplus] - \text{ns}[M] = & \\
& \frac{3d_A d_B u_M (u_A d_M + d_M u_B + u_A u_B) + 2u_A^2 u_M d_B (d_M + d_A)}{(u_A + d_A + d_M)(u_A + d_A)(u_B + d_B)(u_B + d_M + d_B)(u_B + u_A + d_A + d_B + d_M)} \\
& + \frac{2d_A d_B u_M (u_B d_A + u_A d_B) + 2u_B^2 d_A u_M (d_B + d_M)}{(u_A + d_A + d_M)(u_A + d_A)(u_B + d_B)(u_B + d_M + d_B)(u_B + u_A + d_A + d_B + d_M)} \\
& + \frac{d_A u_M d_M (d_M + d_A)}{(u_B + u_A + d_A + d_B + d_M)(u_B + d_M + d_B)(u_A + d_A)(u_A + d_A + d_M)} \\
& + \frac{u_M (u_B^2 d_A + d_B^2 d_M)}{(u_B + u_A + d_A + d_B + d_M)(u_B + d_M + d_B)(u_B + d_B)(u_A + d_A + d_M)} \\
& + \frac{u_M d_B^2 (u_A^2 + d_A^2) + u_A u_M d_B (d_A^2 + d_M^2)}{(u_A + d_A + d_M)(u_A + d_A)(u_B + d_B)(u_B + d_M + d_B)(u_B + u_A + d_A + d_B + d_M)} \\
& + \frac{u_A u_B u_M d_M (d_A + d_B) + u_B d_A u_M (d_B^2 + u_B^2) + u_A^2 u_M d_B (u_B + u_A)}{(u_A + d_A + d_M)(u_A + d_A)(u_B + d_B)(u_B + d_M + d_B)(u_B + u_A + d_A + d_B + d_M)},
\end{aligned}$$

which is clearly positive. The corresponding difference for the protein levels, $\text{ns}[P^\oplus] - \text{ns}[P]$, is too complicated to display, but is also positive for all parameter values.

To illustrate the results, in Figure 5.6, using the same rate constants and initial conditions as Figure 5.4, except $u_A = 0.1, d_A = 0.3, u_B = 0.3, d_B = 0.1$ and $Y_4(0) = 1$, we show the difference between noise strengths for mRNA and protein. The values at steady state are 0.524 and 7.215 for mRNA and protein, respectively, but we see that the difference between noise strengths changes sign over time. Figure 5.7 shows an example where the difference between noise strengths is positive for all time. Here, the difference at steady state is 1.425 and 43.294 for mRNA and protein, respectively. In this case we used the same rate constants and initial conditions as Figure 5.5 together with $u_A = 0.1, d_A = 0.1, u_B = 0.1, d_B = 0.1$ and the deterministic initial condition $Y_4(0) = 1$.

In summary, like the one-switch model, the two-switch model always gives greater noise strengths at steady state than the zero-switch model, but not generally for all time.

5.3.3 One-Switch versus Two-Switch

Using the results from the previous subsections, we can characterise the difference in noise strengths of mRNA and protein between the two-switch model (5.1)–(5.12) and one-switch model (4.25)–(4.28), with $m = 1$. The expressions are too complicated to display, but a key fact is that they contain both negative and positive terms, and their overall sign depends on the model parameters.

To illustrate this, in Figure 5.8 we use the same rate constants and initial conditions as Figure 5.6, with $u_C = u_A$ and $d_C = d_A$. We see that the differences $\text{ns}[\widetilde{M}(t)] - \text{ns}[M^\oplus(t)]$ and $\text{ns}[\widetilde{P}(t)] - \text{ns}[P^\oplus(t)]$ are negative for all time. The steady

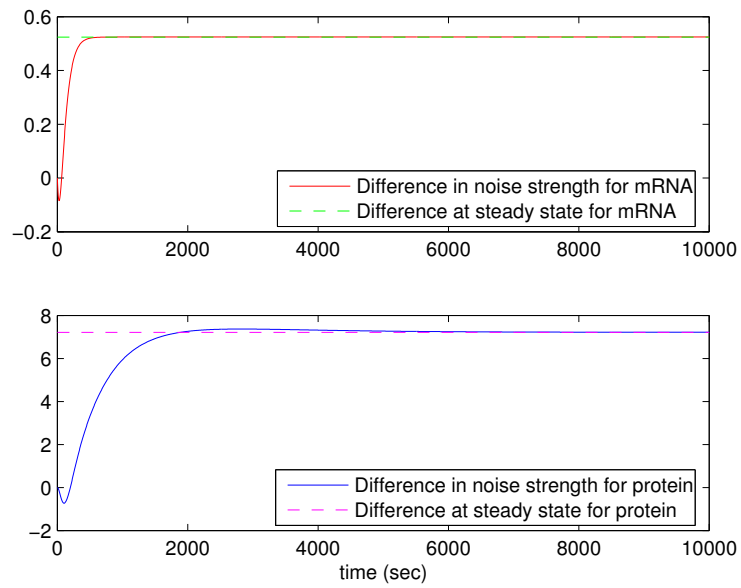


Figure 5.6: As for Figure 5.4, but with the differences between two and zero switches, $\text{ns}[M^\oplus(t)] - \text{ns}[M(t)]$ and $\text{ns}[P^\oplus(t)] - \text{ns}[P(t)]$.

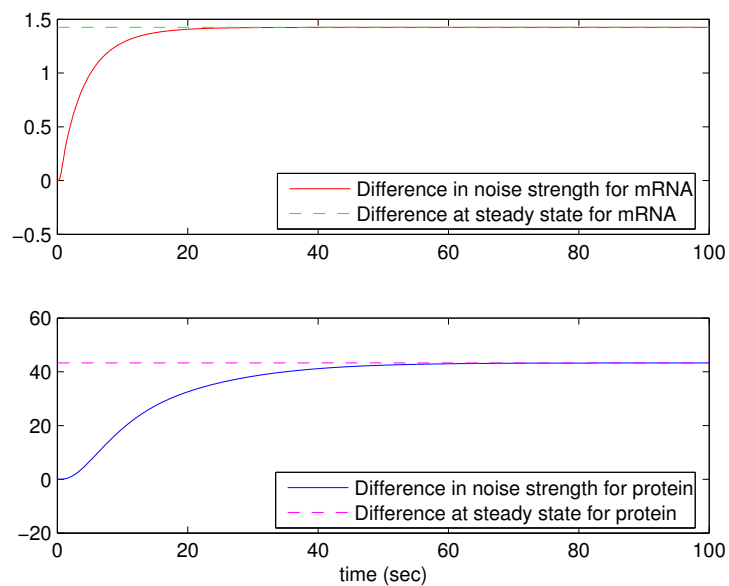


Figure 5.7: As for Figure 5.6 with different parameters and initial conditions.

state differences are -0.022 and -0.314 for mRNA and protein, respectively. On the other hand, Figure 5.9 shows a case where the differences are positive for all time. Here we used the same rate constants and initial conditions as in Figure 5.7 together with $u_C = u_A$ and $d_C = d_A$. In this case, the steady state values are 0.463 and 9.985 for mRNA and protein, respectively. Figure 5.10 shows that the differences in both mRNA and protein can change sign. Here we used the same rate constants and initial conditions as in Figure 5.9, except $u_C = u_A u_B$ and $d_C = u_A d_B + d_A u_B + d_A d_B$. The differences at steady state are -0.064 and -63.833 for mRNA and protein, respectively.

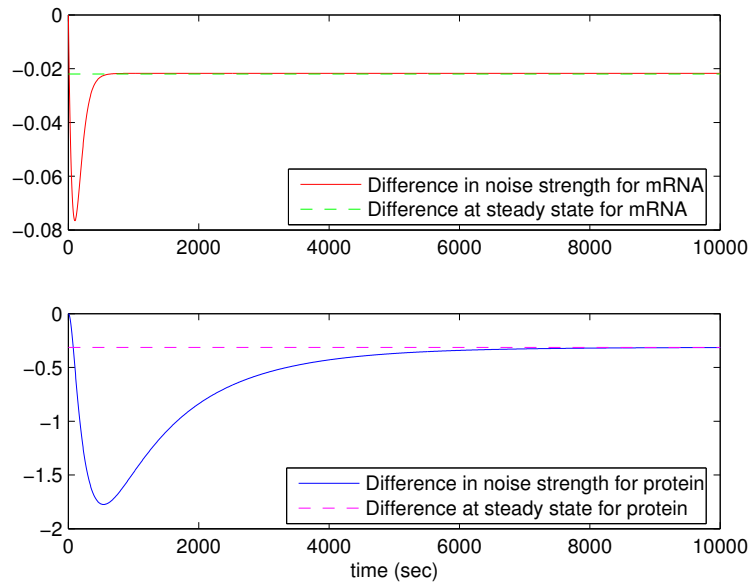


Figure 5.8: Difference in noise strengths between the two and one-switch models.

5.4 Hybrid Moments

As we already showed in Chapter 4, the hybrid SDE setting for the zero, and one-switch models is better at recovering the moments of the underlying exact model

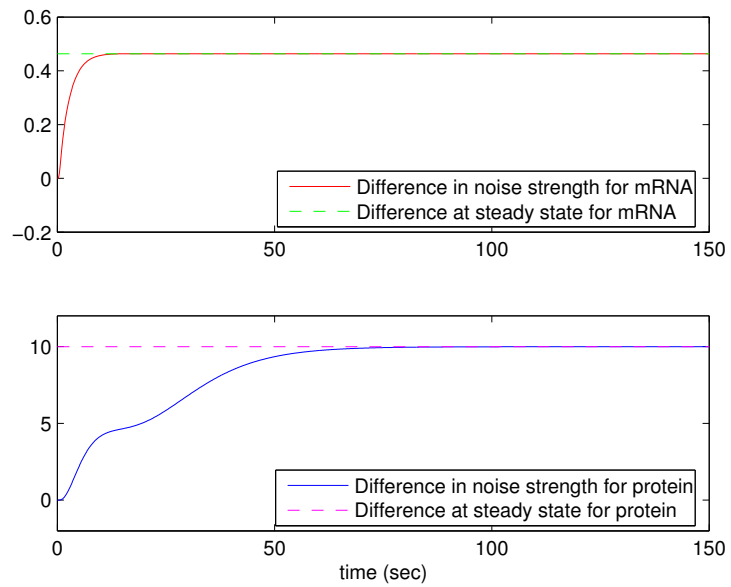


Figure 5.9: As for Figure 5.8 with different parameters.

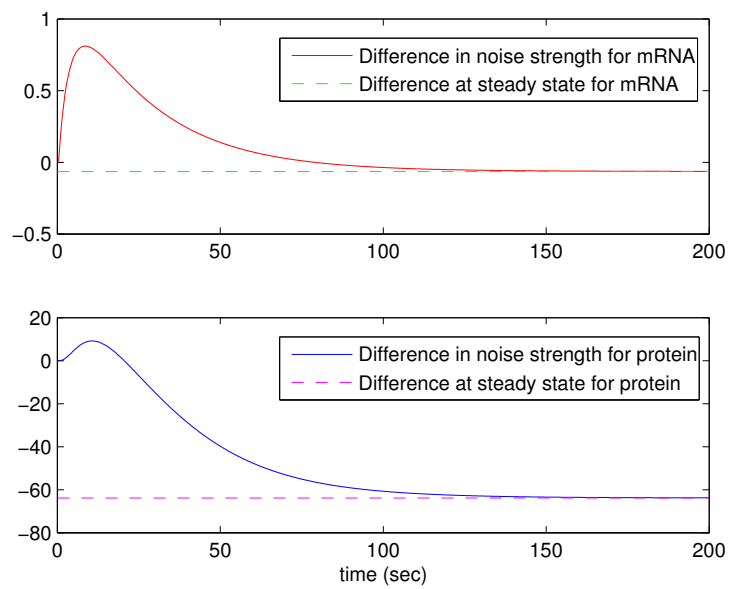


Figure 5.10: As for Figure 5.8 with different parameters.

than the hybrid ODE setting. Our aim in this section is therefore to study hybrid versions of the new two-switch model (5.1)–(5.12). We will show that, as in the Markov jump setting, although it appears to be a second order reaction network, moments of the hybrid SDE model can be analysed.

5.4.1 Hybrid Diffusion Moments

In order to describe the two-switch model as a hybrid SDE, we let $r(t)$ be a Markov switch with state space $\mathbb{S} = \{1, 2, 3, 4\}$ and let γ_{ij} denote the transition rate for the switch from state i to j . Hence, for $i \neq j$,

$$\mathbb{P}(r(t + \Delta) = j \mid r(t) = i) := \gamma_{ij}\Delta + o(\Delta),$$

and $\gamma_{ii} = -\sum_{j \neq i} \gamma_{ij}$ is such that

$$\mathbb{P}(r(t + \Delta) = i \mid r(t) = i) := 1 + \gamma_{ii}\Delta + o(\Delta).$$

Here,

- state 1 corresponds to $A(t) = 0$ and $B(t) = 0$,
- state 2 corresponds to $A(t) = 0$ and $B(t) = 1$,
- state 3 corresponds to $A(t) = 1$ and $B(t) = 0$,
- state 4 corresponds to $A(t) = 1$ and $B(t) = 1$.

For this switch, we move from state 1 to 2 when the TF binds, so we have

$$\gamma_{12} = u_B.$$

Similarly, we move from state 1 to 3 when the TF activates, so that

$$\gamma_{13} = u_A.$$

state		j			
		1	2	3	4
i	1	$-(u_A + u_B)$	u_B	u_A	0
	2	d_B	$-(u_A + d_B)$	0	u_A
	3	d_A	0	$-(d_A + u_B)$	u_B
	4	0	d_A	d_B	$-(d_A + d_B)$

Table 5.1: Transition rates γ_{ij} for switch $r(t)$.

Continuing this manner, we obtain the transition rates in Table 5.1.

Now, let $g(r(t))$ be any function such that

$$g(r(t)) = \begin{cases} 1 & \text{when } r(t) = 4, \\ 0 & \text{otherwise.} \end{cases}$$

We may then express the two-switch model as



Now we look at a hybrid model based on (5.39)–(5.42) where the effect of the TF is modelled as a Markov jump process $r(t)$, and the evolutions of the mRNA and protein levels are modelled with the CLE regime. This gives rise to Itô SDEs driven by an independent switch, of the form

$$dM^\dagger(t) = (u_M g(r) - d_M M^\dagger)dt + \sqrt{u_M g(r)}dW_1 - \sqrt{d_M M^\dagger}dW_2, \quad (5.43)$$

$$dP^\dagger(t) = (u_P M^\dagger - d_P P^\dagger)dt + \sqrt{u_P M^\dagger}dW_3 - \sqrt{d_P P^\dagger}dW_4. \quad (5.44)$$

We use $M^\dagger(t)$ and $P^\dagger(t)$ to distinguish this process from the mRNA and protein levels, $M^\oplus(t)$ and $P^\oplus(t)$, arising from the full CME regime, while $W_i, i = 1, 2, 3, 4$, are mutually independent Brownian motions that are also independent of $r(t)$. Taking expectations, we find immediately that

$$\frac{d}{dt}\mathbb{E}[M^\dagger(t)] = u_M\mathbb{E}[g(r(t))] - d_M\mathbb{E}[M^\dagger(t)], \quad (5.45)$$

$$\frac{d}{dt}\mathbb{E}[P^\dagger(t)] = u_P\mathbb{E}[M^\dagger(t)] - d_P\mathbb{E}[P^\dagger(t)]. \quad (5.46)$$

Since $g(r(t)) \equiv Y_4(t)$, comparing (5.45) and (5.46) with (5.16) and (5.17), we see that this hybrid diffusion regime gives the same first moments as the full Markov jump model.

Applying the generalised Itô formula Theorem 2.2.2 in (5.43) and (5.44), we find

$$\begin{aligned} d(M^{\dagger 2}) &= (2M^\dagger(u_M g(r) - d_M M^\dagger) + (u_M g(r) + d_M M^\dagger)) dt + d(\text{mart.}), \\ d(M^\dagger P^\dagger) &= (P^\dagger(u_M g(r) - d_M M^\dagger) + M^\dagger(u_P M^\dagger - d_P P^\dagger)) dt + d(\text{mart.}), \\ d(P^{\dagger 2}) &= (2P^\dagger(u_P M^\dagger - d_P P^\dagger) + (u_P M^\dagger + d_P P^\dagger)) dt + d(\text{mart.}), \\ d(M^\dagger g(r)) &= (g(r)(u_M g(r) - d_M M^\dagger) + M^\dagger \gamma_{r,4}) dt + d(\text{mart.}), \\ d(P^\dagger g(r)) &= (g(r)(u_P M^\dagger - d_P P^\dagger) + P^\dagger \gamma_{r,4}) dt + d(\text{mart.}), \end{aligned}$$

where “mart.” denotes a martingale. Therefore,

$$\frac{d}{dt}\mathbb{E}[M^{\dagger 2}] = 2u_M\mathbb{E}[M^\dagger g(r)] - 2d_M\mathbb{E}[M^{\dagger 2}] + u_M\mathbb{E}[g(r)] + d_M\mathbb{E}[M^\dagger], \quad (5.47)$$

$$\frac{d}{dt}\mathbb{E}[M^\dagger P^\dagger] = u_M\mathbb{E}[P^\dagger g(r)] - (d_M + d_P)\mathbb{E}[M^\dagger P^\dagger] + u_P\mathbb{E}[M^{\dagger 2}], \quad (5.48)$$

$$\frac{d}{dt}\mathbb{E}[P^{\dagger 2}] = 2u_P\mathbb{E}[M^\dagger P^\dagger] - 2d_P\mathbb{E}[P^{\dagger 2}] + u_P\mathbb{E}[M^\dagger] + d_P\mathbb{E}[P^\dagger], \quad (5.49)$$

$$\frac{d}{dt}\mathbb{E}[M^\dagger g(r)] = u_M\mathbb{E}[g(r)] - d_M\mathbb{E}[M^\dagger g(r)] + \mathbb{E}[M^\dagger \gamma_{r,4}], \quad (5.50)$$

$$\frac{d}{dt}\mathbb{E}[P^\dagger g(r)] = u_P\mathbb{E}[M^\dagger g(r)] - d_P\mathbb{E}[P^\dagger g(r)] + \mathbb{E}[P^\dagger \gamma_{r,4}]. \quad (5.51)$$

(Note that the expectation of the martingale is zero.)

Now, considering the case where $r(t) = 4$, we have that $\gamma_{r,4} = -(d_A + d_B)$, $Y_2 = Y_3 = 0$, $Y_4 = g(r) = 1$, therefore

$$\begin{aligned}\frac{d}{dt}\mathbb{E}[M^\dagger g] &= u_M - d_M\mathbb{E}[M^\dagger] - (d_A + d_B)\mathbb{E}[M^\dagger], \\ \frac{d}{dt}\mathbb{E}[Y_4 M^\oplus] &= u_M - (d_A + d_B + d_M)\mathbb{E}[M^\oplus],\end{aligned}$$

and

$$\begin{aligned}\frac{d}{dt}\mathbb{E}[P^\dagger g] &= u_P\mathbb{E}[M^\dagger] - d_P\mathbb{E}[P^\dagger] - (d_A + d_B)\mathbb{E}[P^\dagger], \\ \frac{d}{dt}\mathbb{E}[Y_4 P^\oplus] &= u_P\mathbb{E}[M^\oplus] - (d_A + d_B + d_P)\mathbb{E}[P^\oplus].\end{aligned}$$

So, letting $r(t) = 4$, $\mathbb{E}[Y_4 M^\oplus]$ satisfies the same ODE as $\mathbb{E}[M^\dagger g]$ and $\mathbb{E}[Y_4 P^\oplus]$ satisfies the same ODE as $\mathbb{E}[P^\dagger g]$. In a similar manner, letting $r(t) = 1, 2, 3$, also gives a perfect match. We conclude that $\mathbb{E}[Y_4 M^\oplus] = \mathbb{E}[M^\dagger g]$ and $\mathbb{E}[Y_4 P^\oplus] = \mathbb{E}[P^\dagger g]$ for all time. By comparing (5.47)–(5.51) and (5.18)–(5.26) we then conclude that the hybrid diffusion regime preserves the second moments and correlations of the full Markov jump model.

5.4.2 Hybrid ODE Moments

In this subsection we consider the case where, as in subsection 5.4.1, the binding/unbinding and activation/deactivation of the TF is modelled as a Markov jump process $r(t)$, but now the evolutions of the mRNA and protein levels are modelled with a simple ODE arising from the law of mass action. In this case, we have two ODEs driven by an independent switch, of the form

$$\begin{aligned}dM^\ddagger(t) &= (u_M g(r(t)) - d_M M^\ddagger(t))dt, \\ dP^\ddagger(t) &= (u_P M^\ddagger(t) - d_P P^\ddagger(t))dt.\end{aligned}$$

We use $M^\ddagger(t)$ and $P^\ddagger(t)$ to denote the continuous-valued stochastic process that represent the mRNA and protein levels in this regime.

Applying the generalised Itô formula Theorem 2.2.2, we find

$$\begin{aligned} d(M^{\dagger 2}) &= (2M^{\dagger}(u_M g(r) - d_M M^{\dagger})) dt + d(\text{mart.}), \\ d(M^{\dagger} P^{\dagger}) &= (P^{\dagger}(u_M g(r) - d_M M^{\dagger}) + M^{\dagger}(u_P M^{\dagger} - d_P P^{\dagger})) dt + d(\text{mart.}), \\ d(P^{\dagger 2}) &= (2P^{\dagger}(u_P M^{\dagger} - d_P P^{\dagger})) dt + d(\text{mart.}), \\ d(M^{\dagger} g(r)) &= (g(r)(u_M g(r) - d_M M^{\dagger}) + M^{\dagger} \gamma_{r,4}) dt + d(\text{mart.}), \\ d(P^{\dagger} g(r)) &= (g(r)(u_P M^{\dagger} - d_P P^{\dagger}) + P^{\dagger} \gamma_{r,4}) dt + d(\text{mart.}). \end{aligned}$$

Therefore,

$$\frac{d}{dt} \mathbb{E}[M^{\dagger}] = u_M \mathbb{E}[g(r)] - d_M \mathbb{E}[M^{\dagger}], \quad (5.52)$$

$$\frac{d}{dt} \mathbb{E}[P^{\dagger}] = u_P \mathbb{E}[M^{\dagger}] - d_P \mathbb{E}[P^{\dagger}], \quad (5.53)$$

$$\frac{d}{dt} \mathbb{E}[M^{\dagger 2}] = 2u_M \mathbb{E}[M^{\dagger} g(r)] - 2d_M \mathbb{E}[M^{\dagger 2}], \quad (5.54)$$

$$\frac{d}{dt} \mathbb{E}[M^{\dagger} P^{\dagger}] = u_M \mathbb{E}[P^{\dagger} g(r)] - (d_M + d_P) \mathbb{E}[M^{\dagger} P^{\dagger}] + u_P \mathbb{E}[M^{\dagger 2}], \quad (5.55)$$

$$\frac{d}{dt} \mathbb{E}[P^{\dagger 2}] = 2u_P \mathbb{E}[M^{\dagger} P^{\dagger}] - 2d_P \mathbb{E}[P^{\dagger 2}], \quad (5.56)$$

$$\frac{d}{dt} \mathbb{E}[M^{\dagger} g(r)] = u_M \mathbb{E}[g(r)] - d_M \mathbb{E}[M^{\dagger} g(r)] + \mathbb{E}[M^{\dagger} \gamma_{r,4}], \quad (5.57)$$

$$\frac{d}{dt} \mathbb{E}[P^{\dagger} g(r)] = u_P \mathbb{E}[M^{\dagger} g(r)] - d_P \mathbb{E}[P^{\dagger} g(r)] + \mathbb{E}[P^{\dagger} \gamma_{r,4}]. \quad (5.58)$$

Comparing (5.16) and (5.17) with (5.52) and (5.53), we see that the hybrid ODE system preserves the first moments. Also, repeating the arguments from subsection 5.4.1, we can show that $\mathbb{E}[M^{\dagger} g(r)]$ matches $\mathbb{E}[Y_4 M^{\oplus}]$, and $\mathbb{E}[P^{\dagger} g(r)]$ matches $\mathbb{E}[Y_4 P^{\oplus}]$. If we then compare (5.25) and (5.54), we see that $\mathbb{E}[M^{\dagger 2}(t)] < \mathbb{E}[M^{\oplus 2}(t)]$ for all $t > 0$. Then from (5.24) and (5.55) we see that $\mathbb{E}[M^{\dagger}(t) P^{\dagger}(t)] < \mathbb{E}[M^{\oplus}(t) P^{\oplus}(t)]$, whence (5.26) and (5.56) allow us to conclude that $\mathbb{E}[P^{\dagger 2}(t)] < \mathbb{E}[P^{\oplus 2}(t)]$.

In summary, for any set of non-zero rate constants, the hybrid ODE model underestimates the second moments of the mRNA and protein and the mRNA-protein correlation, for all time.

5.5 OR Mode

In this section we consider the case where the gene activity in the two-switch model is controlled by a pair of independent switches in OR mode, instead of the AND mode considered previously in this chapter. This could be regarded as a model for the case where two different TFs, *say TFa and TFb*, are present, in which the gene can transcribe when either TFa or TFb is bound to the gene.

We now define, respectively, scalar processes $A^\diamond(t)$ and $B^\diamond(t)$ to record the binding of the TFa and TFb: at time t

- $A^\diamond(t) = 1$ if TFa is bound and $A^\diamond(t) = 0$ if TFa is unbound,
- $B^\diamond(t) = 1$ if TFb is bound and $B^\diamond(t) = 0$ if TFb is unbound,

in which we may characterise these processes by

$$\begin{aligned}\mathbb{P}(A^\diamond(t + \Delta) = 1 \mid A^\diamond(t) = 0) &= u_A \Delta + o(\Delta), \\ \mathbb{P}(A^\diamond(t + \Delta) = 0 \mid A^\diamond(t) = 1) &= d_A \Delta + o(\Delta), \\ \mathbb{P}(B^\diamond(t + \Delta) = 1 \mid B^\diamond(t) = 0) &= u_B \Delta + o(\Delta), \\ \mathbb{P}(B^\diamond(t + \Delta) = 0 \mid B^\diamond(t) = 1) &= d_B \Delta + o(\Delta).\end{aligned}$$

We also define artificial species $Y^\diamond_i(t)$, for $i = 1, 2, 3, 4$, the same way as for the AND mode in section 5.2:

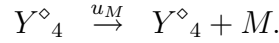
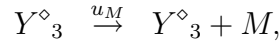
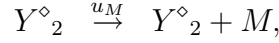
- $Y^\diamond_1(t) = 1 \iff A^\diamond(t) = 0$ and $B^\diamond(t) = 0$,
- $Y^\diamond_2(t) = 1 \iff A^\diamond(t) = 0$ and $B^\diamond(t) = 1$,
- $Y^\diamond_3(t) = 1 \iff A^\diamond(t) = 1$ and $B^\diamond(t) = 0$, and
- $Y^\diamond_4(t) = 1 \iff A^\diamond(t) = 1$ and $B^\diamond(t) = 1$.

Recall that the reaction (5.9) is a catalytic reaction, in which the mRNA is catalysed at a rate proportional to the level of $Y_4(t)$ with rate constant u_M . It will now be more convenient to interpret this as catalytic production from a source with the rate $u_M Y_4(t)$



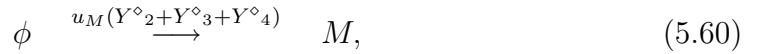
5.5.1 Moments for OR Mode

In OR mode, the gene can transcribe mRNA in the three following ways: when TFa is bound but TFb is unbound, *or* TFa is unbound but TFb is bound, *or* both TFa and TFb are bound. Therefore the three following reactions, *say reactions* j_a, j_b , *and* j_c , summarise the way that mRNA is produced



Replacing the reaction (5.9) in the AND mode with these three reactions, we have the overall system for the OR mode.

Now we introduce catalytic production from a source



and call this reaction *reaction* j_t . Because the reactions j_a, j_b , and j_c are indepen-

dent, we find that in the next infinitesimal time interval $[t, t + dt)$

$$\begin{aligned}
\mathbb{P}(\text{reaction } j_a \text{ or } j_b \text{ or } j_c \text{ happens}) &= \mathbb{P}(\text{reaction } j_a \text{ happens}) \\
&\quad + \mathbb{P}(\text{reaction } j_b \text{ happens}) \\
&\quad + \mathbb{P}(\text{reaction } j_c \text{ happens}) + o(dt) \\
&= u_M Y_2 dt + u_M Y_3 dt + u_M Y_4 dt + o(dt) \\
&= \mathbb{P}(\text{reaction } j_t \text{ happens}) + o(dt).
\end{aligned}$$

Thus, in OR mode, we can use the reaction (5.60) instead of those three reactions, j_a , j_b , and j_c . It follows that the reaction (5.60) is more complicated than the reaction (5.59). Intuitively, the means of mRNA and protein for the OR mode should be larger than those of the AND mode. Do the variances and noise strengths have the same property? To investigate this, we first have to obtain the moments of the OR mode. Using the same trick as in section 5.2, we find that the moments of the OR mode satisfy the same ODEs (5.13)–(5.26) except

$$\begin{aligned}
\frac{d}{dt}\mathbb{E}[M^\diamond] &= u_M(\mathbb{E}[Y^\diamond_2] + \mathbb{E}[Y^\diamond_3] + \mathbb{E}[Y^\diamond_4]) - d_M\mathbb{E}[M^\diamond], \\
\frac{d}{dt}\mathbb{E}[Y^\diamond_2 M^\diamond] &= u_M\mathbb{E}[Y^\diamond_2] + u_B\mathbb{E}[M^\diamond] - (u_A + u_B + d_B + d_M)\mathbb{E}[Y^\diamond_2 M^\diamond] \\
&\quad - u_B\mathbb{E}[Y^\diamond_3 M^\diamond] - (u_B - d_A)\mathbb{E}[Y^\diamond_4 M^\diamond], \\
\frac{d}{dt}\mathbb{E}[Y^\diamond_3 M^\diamond] &= u_M\mathbb{E}[Y^\diamond_3] + u_A\mathbb{E}[M^\diamond] - u_A\mathbb{E}[Y^\diamond_2 M^\diamond] - (u_A - d_B)\mathbb{E}[Y^\diamond_4 M^\diamond] \\
&\quad - (u_A + u_B + d_A + d_M)\mathbb{E}[Y^\diamond_3 M^\diamond], \\
\frac{d}{dt}\mathbb{E}[M^\diamond P^\diamond] &= u_M(\mathbb{E}[Y^\diamond_2 P^\diamond] + \mathbb{E}[Y^\diamond_3 P^\diamond] + \mathbb{E}[Y^\diamond_4 P^\diamond]) + u_P\mathbb{E}[M^\diamond] \\
&\quad - (d_M + d_P)\mathbb{E}[M^\diamond P^\diamond], \\
\frac{d}{dt}\mathbb{E}[M^\diamond{}^2] &= u_M(\mathbb{E}[Y^\diamond_2] + \mathbb{E}[Y^\diamond_3] + \mathbb{E}[Y^\diamond_4]) + d_M\mathbb{E}[M^\diamond] - 2d_M\mathbb{E}[M^\diamond{}^2] \\
&\quad + 2u_M(\mathbb{E}[Y^\diamond_2 M^\diamond] + \mathbb{E}[Y^\diamond_3 M^\diamond] + \mathbb{E}[Y^\diamond_4 M^\diamond]).
\end{aligned}$$

We have used the superscript \diamond to indicate the species for the OR mode.

5.5.2 Mean, Variance, and Noise Strength:

AND Mode versus OR Mode

From the previous subsection we know that the OR mode has the same ODEs for $\mathbb{E}[Y_2]$, $\mathbb{E}[Y_3]$, and $\mathbb{E}[Y_4]$ as the AND mode, and the ODE involves only $\mathbb{E}[Y_2]$, $\mathbb{E}[Y_3]$, and $\mathbb{E}[Y_4]$. Therefore, the means $\mathbb{E}[Y_i]$, $i = 1, 2, 3, 4$, of AND mode are identical to $\mathbb{E}[Y^\diamond_i]$ of OR mode for all time. This is also obvious from first principles—the switches operate independently and their states do not depend on the mode. We now consider

$$\begin{aligned} \frac{d}{dt}(\mathbb{E}[M^\oplus] - \mathbb{E}[M^\diamond]) &= -u_M(\mathbb{E}[Y^\diamond_2] + \mathbb{E}[Y^\diamond_3]) + u_M(\mathbb{E}[Y_4] - \mathbb{E}[Y^\diamond_4]) \\ &\quad - d_M(\mathbb{E}[M^\oplus] - \mathbb{E}[M^\diamond]), \end{aligned}$$

which becomes

$$\mathbb{E}[M^\oplus(t)] - \mathbb{E}[M^\diamond(t)] = e^{-d_M t} \int_0^t h(s) e^{d_M s} ds,$$

where $h(t) := -u_M(\mathbb{E}[Y^\diamond_2] + \mathbb{E}[Y^\diamond_3]) \leq 0$ for all $t \geq 0$. Therefore, the OR mode has a larger mean of mRNA than the AND mode for all time. This leads to the conclusion that the OR mode has also a larger mean of protein than the AND mode for all time as follows:

$$\frac{d}{dt}(\mathbb{E}[P^\oplus] - \mathbb{E}[P^\diamond]) = u_P(\mathbb{E}[M^\oplus] - \mathbb{E}[M^\diamond]) - d_P(\mathbb{E}[P^\oplus] - \mathbb{E}[P^\diamond]),$$

so

$$\mathbb{E}[P^\oplus(t)] - \mathbb{E}[P^\diamond(t)] = e^{-d_P t} \int_0^t u_P(\mathbb{E}[M^\oplus] - \mathbb{E}[M^\diamond]) e^{d_P s} ds \leq 0.$$

Next we investigate the variance and noise strength for the two modes at steady state. Unfortunately the expressions, in terms of the relative rates of transcription, translation and degradation, of the differences of variances in mRNA and protein between OR mode and AND mode have too many terms to display, but there

are very many more positive terms than negative terms. We experimented by numerically varying the rate constants, and found that the variance differences were all positive. Therefore, we expect that, at steady state, the variances in mRNA and protein of OR mode are typically larger than those of AND mode. On the other hand, the differences of noise strengths have lots of negative terms while only few positive terms are present at steady state. We also tried numerically changing the rates, and found unsurprisingly that the differences of noise strengths could change their sign depending on the model parameters. Therefore the OR mode may create more or less noise strength than the AND mode, depending on the rate constants.

Figures 5.11–5.12, and 5.13–5.14, in which the rate constants and initial conditions match those in Figure 5.6, and 5.7, respectively, support the claim. Using the same rate constants as in Figure 5.14 except $d_A = 100$, Figure 5.15 shows that the steady state noise strength differences are not always negative while the steady state variance differences remain positive as shown in Figure 5.16.

5.6 Summary

Some surprisingly simple stochastic models based on Markov jump processes have been successful at describing the level of intrinsic noise in gene regulation activities inside the cell. These models allow the important, and measurable, *noise strength* to be characterised in terms of the relative rates of transcription, translation and degradation.

In this chapter, we introduced a more general model that attempts to account more accurately for the indirect control exerted by a transcription factor. This new model does not fit naturally into the framework of first order reaction networks,

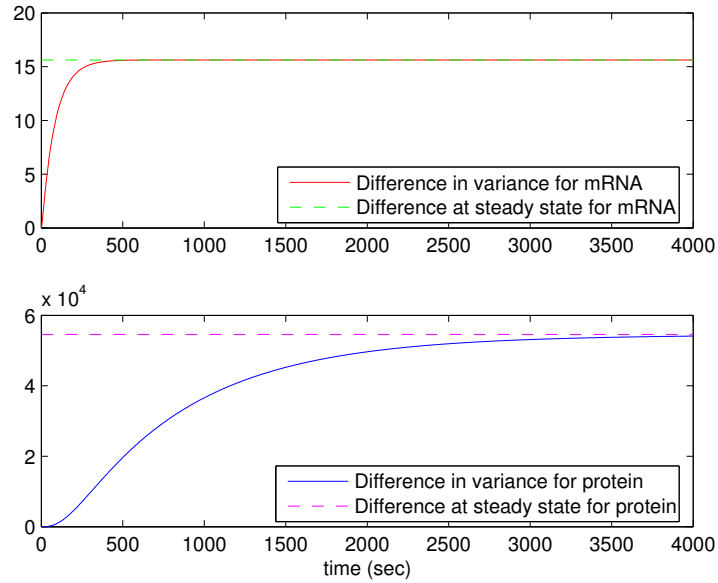


Figure 5.11: Difference in variances between the OR and AND modes, $\text{var}[M^\circ(t)] - \text{var}[M^\oplus(t)]$ and $\text{var}[P^\circ(t)] - \text{var}[P^\oplus(t)]$.

but we showed that its noise strength is amenable to analysis.

Regarding this model as the two-switch successor to previously studied one-switch and zero-switch versions, we were able to show the intuitively reasonable results that, given a set of rate constants,

- the one and two-switch models always have greater *steady state mRNA and protein noise strengths* than the underlying zero-switch model, although the *variances* may be smaller.

So incorporating transcription factor effects in this way leads to a prediction of larger intrinsic noise. However, somewhat less intuitively,

- before equilibrium is reached, the noise strengths of the one and two-switch models may be less than that of the zero-switch model,

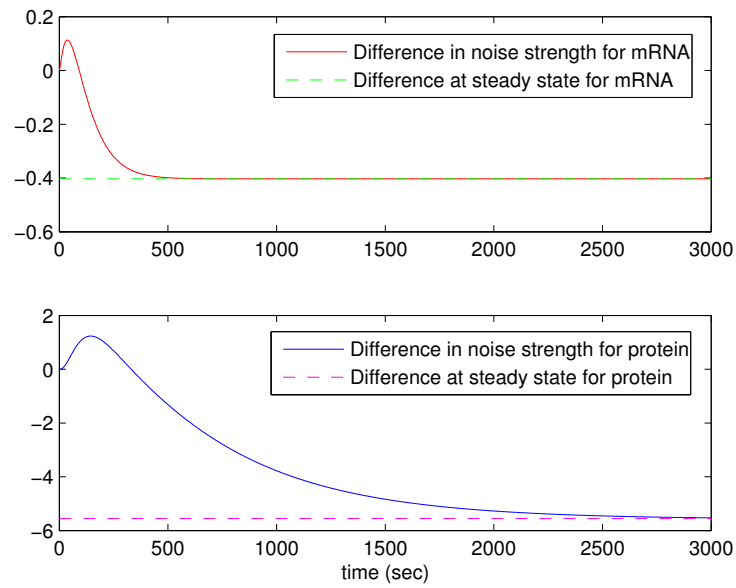


Figure 5.12: Difference in noise strengths between the OR and AND modes, $ns[M^\diamond(t)] - ns[M^\oplus(t)]$ and $ns[P^\diamond(t)] - ns[P^\oplus(t)]$.

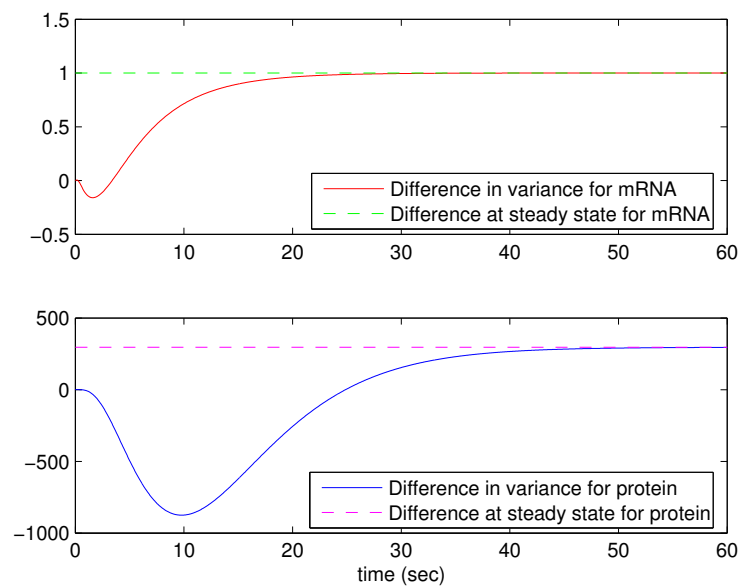


Figure 5.13: As for Figure 5.11 with different parameters.

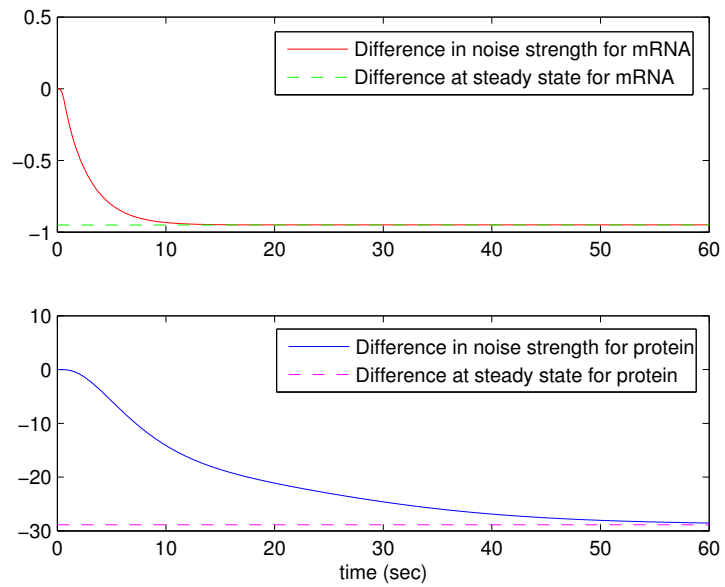


Figure 5.14: As for Figure 5.12 with different parameters.

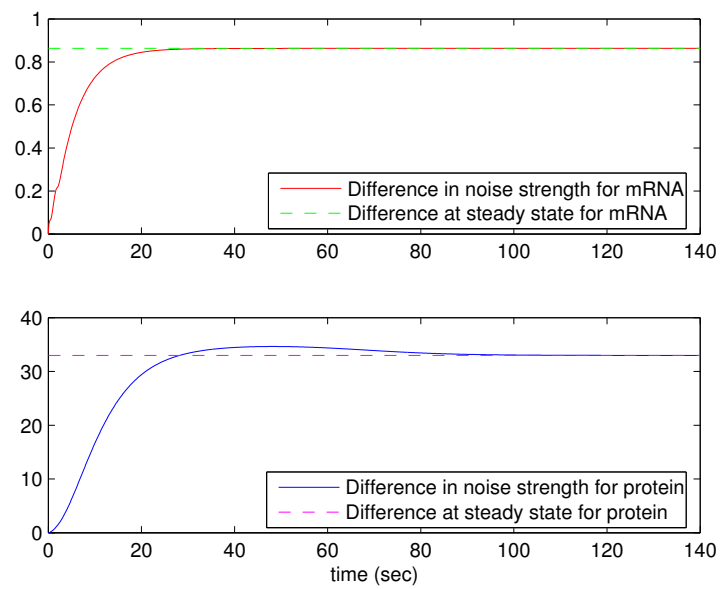


Figure 5.15: As for Figure 5.14 except $d_A = 100$.

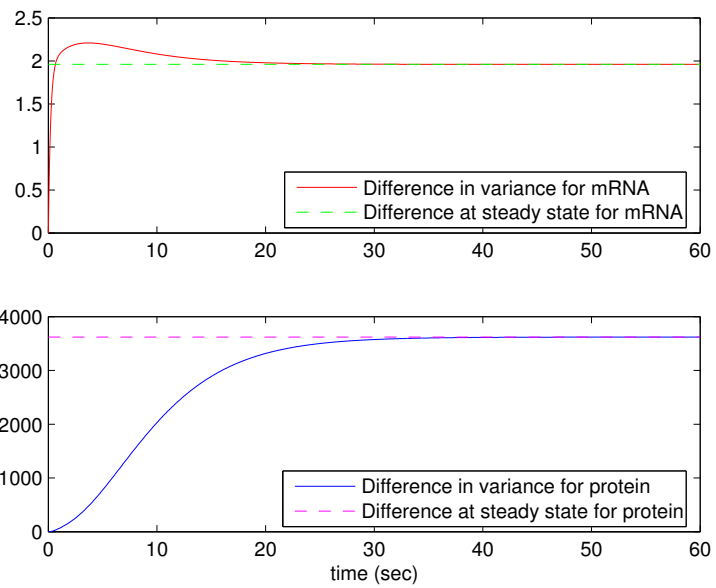


Figure 5.16: As for Figure 5.15 except that the variance errors are measured.

- the two-switch model may be more or less noisy than the one-switch model, depending on the rate constants.

Also,

- according our numerical experiments, depending on the model parameters the OR mode may be more or less noisy than the AND mode.

We also analysed hybrid SDE and ODE approximations to the two-switch model and showed that it is necessary to retain the diffusion term in order to avoid underestimating the mRNA and protein variances and correlation.

Chapter 6

Autoregulation Models for Gene Regulation Networks

In gene regulation, stochastic process using a switch for gene activation and inactivation have been widely studied [31, 43, 44]. The analysis of such stochastic processes is more complex when the state of active/inactive gene is affected by the corresponding protein level [3, 34]. It has been shown that negative feedback of protein reduces protein noise level [34]. There was the same conclusion in [49] when a gene activity is assumed be always active.

In this chapter, which continues the work in Chapter 4, we investigate the effect of protein feedback that enhances its own production. In this case we are able to derive explicit expressions for the first moment of the mRNA and protein for all time. At steady state, we also have explicit expressions for the first and second moments of the mRNA and protein and make the clear statement that positive protein feedback increases the variances and noise strengths of both mRNA and protein.

6.1 Feedback Gene Regulation Model

Figure 6.1 illustrates a schematic of the process that extends the process described in Figure 5.1 by adding a protein feedback loop, enhancing the transcription process.

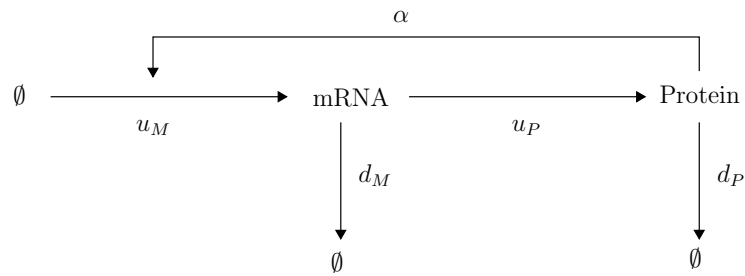


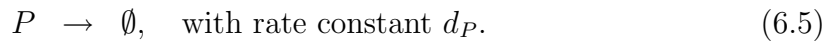
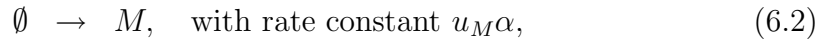
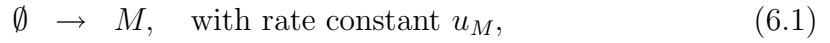
Figure 6.1: Feedback gene regulation diagram.

Here, we assume that an mRNA is produced in two ways; first *production from a source* with rate constant u_M , and second *catalytic production* proportional to the level of protein $P(t)$ with rate constant α . The mRNA can translate a protein with rate constant u_P , and the mRNA and protein can decay with rate constants d_M and d_P respectively.

To simplify the language, we will say that Figure 6.1 represents the feedback model.

6.2 Feedback Moments

We now interpret the feedback model as a Gillespie/population dynamics/Markov jump process, where both species are discrete. This could be written



Here

- (6.1) is production from a source (constant rate),
- (6.2) is catalytic production (rate proportional to level of $P(t)$),
- (6.3) is decay (rate proportional to level of $M(t)$),
- (6.4) is catalytic production (rate proportional to level of $M(t)$),
- (6.5) is decay (rate proportional to level of $P(t)$).

Letting the state vector $X(t) \in \mathbb{R}^2$ be

$$\begin{bmatrix} M^\otimes(t) \\ P^\otimes(t) \end{bmatrix},$$

the stoichiometric vectors are

$$\boldsymbol{\nu}_1 = \begin{bmatrix} 1 \\ 0 \end{bmatrix}, \quad \boldsymbol{\nu}_2 = \begin{bmatrix} 1 \\ 0 \end{bmatrix}, \quad \boldsymbol{\nu}_3 = \begin{bmatrix} -1 \\ 0 \end{bmatrix}, \quad \boldsymbol{\nu}_4 = \begin{bmatrix} 0 \\ 1 \end{bmatrix}, \quad \boldsymbol{\nu}_5 = \begin{bmatrix} 0 \\ -1 \end{bmatrix},$$

with corresponding propensity functions

$$\begin{aligned} a_1(X) &= u_M, \\ a_2(X) &= u_M \alpha X_2(t), \\ a_3(X) &= d_M X_1(t), \\ a_4(X) &= u_P X_1(t), \\ a_5(X) &= d_P X_2(t). \end{aligned}$$

Here we have used the superscript \otimes to denote the species for the feedback model.

We can see that the reactions (6.1)-(6.5) fit into the framework of a *first-order reaction network*. Using the general result of [11], we obtain a closed system of ODEs that describe the evolution of the first and second moments and correlations.

In their notation, we find

$$K^s = \begin{bmatrix} u_M & 0 \\ 0 & 0 \end{bmatrix}, K^d = \begin{bmatrix} d_M & 0 \\ 0 & d_P \end{bmatrix}, K^{\text{cat}} = \begin{bmatrix} 0 & u_M \alpha \\ u_P & 0 \end{bmatrix}, K^{\text{con}} = \begin{bmatrix} 0 & 0 \\ 0 & 0 \end{bmatrix}.$$

We also have

$$\mathcal{K} = \begin{bmatrix} -d_M & u_M \alpha \\ u_P & -d_P \end{bmatrix}, \quad \text{and} \quad \Gamma(t) = \begin{bmatrix} u_M \mathbb{E}[M^\otimes(t)] & u_M(1 + \alpha) \mathbb{E}[P^\otimes(t)] \\ u_P \mathbb{E}[M^\otimes(t)] & 0 \end{bmatrix}.$$

These lead to

$$\frac{d}{dt}\mathbb{E}[M^\otimes(t)] = -d_M\mathbb{E}[M^\otimes(t)] + u_M\alpha\mathbb{E}[P^\otimes(t)] + u_M, \quad (6.6)$$

$$\frac{d}{dt}\mathbb{E}[P^\otimes(t)] = u_P\mathbb{E}[M^\otimes(t)] - d_P\mathbb{E}[P^\otimes(t)], \quad (6.7)$$

$$\begin{aligned} \frac{d}{dt}\mathbb{E}[M^\otimes(t)^2] &= (2u_M + d_M)\mathbb{E}[M^\otimes(t)] + u_M\alpha\mathbb{E}[P^\otimes(t)] - 2d_M\mathbb{E}[M^\otimes(t)^2] \\ &\quad + 2u_M\alpha\mathbb{E}[M^\otimes(t)P^\otimes(t)] + u_M, \end{aligned} \quad (6.8)$$

$$\begin{aligned} \frac{d}{dt}\mathbb{E}[P^\otimes(t)^2] &= u_P\mathbb{E}[M^\otimes(t)] + d_P\mathbb{E}[P^\otimes(t)] + 2u_P\mathbb{E}[M^\otimes(t)P^\otimes(t)] \\ &\quad - 2d_P\mathbb{E}[P^\otimes(t)^2], \end{aligned} \quad (6.9)$$

$$\begin{aligned} \frac{d}{dt}\mathbb{E}[M^\otimes(t)P^\otimes(t)] &= u_M\mathbb{E}[P^\otimes(t)] + u_P\mathbb{E}[M^\otimes(t)^2] - (d_M + d_P)\mathbb{E}[M^\otimes(t)P^\otimes(t)] \\ &\quad + u_M\alpha\mathbb{E}[P^\otimes(t)^2]. \end{aligned} \quad (6.10)$$

Letting

$$z(t) := \begin{bmatrix} \mathbb{E}[M^\otimes(t)] \\ \mathbb{E}[P^\otimes(t)] \\ \mathbb{E}[M^\otimes(t)^2] \\ \mathbb{E}[P^\otimes(t)^2] \\ \mathbb{E}[M^\otimes(t)P^\otimes(t)] \end{bmatrix},$$

we find that

$$\frac{dz(t)}{dt} = Nz(t) + B,$$

where

$$N = \begin{bmatrix} -d_M & u_M\alpha & 0 & 0 & 0 \\ u_P & -d_P & 0 & 0 & 0 \\ 2u_M + d_M & u_M\alpha & -2d_M & 0 & 2u_M\alpha \\ u_P & d_P & 0 & -2d_P & 2u_P \\ 0 & u_M & u_P & u_M\alpha & -(d_M + d_P) \end{bmatrix} \quad \text{and} \quad B = \begin{bmatrix} u_M \\ 0 \\ u_M \\ 0 \\ 0 \end{bmatrix}.$$

6.3 Analytical Solutions

For convenience, we let D and D^2 be the operator notations such that $D \equiv \frac{d}{dt}$ and $D^2 \equiv \frac{d^2}{dt^2}$. Then from (6.6) and (6.7), we have

$$(D + d_M)z_1 - u_M\alpha z_2 = u_M, \quad (6.11)$$

$$u_P z_1 - (D + d_P)z_2 = 0. \quad (6.12)$$

Multiplying both sides of (6.11) by u_P , we have

$$u_P(D + d_M)z_1 - u_M u_P \alpha z_2 = u_M u_P. \quad (6.13)$$

Operating on both sides of (6.12) with $D + d_M$ and then subtracting from (6.13), we find

$$(D^2 + (d_M + d_P)D + (d_M d_P - u_M u_P \alpha)) z_2 = u_M u_P. \quad (6.14)$$

It follows that

$$\begin{aligned} z_2 = & c_1 e^{-\frac{(d_M+d_P)-\sqrt{(d_M-d_P)^2+4u_M u_P \alpha}}{2}t} + c_2 e^{-\frac{(d_M+d_P)+\sqrt{(d_M-d_P)^2+4u_M u_P \alpha}}{2}t} \\ & + \frac{u_M u_P}{d_M d_P - u_M u_P \alpha}, \quad \text{if } u_M u_P \alpha \neq d_M d_P, \end{aligned} \quad (6.15)$$

where c_1 and c_2 are arbitrary constants, is a general solution of (6.14). Substituting (6.15) into (6.12), we have

$$\begin{aligned} z_1 = & c_1 e^{-\frac{(d_M+d_P)-\sqrt{(d_M-d_P)^2+4u_M u_P \alpha}}{2}t} \left[\frac{(d_P - d_M) + \sqrt{(d_M - d_P)^2 + 4u_M u_P \alpha}}{2u_P} \right] \\ & + c_2 e^{-\frac{(d_M+d_P)+\sqrt{(d_M-d_P)^2+4u_M u_P \alpha}}{2}t} \left[\frac{(d_P - d_M) - \sqrt{(d_M - d_P)^2 + 4u_M u_P \alpha}}{2u_P} \right] \\ & + \frac{u_M d_P}{d_M d_P - u_M u_P \alpha}, \quad \text{if } u_M u_P \alpha \neq d_M d_P. \end{aligned}$$

We are now considering the case where $\alpha < d_M d_P / u_M u_P$, so

$$\begin{aligned} 0 < (d_M - d_P)^2 + 4u_M u_P \alpha & < (d_M - d_P)^2 + 4d_M d_P \\ & = (d_M + d_P)^2. \end{aligned}$$

Therefore

$$(d_M + d_P) \pm \sqrt{(d_M - d_P)^2 + 4u_M u_P \alpha} > 0.$$

This leads to

$$\begin{aligned} \mathbb{E}[M^\otimes(t)] = z_1 &\rightarrow \frac{u_M d_P}{d_M d_P - u_M u_P \alpha}, \\ \text{and } \mathbb{E}[P^\otimes(t)] = z_2 &\rightarrow \frac{u_M u_P}{d_M d_P - u_M u_P \alpha}, \quad \text{as } t \rightarrow \infty. \end{aligned}$$

If $\alpha > d_M d_P / u_M u_P$, we then can show that

$$(d_M - d_P)^2 + 4u_M u_P \alpha > (d_M + d_P)^2.$$

Therefore

$$\begin{aligned} (d_P + d_M) - \sqrt{(d_M - d_P)^2 + 4u_M u_P \alpha} &< 0, \\ \text{and } (d_P - d_M) + \sqrt{(d_M - d_P)^2 + 4u_M u_P \alpha} &> 0. \end{aligned}$$

This leads to

$$\begin{aligned} \mathbb{E}[M^\otimes(t)] = z_1 &\rightarrow \infty, \\ \text{and } \mathbb{E}[P^\otimes(t)] = z_2 &\rightarrow \infty, \quad \text{as } t \rightarrow \infty. \end{aligned}$$

If $\alpha = d_M d_P / u_M u_P$, by (6.14), we have

$$(D^2 + (d_M + d_P)D)z_2 = u_M u_P. \quad (6.16)$$

Thus

$$z_2 = c_3 + c_4 e^{-(d_M + d_P)t} + \frac{u_M u_P}{d_M + d_P} t \quad (6.17)$$

is a general solution of (6.16). Substituting (6.17) into (6.12), we find that

$$z_1 = -\frac{c_4 d_M}{u_P} e^{-(d_M + d_P)t} + \frac{u_M d_P}{d_M + d_P} t + \frac{c_3 d_P}{u_P} + \frac{u_M}{d_M + d_P}. \quad (6.18)$$

Therefore, in this case,

$$\begin{aligned} \mathbb{E}[M^\otimes(t)] &= z_1 \rightarrow \infty, \\ \text{and } \mathbb{E}[P^\otimes(t)] &= z_2 \rightarrow \infty, \quad \text{as } t \rightarrow \infty. \end{aligned}$$

In summary, we have shown that the first moments of mRNA and protein of the feedback model are stable if and only if the protein feedback rate, α , is less than $d_M d_P / u_M u_P$.

6.4 Feedback Effect

In this section we consider the effect of increasing the feedback rate. Let $0 \leq \alpha_1 < \alpha_2$, and let $M_{\alpha_i}^\otimes$ and $P_{\alpha_i}^\otimes$ denote the number of mRNA and protein molecules at time t for the feedback model (6.6)-(6.10) with $\alpha = \alpha_i$. We then let

$$y(t) := \begin{bmatrix} \mathbb{E}[M_{\alpha_2}^\otimes(t)] - \mathbb{E}[M_{\alpha_1}^\otimes(t)] \\ \mathbb{E}[P_{\alpha_2}^\otimes(t)] - \mathbb{E}[P_{\alpha_1}^\otimes(t)] \\ \mathbb{E}[M_{\alpha_2}^\otimes(t)^2] - \mathbb{E}[M_{\alpha_1}^\otimes(t)^2] \\ \mathbb{E}[P_{\alpha_2}^\otimes(t)^2] - \mathbb{E}[P_{\alpha_1}^\otimes(t)^2] \\ \mathbb{E}[M_{\alpha_2}^\otimes(t)P_{\alpha_2}^\otimes(t)] - \mathbb{E}[M_{\alpha_1}^\otimes(t)P_{\alpha_1}^\otimes(t)] \end{bmatrix}, \quad \text{with } y(0) = \mathbf{0}.$$

We have

$$\frac{dy_1}{dt} = -d_M y_1 + \alpha_1 u_M y_2 + u_M (\alpha_2 - \alpha_1) \mathbb{E}[P_{\alpha_2}^\otimes], \quad (6.19)$$

$$\frac{dy_2}{dt} = u_P y_1 - d_P y_2, \quad (6.20)$$

$$\begin{aligned} \frac{dy_3}{dt} &= (2u_M + d_M) y_1 + u_M \alpha_1 y_2 - 2d_M y_3 + 2u_M \alpha_1 y_5 \\ &\quad + u_M (\alpha_2 - \alpha_1) \mathbb{E}[P_{\alpha_2}^\otimes] + 2u_M (\alpha_2 - \alpha_1) \mathbb{E}[M_{\alpha_2}^\otimes P_{\alpha_2}^\otimes], \end{aligned} \quad (6.21)$$

$$\frac{dy_4}{dt} = u_P y_1 + d_P y_2 + 2u_P y_5 - 2d_P y_4, \quad (6.22)$$

$$\begin{aligned} \frac{dy_5}{dt} &= u_M y_2 + u_P y_3 - (d_M + d_P) y_5 + u_M \alpha_1 y_4 \\ &\quad + u_M (\alpha_2 - \alpha_1) \mathbb{E}[(P_{\alpha_2}^\otimes)^2]. \end{aligned} \quad (6.23)$$

Now, consider the first two equations (6.19) and (6.20). These involve only y_1 and y_2 . We will show that both components remain nonnegative for all time. Here we suppose that the initial moments for the feedback α_1 and α_2 are the same, so $y(0) = \mathbf{0}$, and also note that $\mathbb{E}[M_{\alpha_i}^{\otimes}(0)] > 0$ and $\mathbb{E}[P_{\alpha_i}^{\otimes}(0)] > 0$. From (6.19), we see that $y_1(t)$ has a positive derivative at $t = 0$, so for a small time interval $(0, \Delta t]$,

$$y_1(t) > 0 \quad \forall t \in (0, \Delta t]. \quad (6.24)$$

Consequently, from (6.20),

$$y_2(t) = e^{-d_P t} \int_0^t u_P y_1(s) e^{d_P s} ds > 0 \quad \forall t \in (0, \Delta t]. \quad (6.25)$$

Now, for any t , suppose the solution is such that $y_1(t) = 0$ and $y_2(t) > 0$. Then from (6.19), we see that $y_1(t)$ has a positive derivative, so the solution returns to the first quadrant. Similarly, if $y_2(t) = 0$ and $y_1(t) > 0$ then from (6.20) we see that the solution also returns to the first quadrant. Finally, if $y_1(t) = y_2(t) = 0$, then both derivatives are nonnegative, so neither component can decrease. Together with (6.24) and (6.25), this allows us to conclude that the solution $y_1(t)$ and $y_2(t)$ remains nonnegative for all time.

We may then rewrite (6.21)–(6.23) as

$$\frac{d}{dt} \begin{bmatrix} y_3 \\ y_4 \\ y_5 \end{bmatrix} = \begin{bmatrix} -2d_M & 0 & 2u_M \alpha_1 \\ 0 & -2d_P & 2u_P \\ u_P & u_M \alpha_1 & -(d_M + d_P) \end{bmatrix} \begin{bmatrix} y_3 \\ y_4 \\ y_5 \end{bmatrix} + h(t),$$

where

$$h(t) := \begin{bmatrix} (2u_M + d_M)y_1 + u_M \alpha_1 y_2 + u_M(\alpha_2 - \alpha_1)\mathbb{E}[P_{\alpha_2}^{\otimes}] + 2u_M(\alpha_2 - \alpha_1)\mathbb{E}[M_{\alpha_2}^{\otimes} P_{\alpha_2}^{\otimes}] \\ u_P y_1 + d_P y_2 \\ u_M y_2 + u_M(\alpha_2 - \alpha_1)\mathbb{E}[(P_{\alpha_2}^{\otimes})^2] \end{bmatrix}$$

is nonnegative. The arguments used above for $y_1(t)$ and $y_2(t)$ may now be applied to $y_3(t)$, $y_4(t)$ and $y_5(t)$ and we conclude that all solution components remain nonnegative.

In summary, we have shown that the first and second moments and correlations of mRNA and protein increase monotonically in α . In other words, for any choice of model parameters, increasing the protein feedback rate cannot decrease the moments of mRNA or protein.

Now, let us consider differences of variances of mRNA and protein between the feedback rates α_1 and α_2 where $0 \leq \alpha_1 < \alpha_2$. We let

$$v := \begin{bmatrix} \text{var}[M_{\alpha_2}^{\otimes}] - \text{var}[M_{\alpha_1}^{\otimes}] \\ \text{var}[P_{\alpha_2}^{\otimes}] - \text{var}[P_{\alpha_1}^{\otimes}] \end{bmatrix}.$$

Then

$$\begin{aligned} \frac{dv_1}{dt} &= \frac{d}{dt} \text{var}[M_{\alpha_2}^{\otimes}] - \frac{d}{dt} \text{var}[M_{\alpha_1}^{\otimes}] \\ &= \frac{d}{dt} (\mathbb{E}[(M_{\alpha_2}^{\otimes})^2] - (\mathbb{E}[M_{\alpha_2}^{\otimes}])^2) - \frac{d}{dt} (\mathbb{E}[M_{\alpha_1}^{\otimes}] - (\mathbb{E}[M_{\alpha_1}^{\otimes}])^2) \\ &= d_M y_1 + u_M (\alpha_2 \mathbb{E}[P_{\alpha_2}^{\otimes}] - \alpha_1 \mathbb{E}[P_{\alpha_1}^{\otimes}]) - 2d_M v_1 \\ &\quad + 2u_M (\alpha_2 \mathbb{E}[M_{\alpha_2}^{\otimes} P_{\alpha_2}^{\otimes}] - \alpha_1 \mathbb{E}[M_{\alpha_1}^{\otimes} P_{\alpha_1}^{\otimes}]) \\ &\quad - 2u_M (\alpha_2 \mathbb{E}[M_{\alpha_2}^{\otimes}] \mathbb{E}[P_{\alpha_2}^{\otimes}] - \alpha_1 \mathbb{E}[M_{\alpha_1}^{\otimes}] \mathbb{E}[P_{\alpha_1}^{\otimes}]). \end{aligned}$$

So,

$$v_1 = e^{-2d_M t} \int_0^t h_4(s) e^{2d_M s} ds,$$

where

$$\begin{aligned} h_4(t) &:= u_M (\alpha_2 \mathbb{E}[P_{\alpha_2}^{\otimes}] - \alpha_1 \mathbb{E}[P_{\alpha_1}^{\otimes}]) + 2u_M (\alpha_2 \mathbb{E}[M_{\alpha_2}^{\otimes} P_{\alpha_2}^{\otimes}] - \alpha_1 \mathbb{E}[M_{\alpha_1}^{\otimes} P_{\alpha_1}^{\otimes}]) \\ &\quad - 2u_M (\alpha_2 \mathbb{E}[M_{\alpha_2}^{\otimes}] \mathbb{E}[P_{\alpha_2}^{\otimes}] - \alpha_1 \mathbb{E}[M_{\alpha_1}^{\otimes}] \mathbb{E}[P_{\alpha_1}^{\otimes}]) + d_M y_1. \end{aligned}$$

Hence v_1 can be either positive or negative because h_4 contains both positive and negative terms.

Next, we consider

$$\begin{aligned}
\frac{dv_2}{dt} &= \frac{d}{dt}\text{var}[P_{\alpha_2}^{\otimes}] - \frac{d}{dt}\text{var}[P_{\alpha_1}^{\otimes}] \\
&= \frac{d}{dt}(\mathbb{E}[(P_{\alpha_2}^{\otimes})^2] - (\mathbb{E}[P_{\alpha_2}^{\otimes}])^2) - \frac{d}{dt}(\mathbb{E}[P_{\alpha_1}^{\otimes}] - (\mathbb{E}[P_{\alpha_1}^{\otimes}])^2) \\
&= u_P y_1 + d_P y_2 + 2u_P y_5 - 2d_P v_2 - 2u_P(\mathbb{E}[M_{\alpha_2}^{\otimes}]\mathbb{E}[P_{\alpha_2}^{\otimes}] - \mathbb{E}[M_{\alpha_1}^{\otimes}]\mathbb{E}[P_{\alpha_1}^{\otimes}]).
\end{aligned}$$

Therefore

$$v_2 = e^{-2d_P t} \int_0^t h_5(s) e^{2d_P s} ds,$$

where $h_5(t) := u_P y_1 + d_P y_2 + 2u_P y_5 - 2u_P(\mathbb{E}[M_{\alpha_2}^{\otimes}]\mathbb{E}[P_{\alpha_2}^{\otimes}] - \mathbb{E}[M_{\alpha_1}^{\otimes}]\mathbb{E}[P_{\alpha_1}^{\otimes}])$. Hence v_2 can also be either positive or negative because h_5 contains both positive and negative terms.

Thus, we cannot show explicitly that for all sets of parameter values the mRNA and protein variances increase with the feedback rate. However, we observed such monotonicity in all our simulations that used biologically realistic parameters; see, for example, Figures 6.2–6.5.

Figures 6.2 and 6.3 show the differences of variances in mRNA and protein, respectively, for various feedback rates by using an ODE solver on (6.6)–(6.10). Initial conditions and rate constants were as follows: $M^{\otimes}(0) = 2$, $P^{\otimes}(0) = 4$ and $u_M = 0.3$, $d_M = 0.012$, $u_P = 0.17$ from [47] and $d_P = 0.0007$ from [6]. We set the feedback rates as $\alpha_i = id_M d_P / 5u_M u_P$ for $i = 0, 1, 2, 3, 4$. The horizontal lines are steady state values computed from (6.30) and (6.31). We see that the variances increase monotonically in α . Similarly, Figures 6.4 and 6.5 show the differences of the variances in mRNA and protein with rate constants taken from [44]: $u_M = 10$, $d_M = 5$, $u_P = 10$, and $d_P = 0.1$.

Figures 6.6 and 6.7 show the differences of noise strengths in mRNA and protein, respectively, for the same feedback rates, initial conditions, and rate constants as in Figure 6.2. We see that the noise strengths of the bigger feedback rate models

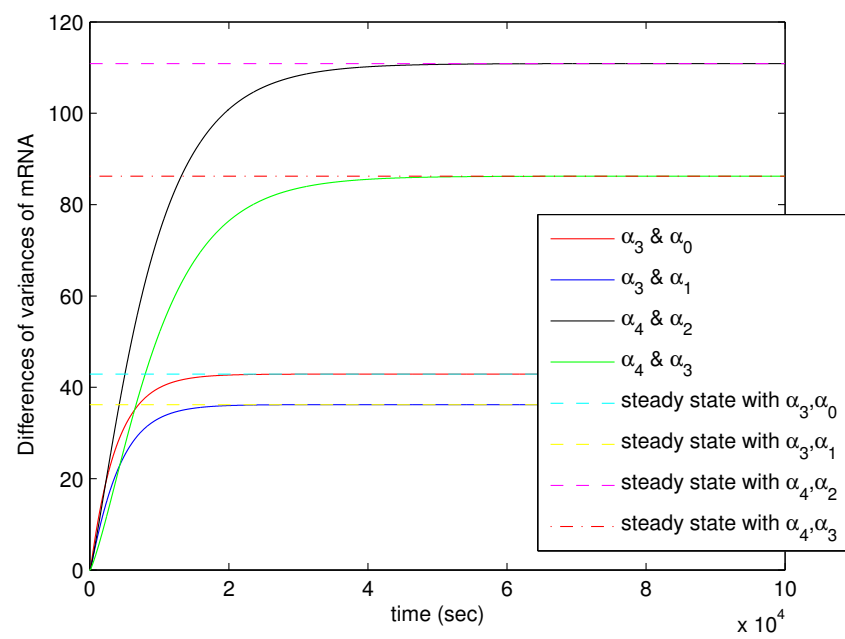


Figure 6.2: Differences of variances in mRNA for the feedback model. Using feedback rates $\alpha_i = id_M d_P / 5u_M u_P$ for $i = 0, 1, 2, 3, 4$.

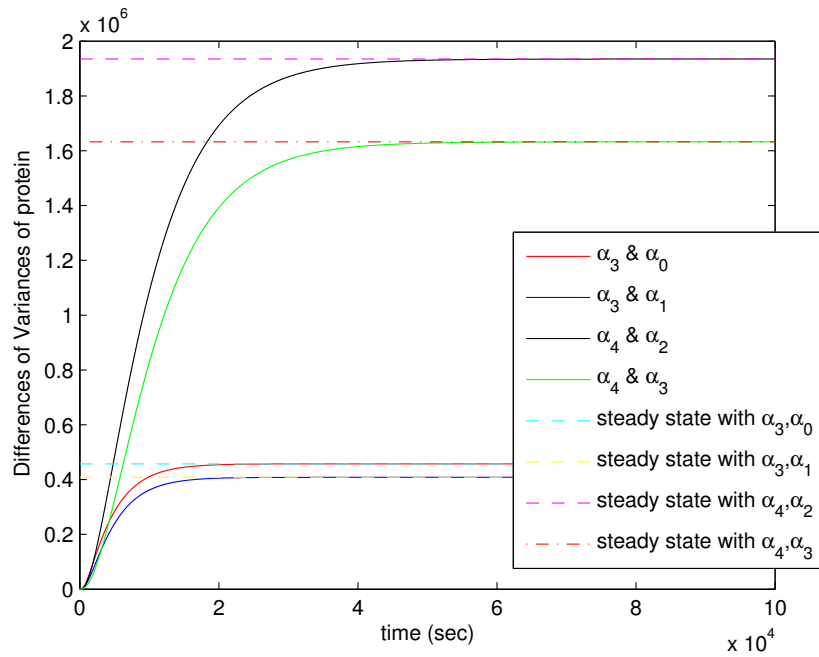


Figure 6.3: Differences of variances in protein for the feedback model. Using feedback rates $\alpha_i = id_M d_P / 5u_M u_P$ for $i = 0, 1, 2, 3, 4$.

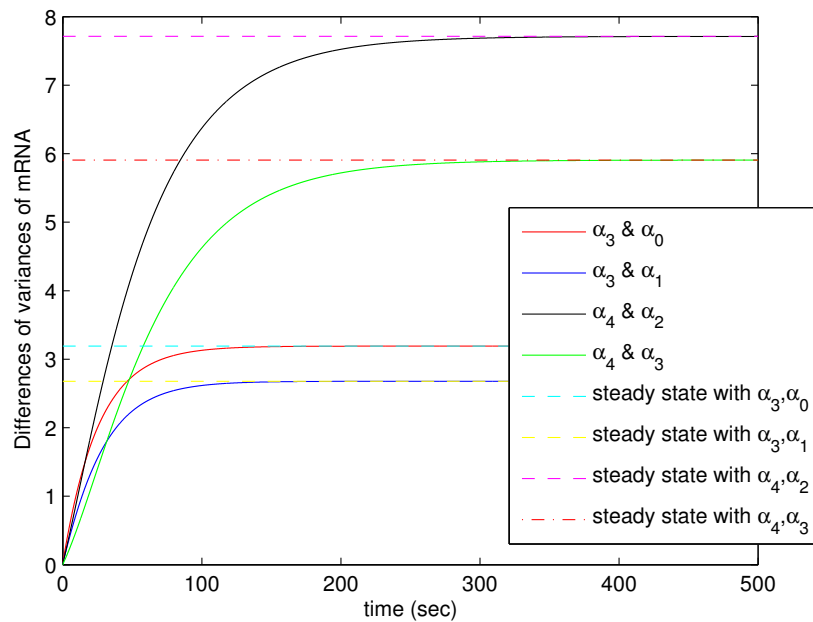


Figure 6.4: The same as Figure 6.2 with different rate constants.

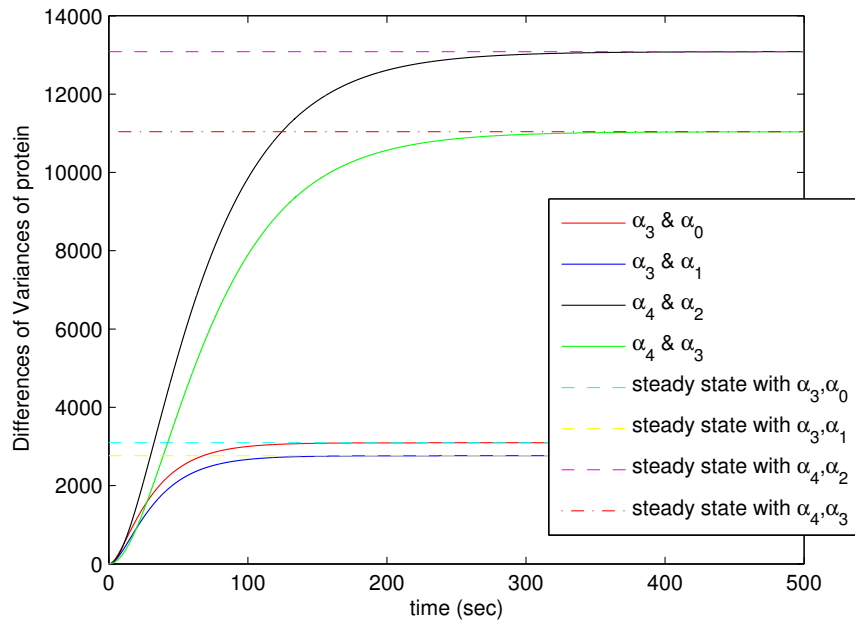


Figure 6.5: The same as Figure 6.3 with different rate constants.

are always larger than those with the smaller feedback rates for all time, whereas the horizontal lines are steady state values computed from (6.32) and (6.33). Figures 6.8 and 6.9, for which the rate constants used were the same as in Figure 6.4, show similar behaviour.

Note that,

- Using the default of relative and absolute error tolerances, *RelTol* and *AbsTol*, of the ODE solver *ode15s* gave qualitatively incorrect results. This was fixed by setting more stringent *RelTol* and *AbsTol* values.

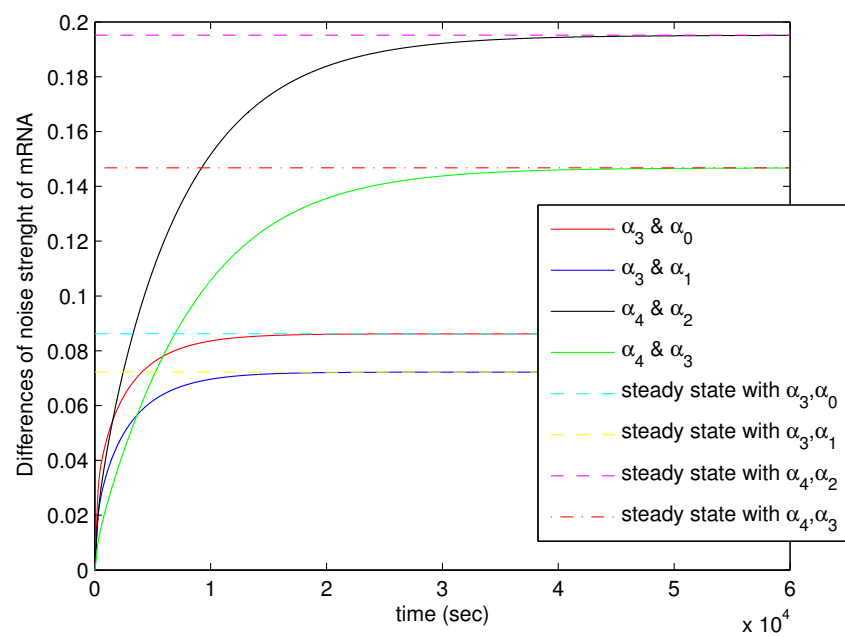


Figure 6.6: Differences of noise strengths in mRNA for the feedback model. Using feedback rates $\alpha_i = id_M d_P / 5u_M u_P$ for $i = 0, 1, 2, 3, 4$.

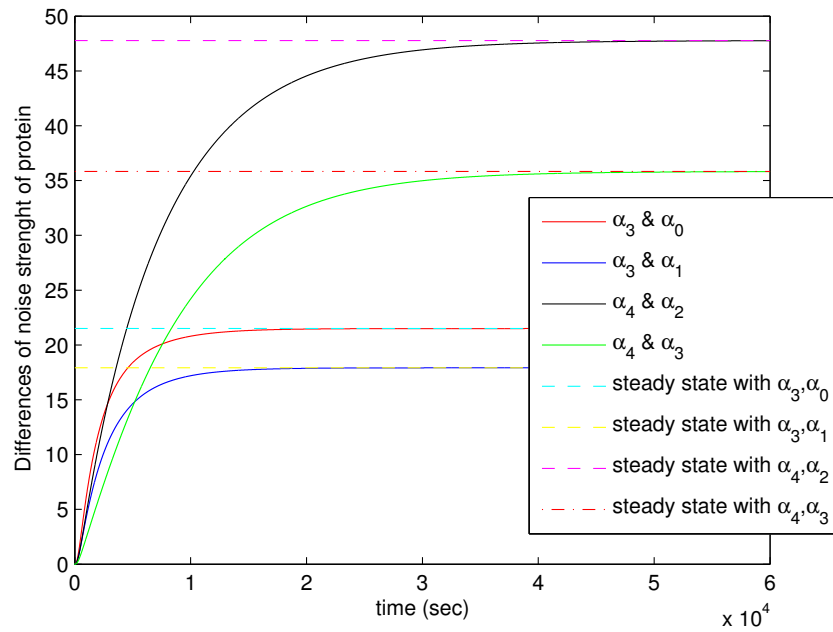


Figure 6.7: Differences of noise strengths in protein for the feedback model. Using feedback rates $\alpha_i = id_M d_P / 5u_M u_P$ for $i = 0, 1, 2, 3, 4$.

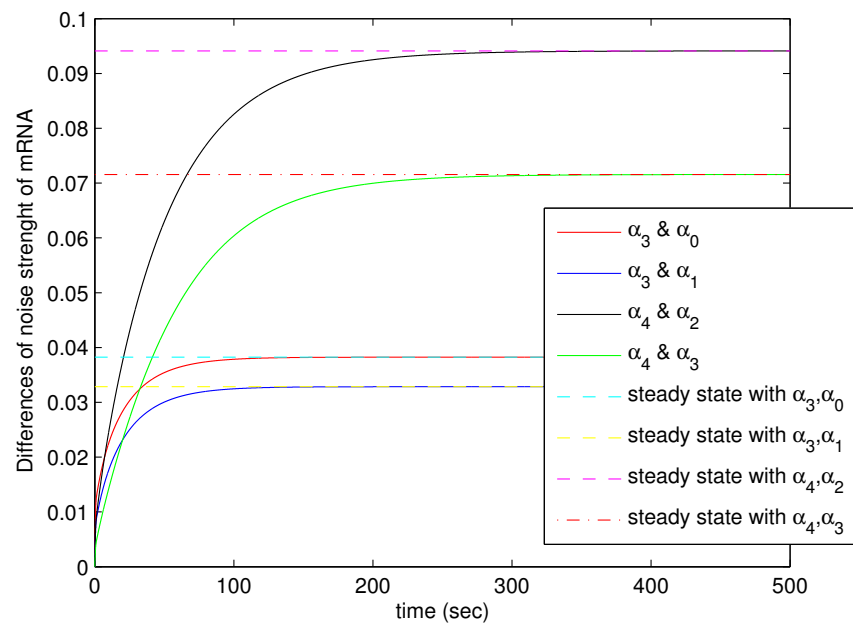


Figure 6.8: The same as Figure 6.6 with different rate constants.

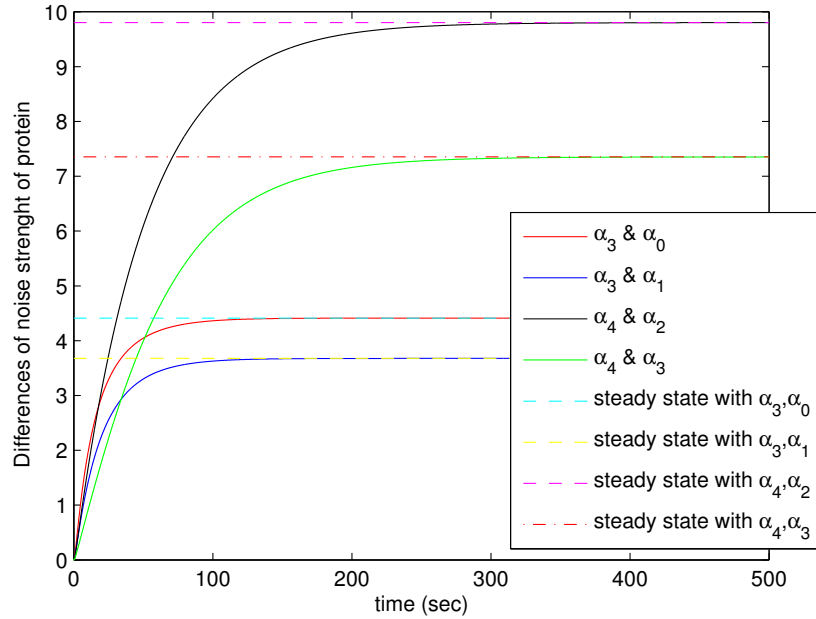


Figure 6.9: The same as Figure 6.7 with different rate constants.

6.5 Steady State Variances and Noise Strengths with Feedback

In this section we compare the variances and noise strengths of mRNA and protein at steady state. To find when the system is stable at steady state, we let $w(t) = z(t) + N^{-1}B$, where w , N and B were defined in section 6.2, so

$$\frac{dw(t)}{dt} = Nw(t).$$

We then find that the system has eigenvalues:

$$\begin{aligned} & -(d_M + d_P), \\ & -(d_M + d_P) \pm \sqrt{(d_M - d_P)^2 + 4u_M u_P \alpha}, \\ & \frac{-(d_M + d_P) \pm \sqrt{(d_M - d_P)^2 + 4u_M u_P \alpha}}{2}. \end{aligned}$$

The system has a stable equilibrium if and only if all eigenvalues are negative, giving

$$-(d_M + d_P) + \sqrt{(d_M - d_P)^2 + 4u_M u_P \alpha} < 0.$$

This leads to the following condition for a linearly stable equilibrium,

$$0 \leq \alpha < \frac{d_M d_P}{u_M u_P}.$$

For the feedback model with $0 \leq \alpha < d_M d_P / u_M u_P$, we find that the steady state moments have the form

$$\mathbb{E}[M^s] = \frac{d_P u_M}{d_M d_P - u_P u_M \alpha}, \quad (6.26)$$

$$\mathbb{E}[P^s] = \frac{u_P u_M}{d_M d_P - u_P u_M \alpha}, \quad (6.27)$$

$$\begin{aligned} \mathbb{E}[(M^s)^2] &= \frac{u_M d_M d_P (d_M d_P - u_P u_M \alpha) + u_M^2 d_P (u_P \alpha^2 u_M + d_M d_P)}{(d_M + d_P)(d_M d_P - u_P u_M \alpha)^2} \\ &\quad + \frac{u_M d_P^3 (u_M + d_M)}{(d_M + d_P)(d_M d_P - u_P u_M \alpha)^2}, \end{aligned} \quad (6.28)$$

$$\begin{aligned} \mathbb{E}[(P^s)^2] &= \frac{u_M u_P d_P (d_M d_P - u_P u_M \alpha) + u_M^2 u_P^2 (d_M + d_P)}{(d_M + d_P)(d_M d_P - u_P u_M \alpha)^2} \\ &\quad + \frac{u_M d_M u_P d_P (d_M + u_P)}{(d_M + d_P)(d_M d_P - u_P u_M \alpha)^2}. \end{aligned} \quad (6.29)$$

We have used the superscript s to denote the level of species at steady state for the feedback model.

We are now in a position to consider differences of variances and noise strengths in mRNA and protein at steady state. Let $0 \leq \alpha_1 < \alpha_2 < d_M d_P / u_M u_P$, and let $M_{\alpha_i}^s$ and $P_{\alpha_i}^s$ denote the number of mRNA and protein molecules at steady state

for the feedback model (6.6)-(6.10) with $\alpha = \alpha_i$, we find that

$$\begin{aligned}
& \text{var}[M_{\alpha_2}^s] - \text{var}[M_{\alpha_1}^s] \\
&= \frac{u_M^2 d_P u_P d_M (\alpha_2 - \alpha_1)}{(d_M d_P - u_P u_M \alpha_2)(d_M d_P - u_P u_M \alpha_1)(d_M + d_P)} \\
&+ \frac{u_M^2 d_P^2 u_P d_M (\alpha_2 - \alpha_1)(d_P + \alpha_2 u_M)}{(d_M d_P - u_P u_M \alpha_1)(d_M + d_P)(d_M d_P - u_P u_M \alpha_2)^2} \\
&+ \frac{u_M^2 d_P^2 u_P d_M (\alpha_2 - \alpha_1)(d_P + \alpha_1 u_M)}{(d_M d_P - u_P u_M \alpha_2)(d_M + d_P)(d_M d_P - u_P u_M \alpha_1)^2}, \tag{6.30}
\end{aligned}$$

$$\begin{aligned}
& \text{var}[P_{\alpha_2}^s] - \text{var}[P_{\alpha_1}^s] \\
&= \frac{u_M^2 u_P^2 d_P d_M (\alpha_2 - \alpha_1)(d_M + u_P)(2d_M d_P - u_P u_M \alpha_1 - u_P u_M \alpha_2)}{(d_M + d_P)(d_M d_P - u_P u_M \alpha_1)^2 (d_M d_P - u_P u_M \alpha_2)^2} \\
&+ \frac{u_M^2 u_P^2 d_P (\alpha_2 - \alpha_1)}{(d_M d_P - u_P u_M \alpha_2)(d_M d_P - u_P u_M \alpha_1)(d_M + d_P)} \tag{6.31}
\end{aligned}$$

and

$$\begin{aligned}
& \text{ns}[M_{\alpha_2}^s] - \text{ns}[M_{\alpha_1}^s] \\
&= \frac{u_M u_P (\alpha_2 - \alpha_1)(\alpha_1 u_M (d_M d_P - u_P u_M \alpha_2) + d_P^2 d_M + \alpha_2 u_M d_M d_P)}{(d_M + d_P)(d_M d_P - u_P u_M \alpha_1)(d_M d_P - u_P u_M \alpha_2)}, \tag{6.32}
\end{aligned}$$

$$\begin{aligned}
& \text{ns}[P_{\alpha_2}^s] - \text{ns}[P_{\alpha_1}^s] \\
&= \frac{d_P u_M u_P d_M (\alpha_2 - \alpha_1)(d_M + u_P)}{(d_M + d_P)(d_M d_P - u_P u_M \alpha_1)(d_M d_P - u_P u_M \alpha_2)}. \tag{6.33}
\end{aligned}$$

Since $0 \leq \alpha_1 < \alpha_2 < d_M d_P / u_M u_P$, at steady state we can see from (6.30)-(6.33) that both differences of variances and noise strengths increase monotonically in α in the interval $[0, \beta)$ where $\beta = d_M d_P / u_M u_P$. Thus, at stable steady state, increasing the protein feedback rate causes the variances and noise strengths of both mRNA and protein to increase monotonically in α .

6.6 Summary

In this chapter we studied a feedback model in which protein enhances its own production, and indicated

- all moments increase monotonically in the feedback rate, independent of rate constants and initial conditions,
- the ranges of the protein feedback rate to guarantee the system has a stable equilibrium.

In this range of the feedback rate,

- the steady state first and second moments can be established,
- variances and noise strengths increase monotonically in the feedback rate at steady state for any choice of model parameters.

Chapter 7

Conclusions and Further Work

7.1 Conclusions

In this thesis we have conducted research on gene regulation networks using modelling and numerical simulation. We focused on comparing the noise strength between the true solutions arising from CME models and the approximate solutions arising from hybrid models to decide whether a model is good.

In Chapter 4, we established existence and uniqueness, and numerical simulation theories for solutions of the hybrid models driven by an independent Markovian switch with infinite state space. We also showed that simple multi-scale diffusion models in gene regulation have advantages over their ODE counterparts.

In Chapter 5, we introduced a more general model where gene activity is controlled by a transcription factor. We focussed on this control in two senses; AND and OR modes. In AND mode, even though this model is a second order reaction network, noise strength is amenable to analysis. We found that steady state mRNA and protein noise strengths of the one and two-switch models are greater than those of the zero-switch model, while the two-switch model may be more or

less noisy than the one-switch model, depending on the choice of the model parameters. We further showed that the hybrid SDE approximation is better than the hybrid ODE approximation in order to recover the mRNA and protein variances and correlation. In addition, we showed that the OR mode may be more or less noisy than the AND mode, depending on the rate constants.

In the final chapter of research, we examined the variance and noise strength of gene regulation when protein feedback is allowed. Not surprisingly, increasing the feedback rate causes the first and second moments and correlations to increase. We also showed that, in the stable range of protein feedback rate, the steady state variances and noise strengths of mRNA and protein increase monotonically in the feedback rate.

7.2 Further Work

There are many interesting open questions in this area, including:

- How general is the phenomenon shown in this thesis that replacing a Langevin component with the reaction rate ODE causes the overall variance to be underestimated?
- Is there a general existence/uniqueness/numerical convergence theory for diffusion coefficients that involve the square root function?
- Is it possible to develop a theory for infinite state-dependent Markov switches, which arise, for example, when the transcription rate is affected by a protein as discussed in the previous chapter?

Bibliography

- [1] U. ALON, *An Introduction to Systems Biology: Design Principles of Biological Circuits*, Chapman & Hall, London, 2006.
- [2] W. J. ANDERSON, *Continuous-time Markov chains*, Springer Series in Statistics: Probability and its Applications, Springer-Verlag, New York, 1991. An applications-oriented approach.
- [3] A. BOBROWSKI, T. LIPNIACKI, K. PICHÓR, AND R. RUDNICKI, *Asymptotic behavior of distributions of mRNA and protein levels in a model of stochastic gene expression*, Journal of Mathematical Analysis and Applications, 333 (2007), pp. 753–769.
- [4] H. BOLOURI AND E. H. DAVIDSON, *Modeling transcriptional regulatory networks*, BioEssays, 24 (2002), pp. 1118–1129.
- [5] N. E. BUCHLER, U. GERLAND, AND T. HWA, *Nonlinear protein degradation and the function of genetic circuits*, Proc. Natl. Acad. Sci. USA, 102 (2005), pp. 9559–64.
- [6] R. BUNDSCHUH, F. HAYOT, AND C. JAYAPRAKASH, *The role of dimerization in noise reduction of simple genetic networks*, Journal of Theoretical Biology, 220 (2003), pp. 261–269.

- [7] Y. CAO, D. T. GILLESPIE, AND L. PETZOLD, *The slow-scale stochastic simulation algorithm*, The Journal of Chemical Physics, 122 (2005), p. 014116.
- [8] —, *Efficient step size selection for the Tau-leaping simulation method*, The Journal of Chemical Physics, 124 (2006), p. 044109.
- [9] H. DE JONG, *Modeling and simulation of genetic regulatory systems: A literature review*, Journal of Computational Biology, 9 (2002), pp. 69–105.
- [10] W. E, D. LIU, AND E. VANDEN-ELJNDEN, *Nested stochastic simulation algorithms for chemical kinetic systems with multiple time scales*, The Journal of Chemical Physics, 123 (2005), p. 194107.
- [11] C. GADGIL, C. H. LEE, AND H. G. OTHMER, *A stochastic analysis of first-order reaction networks*, Bulletin of Mathematical Biology, 67 (2005), pp. 901–946.
- [12] M. GIBSON AND J. BRUCK, *Efficient exact stochastic simulation of chemical systems with many species and many channels*, The Journal of Physical Chemistry A, 104 (2000), pp. 1876–1889.
- [13] Ī. Ī. GĪHMAN AND A. V. SKOROHOD, *Stochastic Differential Equations*, Springer-Verlag, New York, 1972. Translated from the Russian by Kenneth Wickwire, Ergebnisse der Mathematik und ihrer Grenzgebiete, Band 72.
- [14] D. T. GILLESPIE, *A general method for numerically simulating the stochastic time evolution of coupled chemical reactions*, Journal of Computational Physics, 22 (1976), pp. 403–434.
- [15] —, *Exact stochastic simulation of coupled chemical reactions*, The Journal of Physical Chemistry, 81 (1977), pp. 2340–2361.

- [16] —, *A rigorous derivation of the chemical master equation*, *Physica A Statistical Mechanics and its Applications*, 188 (1992), pp. 404–425.
- [17] —, *Markov Processes: An Introduction for Physical Scientists*, Academic Press, Inc., Boston, 1992.
- [18] —, *The chemical Langevin equation*, *The Journal of Chemical Physics*, 113 (2000), pp. 297–306.
- [19] —, *Approximate accelerated stochastic simulation of chemically reacting systems*, *The Journal of Chemical Physics*, 115 (2001), pp. 1716–1733.
- [20] —, *Stochastic simulation of chemical kinetics*, *Annual Review of Physical Chemistry*, 58 (2007), pp. 35–55.
- [21] F. B. HANSON AND J. J. WESTMAN, *Optimal consumption and portfolio control for jumpdiffusion stock process with lognormal jumps*, *Proceedings of American Control Conference*, (2002), pp. 4256–4261.
- [22] D. J. HIGHAM, *An algorithmic introduction to numerical simulation of stochastic differential equations*, *SIAM Review*, 43 (2001), pp. 525–546.
- [23] —, *Modeling and simulating chemical reactions*, *SIAM Review*, 50 (2008), pp. 347–368.
- [24] —, *Stochastic ordinary differential equations in applied and computational mathematics*, *University of Strathclyde Mathematics and Statistics Research Report*, #7 (2010), pp. 1–32. To appear in *IMA Journal of Applied Mathematics*.

- [25] D. J. HIGHAM AND R. KHANIN, *Chemical master versus chemical Langevin for first-order reaction networks*, Open Applied Mathematics Journal, 2 (2008), pp. 59–79.
- [26] D. J. HIGHAM, X. MAO, AND A. STUART, *Strong convergence of Euler-type methods for nonlinear stochastic differential equations*, SIAM Journal on Numerical Analysis, 40 (2002), pp. 1041–1063.
- [27] P. J. INGRAM, M. P. STUMPF, AND J. STARK, *Network motifs: structure does not determine function*, BMC Genomics, 7 (2006), p. 108.
- [28] S. INTEP AND D. J. HIGHAM, *Zero, one and two-switch models of gene regulation*, Discrete and Continuous Dynamical Systems Series B, 14 (2010), pp. 495–513.
- [29] S. INTEP, D. J. HIGHAM, AND X. MAO, *Switching and diffusion models for gene regulation networks*, Multiscale Modeling & Simulation, 8 (2009), pp. 30–45.
- [30] R. KARMAKAR AND I. BOSE, *Stochastic model of transcription factor-regulated gene expression*, Physical Biology, 3 (2006), pp. 200–208.
- [31] R. KHANIN AND D. J. HIGHAM, *Chemical master equation and Langevin regimes for a gene transcription model*, Theoretical Computer Science, 408 (2008), pp. 31–40.
- [32] F. C. KLEBANER, *Introduction to Stochastic Calculus with Applications*, Imperial College Press, London, 1998.
- [33] T. G. KURTZ, *Approximation of Population Processes*, SIAM, 1981.

- [34] T. LIPNIACKI, P. PASZEK, A. MARCINIAK-CZOCHRA, A. R. BRASIER, AND M. KIMMEL, *Transcriptional stochasticity in gene expression*, Journal of Theoretical Biology, 238 (2006), pp. 348–367.
- [35] S. MACNAMARA, K. BURRAGE, AND R. B. SIDJE, *Multiscale modeling of chemical kinetics via the master equation*, Multiscale Modeling & Simulation, 6 (2008), pp. 1146–1168.
- [36] X. MAO, *Stochastic Differential Equations and Applications*, Horwood, Chichester, 1997.
- [37] X. MAO AND C. YUAN, *Stochastic Differential Equations with Markovian Switching*, Imperial College Press, London, 2006.
- [38] X. MAO, C. YUAN, AND G. YIN, *Approximations of Euler-Maruyama type for stochastic differential equations with Markovian switching, under non-Lipschitz conditions*, Journal of Computational and Applied Mathematics, 205 (2007), pp. 936–948.
- [39] D. A. MCQUARRIE, *Stochastic approach to chemical kinetics*, Journal of Applied Probability, 4 (1967), pp. 413–478.
- [40] J. D. MURRAY, *Mathematical Biology*, Springer-Verlag, Berlin, second, corrected ed., 1993.
- [41] J. R. NORRIS, *Markov Chains*, Cambridge University Press, Cambridge, 1997.
- [42] B. OKSENDAL, *Stochastic Differential Equations: an Introduction with Applications*, Springer-Verlag, Berlin, fifth ed., 1998.

- [43] P. PASZEK, *Modeling stochasticity in gene regulation: characterization in the terms of the underlying distribution function*, *Bulletin of Mathematical Biology*, 69 (2007), pp. 1567–601.
- [44] J. RASER AND E. O’SHEA, *Control of stochasticity in eukaryotic gene expression*, *Science*, 304 (2004), pp. 1811–4.
- [45] E. RENSHAW, *Modelling Biological Populations in Space and Time*, Cambridge University Press, 1991.
- [46] A. V. SKOROHOD, *Asymptotic Methods in the Theory of Stochastic Differential Equations*, American Mathematical Society, 1989.
- [47] P. S. SWAIN, M. B. ELOWITZ, AND E. D. SIGGIA, *Intrinsic and extrinsic contributions to stochasticity in gene expression*, *Proc. Natl. Acad. Sci. USA*, 99 (2002), pp. 12795–800.
- [48] L. SZPRUCH AND D. J. HIGHAM, *Comparing hitting time behavior of Markov jump processes and their diffusion approximations*, *Multiscale Modeling & Simulation*, 8 (2010), pp. 605–621.
- [49] M. THATTAI AND A. VAN OUDENAARDEN, *Intrinsic noise in gene regulatory networks*, *Proc. Natl. Acad. Sci. USA*, 98 (2001), pp. 8614–19.
- [50] T. TIAN AND K. BURRAGE, *Stochastic models for regulatory networks of the genetic toggle switch*, *Proc. Natl. Acad. Sci. USA*, 103 (2006), pp. 8372–8377.
- [51] T. E. TURNER, S. SCHNELL, AND K. BURRAGE, *Stochastic approaches for modelling in vivo reactions*, *Computational Biology and Chemistry*, 28 (2004), pp. 165–178.

- [52] M. ULLAH, H. SCHMIDT, K.-H. CHO, AND O. WOLKENHAUER, *Deterministic modelling and stochastic simulation of biochemical pathways using MATLAB*, IEE Proceedings Systems Biology, 153 (2006), pp. 53–60.
- [53] V. VYSHEMIRSKY AND M. GIROLAMI, *Bayesian ranking of biochemical system models*, Bioinformatics, 24(6) (2008), pp. 833–839.
- [54] J. WANG, J. ZHANG, Z. YUAN, AND T. ZHOU, *Noise-induced switches in network systems of the genetic toggle switch*, BMC Systems Biology, 1:50 (2007).
- [55] D. J. WILKINSON, *Stochastic Modelling for Systems Biology*, Chapman & Hall/CRC, 2006.
- [56] G. YAN AND F. B. HANSON, *Option pricing for a stochastic-volatility jump-diffusion model with log-uniform jump-amplitudes*, Proceedings of American Control Conference, (2006), pp. 1–7.
- [57] G. G. YIN AND Q. ZHANG, *Discrete-Time Markov Chains*, Springer, Berlin, 2005.